Evaluation on the Biocompatibility of Selected Nanoparticles: *In vitro* and *In vivo* Studies

Thesis submitted for the degree of

DOCTOR OF PHILOSOPHY

By

Jyotsna Radhika G.

Department of Animal Sciences
School of Life Sciences
University of Hyderabad
Hyderabad 500 046, India

Enrolment No. 07LAPH03

July, 2013

University of Hyderabad

(A Central University established in 1974 by act of parliament)

HYDERABAD- 500 046, INDIA

DECLARATION

I hereby declare that the work embodied in this thesis entitled **"Evaluation on the Biocompatibility of Selected Nanoparticles: *In vitro* and *In vivo* studies."** has been carried out by me under the supervision of Prof. P. Reddanna and this has not been submitted for any degree or diploma of any other university earlier.

Prof. P. Reddanna	**Jyotsna Radhika G.**
(Research Supervisor)	(Research Scholar)

University of Hyderabad

(A Central University established in 1974 by act of parliament)

HYDERABAD- 500 046, INDIA

CERTIFICATE

This is to certify that **Mrs. Jyotsna Radhika Giddaluri** has carried out the research work embodied in the present thesis under my supervision and guidance for a full period prescribed under the Ph.D. ordinance of this University. We recommend her thesis "**Evaluation on the Biocompatibility of Selected Nanoparticles: *In vitro* and *In vivo* studies."** for submission for the degree of Doctor of Philosophy of this University.

Prof. P. Reddanna _____
Research Supervisor

Head _____
Department of Animal Sciences

Dean _____
School of Life Sciences

ACKNOWLEDGEMENTS

I express my deep sense of gratitude to ***Prof. Pallu Reddanna****, my research supervisor for believing in me and having given me the opportunity to work under his guidance. As a man of great integrity and strength he has been a great inspiration throughout my doctoral tenure and helped me believe in hard work and perseverance. I have not only been able to improve my research abilities under his able guidance but also have bettered my personality. I thank him for the constant support and encouragement he extended during times of thick and thin.*

I thank my doctoral committee members ***Dr. Nareshbabu V. Sepuri*** *and* ***Dr Bramanandam Manavathi*** *for their constant support and valuable suggestions during my research period.*

I thank the Head of the department, Animal Sciences, ***Prof. B.Senthilkuaran*** *and the former Heads of the department* ***Prof. Aparna Dutta Gupta****,* ***Prof. S. Dayananda****,* ***Prof. Manjula Sritharan*** *for their support and encouragement and for letting me use the department facilities.*

I thank the Dean of School of Life Sciences, ***Prof R.P.Sharma*** *and the former Deans of School of life sciences,* ***Prof. A.S.Raghavendra****,* ***Prof. M. Ramanadham****, Prof.* ***Aparna Dutta Gupta*** *for their support and encouragement during my research tenure and also for allowing me to use the School facilities.*

I thank ***Prof. Agapios Sachinidis****, my co-supervisor at University of Cologne for giving me an opportunity to work in his laboratory as a DAAD exchange scholar. I thank him for agreeing to guide me to get some insights into stem cell technology and helping me develop the skill of stem cell culturing.*

I thank ***Dr. Saber Hussain*** *and* ***Prof. Lakshmipathi*** *for their valuable suggestions through the course of my research work.*

I thank ***Dr. M.K, Arunasree*** *and* ***Dr. A. Bindu Madhava Reddy*** *for their support and encouragement.*

Special heartfelt thanks to my doyen ***Dr. P. Nishanth*** *for his unwavering support and constant encouragement during my entire research period. His conviction and confidence have always been an inspiration. His critical comments and patience have helped me improve my research skills largely.*

I thank my colleagues ***Suresh****,* ***Kumar,*** ***Geetika****,* ***Naresh****,* ***Naireen,*** *and* ***Azad*** *for making the lab atmosphere congenial and lively to work in.*

I thank my senior colleagues ***Dr. G.V.Reddy****,* ***Dr. Roy****,* ***Dr. Bharath****,* ***Dr. Sreekanth****,* ***Dr. Sreedevi****,* ***Dr. Anil Kumar****,* ***Dr. Smitha,*** ***Dr. Chandramohan****,* ***Dr. Ramakrishna****,* ***Dr.***

Aparoy, Dr. Pulla reddy and Dr. Kishore for their guidance and help in acquiring the technical skills and scientific insight.

I thank my friends at school of life sciences Ushodaya, Jyotsna, Swetha, Pandey, Sunil, Chandrani, Lakshmi, Preethi, Subha and Venkat for their friendship and support. Their lively company has been a refreshing sneak away from the mundaneness. I also thank all my colleagues at school of life sciences for maintaining a lively and amicable atmosphere.

My special thanks to Gangadhar, Susheel and Aishwarya for their ever responsiveness and timely help.

I thank the CSIR RFSMS for the research fellowship and DAAD for funding my stay at University of Cologne, Germany.

I thank the DST FIST and central Proteomics and Genomics facilities for providing us the accesses to the advanced research facilities.

I thank the administrative and technical staff of department of Animal sciences Mr. Ankineedu, Mr. Shiva kumar, Ms. Jyothi, Mr. Jagan for their timely help. Assistance from lab attendants Mr. Balram, Mr. Nagesh, Mr. Sivaram and Mr. Bangariah is greatly appreciated.

I would like to make a special mention of my friends Chaithu, Sujana, Apoorva and Divya, for always being there for me when I needed. Their emotional support through all times kept me going. Thank you for being the very special part of my life.

Special thanks to Jayakant, Balaji and Felcy for their new refreshing thoughts and quick responses to my emails requesting for research articles.

Words can't express the magnanimity of appreciation that I hold in my heart for the man of my life, Kesava. He has been a towering support and a rock of strength emotionally. His trust and encouragement helped me pull off to the finish line. His unwavering patience in dealing with me and the 'complete what you initiate' attitude of his, kept me going till the end.

I fall short of words when it comes to thanking my parents, my brother, my mother in law, my grandparents and my extended family. My parents have been a true inspiration all along, they stood by me in every step I took and every decision I made. Their simplicity, revered advice, love and affection have helped me be what I am. "Behind every man's success there is a woman and behind every woman's success there is a loving and caring family." I am grateful to God for having given me such wonderful family and friends.

Jyotsna Radhika G.

Table of Contents

List of Figures and Tables

Abbreviations

°C	:	Degree centigrade/ Degree Celsius
µg	:	Micro gram
µl	:	Micro liter
AA	:	Arachidonic Acid
ATP	:	Adenosinetriphosphate
CHAPS	:	3-[(3-cholamidopropyl) dimethylammonia]-1-propane sulphonate
COX	:	Cyclooxygenase
DCF	:	Dichloro fluorescein
DCFHDA	:	2, 7 dichloro dihydro fluorescein diacetate
DLS	:	Dynamic light scattering
DTT	:	Dithiothreitol
DMSO	:	Dimethyl sulfoxide
EDTA	:	Ethylene diamine tetra acetic acid
FBS	:	Fetal bovine serum
g	:	Gram
h	:	Hour (s)
H_2O_2	:	Hydrogen peroxide
Hsp 70	:	Heat shock protein 70
IAA	:	Iodoacetamide
IEF	:	Isoelectric focusing
IL	:	Interleukin
kDa	:	Kilodalton
l	:	Litre
LT	:	Leukotriene
LPS	:	Lipopolysaccharide
MAPK	:	Mitogen activated protein kinase
min	:	Minute(s)
ml	:	Milliliter
mM	:	Millimolar
MTT	:	[3-(4, 5-dimethylthiazol-2-yl)-2,5- Diphenyl tetrazolium bromide]
NBT	:	Nitroblue tetrazolium
NF-κB	:	Nuclear factor-kappa B
nm	:	Nanometers
nM	:	Nanomolar
OD	:	Optical density

PAGE	:	Polyacrylamide gel electrophoresis
PBS	:	Phosphate buffered saline
PG	:	Prostaglandin
PMSF	:	Phenylmethanesulphonylfluoride
ROS	:	Reactive oxygen species
RT-PCR	:	Reverse transcriptase-polymerase chain Reaction
SDS	:	Sodium dodecyl sulfate
TEM	:	Transmission electron microscopy
TNF-α	:	Tumor Necrosis Factor-α
UV	:	Ultraviolet

General Introduction

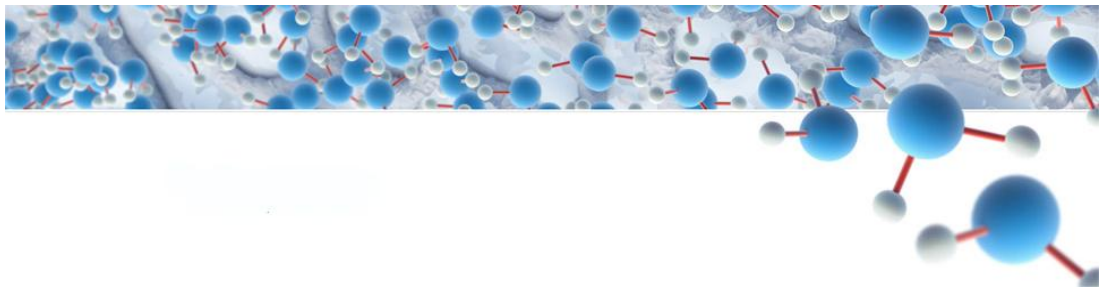

General Introduction

1. Nanotechnology and Nanomaterials

Nanotechnology is one of the fastest growing technologies globally, that has found its use in every field. The idea of nanotechnology spun off from the seminal lecture "There is plenty of room at the bottom" by American physicist Richard Feynman in the year 1959. In his lecture, he discussed the exciting ideas of miniaturizing the things to atomic sizes that would work as tiny hands, the nanorobots. This idea of his was conceived much later in 1979 when Norio Taniguchi researched on developing the ultra precision machines. It was during that time that the word "Nanotechnology" was coined by him, which was popularized by Eric Drexler through his book "Engines of creation: the coming Era of Nanotechnology".

Nanotechnology could be defined as, "The design, characterization, production, and application of structures, devices, and systems by controlled manipulation of size and shape at the nanometer scale (atomic, molecular, and macromolecular scale) that produces structures, devices, and systems with at least one novel/superior characteristic or property."

In simpler terms nanotechnology is the research and development of materials and species that are of nanometer dimensions. Although nanoscale materials exist in nature and are not a novelty, it is the advent of instruments and techniques such as Scanning Tunneling Microscope and Atomic Force Microscope that helped scientists to learn more about materials at nanoscale. The parallel

development of methods to produce materials at nanoscale and techniques to characterize them increased the interest in exploring the use of nanomaterials in various applications.

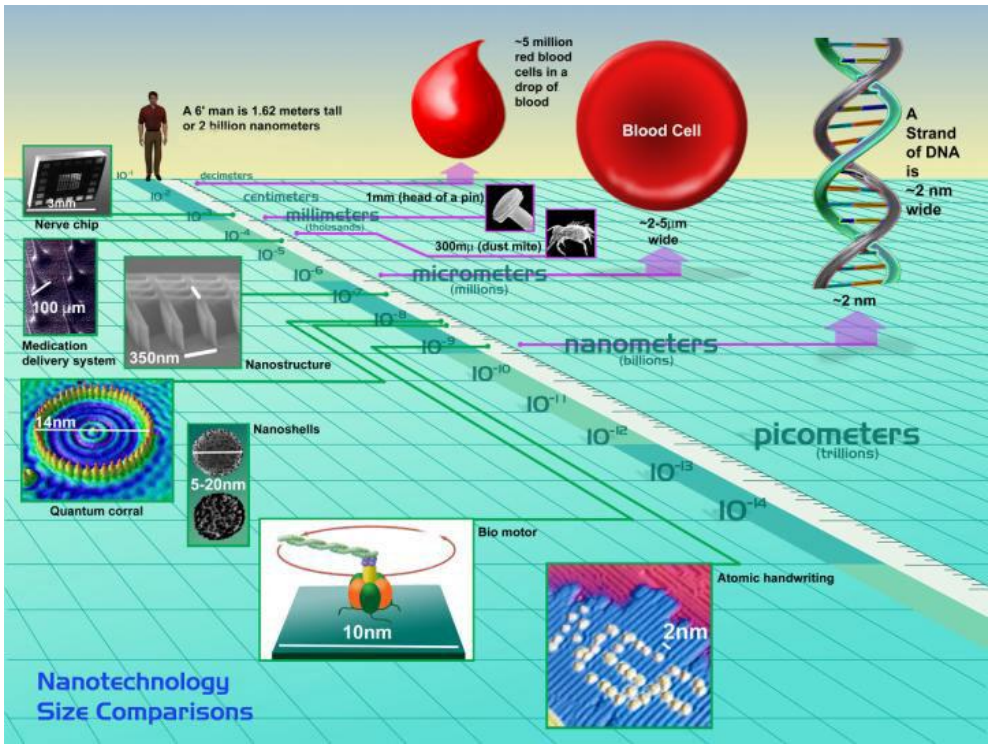

Figure 1. Examples of human-made devices created using nanotechnology, juxtaposed along a measurement ruler which depicts their relative size in the nanometer.

(Source: www.nsf.gov)

Nanomaterials are defined as structured components with at least one dimension less than 100 nm. Nanomaterials can be classified into three groups depending on the number of dimensions that are of nanometer range.

- Nanoparticles are materials that are of nanoscale in three dimensions are particles, for example precipitates, colloids of metals and quantum dots etc.

- Nanowires and nanotubes are materials that possess nanoscale in two dimensions, for example carbon nanotubes.
- Nanolayers, such as a thin films or surface coatings are the materials that have one dimension in the nanoscale. Some of the features on computer chips come in this category.

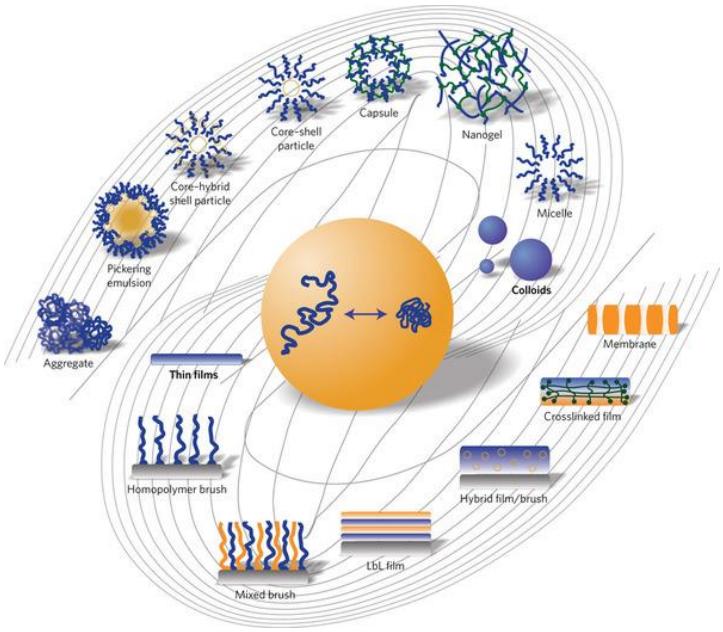

Figure 2. Nanomaterials in various forms (Source: www.nature.com)

Nanomaterials have unique physicochemical properties that result from the combination of their small size, chemical composition, surface structure, solubility, shape, and aggregation. The two principal factors which bring about a significant difference in the properties exhibited by nanomaterials include; increased relative surface area, and quantum effects. Properties such as reactivity, strength and electrical characteristics are altered or improved due to these two factors. As the particle size decreases, a greater proportion of atoms are found at

the surface compared to those inside. For example, a particle of size 30 nm has 5% of its atoms on its surface, at 10 nm 20% and at 3 nm 50% of its atoms. Thus nanoparticles have a much greater surface area per unit mass compared with larger particles and will be much more reactive than the same mass of material made up of larger particles. Because of these improved properties compared to their bulk counter parts nanomaterials seem to find a lot of applications. As we recognize new applications for NPs, the number of products containing such nanomaterials continues to grow exponentially.

2. Applications of Nanomaterials

Nanomaterials are finding use in every walk of human life from energy management to automobiles, from medicine and drugs to cosmetics, etc,.

- Cosmetics: Nanosized titanium oxide and zinc oxide absorb UV rays and are used in sunscreen lotions.
- Nanocomposite materials are not only used to increase mechanical properties but also to impart new properties (optical, electronic, etc,.)
- Nanocoatings: Surface coating with nanometer thickness of nanomaterial can be used to improve properties like wear and scratch-resistant, optoelectronics, hydrophobic properties.
- Hard cutting tools: Current cutting tools (e.g. mill machine tools) are made using a sort of metal nanocomposites such as tungsten carbide, tantalum

carbide and titanium carbide that have more wear and erosion-resistant, and last longer than their conventional (large grained) materials.

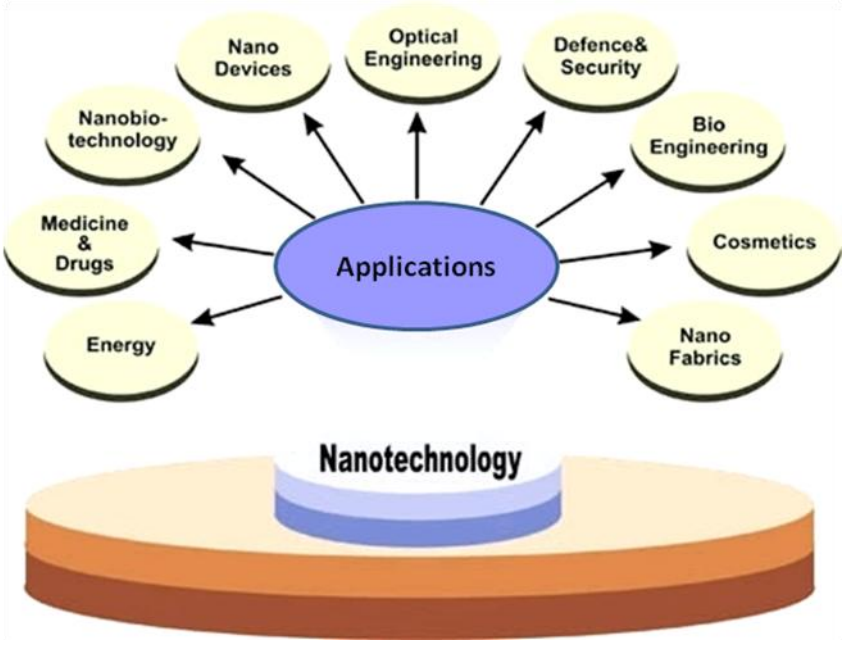

Figure 3. Applications of nanotechnology (Source: nanorev.in)

- Nanoparticles are being used to improve the paint and various dye properties.
- Nano-engineered membranes are being used to improve efficiency of small-scale fuel cells.
- Displays: New class of display using carbon nanotubes as emission device for the next generation of monitor and television (FED-field emission displays).
- Nanotechnology based knowledge may produce more efficient, lightweight, high-energy density batteries.
- Nanoparticles can be used as fuel additives and lubricants to improve the efficiency of the machines.

- Nanostructured membranes are being used for deionization of salt water for drinking purpose and also for making the water virus free. Remediation of industrial waste waters is also possible by use of nanoparticles that can convert the highly toxic substances into non-toxic ones.
- Nanoelectronics: Currently nanomaterials are being used in computer chips, information storage devices, and sensors.
- Nanomaterials are finding applications in the field of medicine such as disease diagnosis, drug delivery and molecular imaging.

2.1. Applications of Widely used Nanomaterials

Silver nanoparticles are finding lot of applications mainly due to the improved antimicrobial abilities. Silver nanoparticles based wound dressings and band-aids are available in the market. Silver nanoparticles are used for sterilizing medical equipments and also used to coat the bioengineered prosthesis (Bosetti *et al.,* 2002). Silver nanoparticle based substances are being used in dental restorative material, endodontic retrofill cements and dental implants (García-Contreras *et al.,* 2011). They are used in water treatment, to purify the water and reduce the microbial loads. Silver nanoparticles are incorporated into the polyurethane foams that can be used as filters for water treatment (Jain *et al.,* 2005). More recently, silver nanoparticles have also found their use in textile industry, to make the fabrics microbe resistant (Lee *et al.,* 2003, Ilic *et al.,* 2009, An *et al.,* 2010). Silver

nanoparticles also possess good catalytic properties because of which they are used to speed up some of the reactions such as bleaching of organic dyes (Kohler *et al.,* 2008) and reduction of 4-nitrophenol (Liu and Zhao 2009). Its electrochemical properties are exploited in the development of sensors as well (Manno *et al.,* 2008).

Aluminium nanoparticles have commercial, industrial applications starting from their use as in alloys that increase the mechanical strength (Ruan and Schuh 2012). Alumina nanoparticles are used as catalysts in gas purification (Buzdugan and Beckman, 2007; Platonov *et al.,* 2007). It is also used in preparation of ceramics to improve their strength, hardness and wear resistance. Alumina nanoparticles are also used in cosmetics, dental and bone implants (Lukin *et al.,* 2001). Aluminium nanoparticles are used in military for solid rocket fuel propellants (Miziolek, 2002).

Carbon based nanomaterials such as fullerenes, nanotubes and nanofibres are finding lot of applications. The graphite nanofibers are being used in the electronics and electrochemistry. They are being used for developing sensor devices (Quercia *et al.,* 2004). Carbon dots and diamond based nanoparticles are being studied for uses in bioimaging and long term cell tracking (Cao *et al.,* 2007, Fang *et al.,* 2011). Mesoporous carbon nanoparticles are now being considered for use as drug delivery agents (Kim *et al.,* 2008, Liu *et al.,* 2008). More recently the carbon nanoparticles that exhibit fluorescent properties have been prepared that can be used in imaging (Chandra *et al.,* 2011).

Gold is one of the noble metals that have been of great commercial and biomedical importance. Gold, in the form of nanoparticles, has also found new applications in the biomedical field.

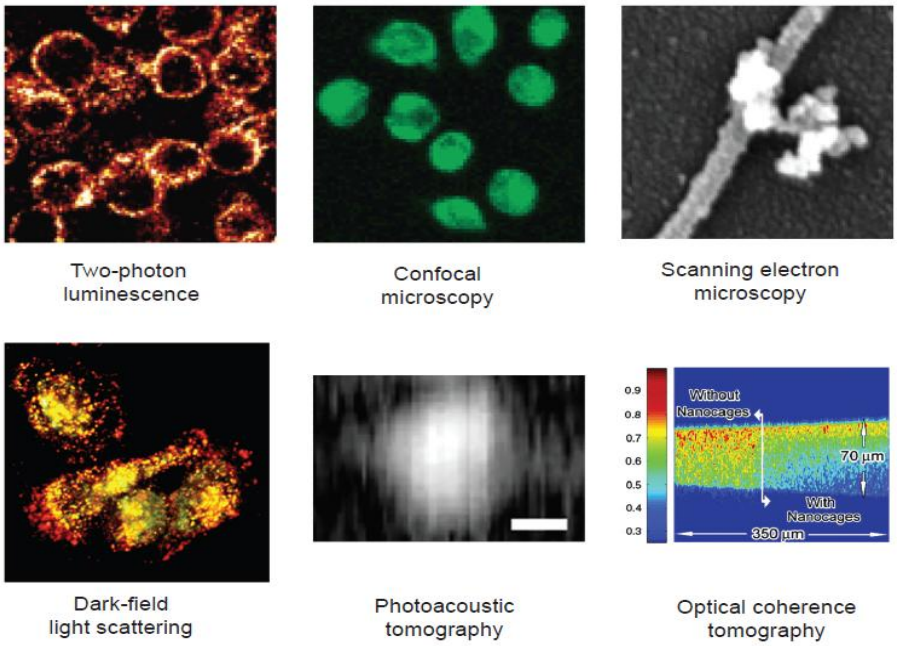

Figure 4. Bioimaging applications of nanoparticles (Source: From Chen et al., 2005; Yang et al., 2005; Fuente et al., 2006; Durr et al., 2007; Li et al., 2007a; Oyelere et al., 2007)

Gold nanoparticles are being used to deliver the biomolecules such as proteins and DNA into the cells in order to transform them (Niemeyer, 2001; Sanford *et al.,* 1993). They are being used in developing sensors for the detection of various biomolecules (Olofsson *et al.,* 2003), and thus in drug delivery and cancer therapy. The nanoparticles coated with drug molecules and antibodies are being considered for targeted drug delivery to the cancer tissues (Chen *et al.,* 2007b). Gold nanoparticles are being considered for the thermal cancer therapy because of their improved photothermal properties (Chen *et al.,* 2007a). The surface enhanced

Raman scattering (SERS) property of the gold nanoparticles is being applied for *in vivo* bioimaging and cell tracking (Keren *et al.,* 2008).

3. Nanomaterials and Associated Risks

Nanomaterials, with their improved physicochemical properties, have found varied application. They are already being used in a wide range of consumer products such as sunscreens, cosmetics, composites, medical and electronic devices, and are also being used as chemical catalysts. While it is likely that most nanomaterials are reasonably safe, some created with unique properties may exhibit deleterious effects on living cells. Importantly, the substances that are inert in bulk may be toxic at nanosize, due to their altered chemical and physical properties (Nel *et al.,* 2006), arguing that most of the nanomaterials must be methodically evaluated for their toxic potential. Recently, a number of studies have shown toxicity of NPs in different organs of animal models (Kaewamatawong *et al.,* 2006; Niwa *et al.,* 2008). NPs have been reported to induce a pro-oxidant environment within the cells, and thereby leading to adverse biological consequences ranging from the loss of normal cellular functional response to cell death (Braydich-Stolle *et al.,* 2005; Hussain *et al.,* 2005). Many studies have demonstrated the ability of NPs to generate reactive oxygen species (ROS) (Stone *et al.,* 1998). This oxidative stress may be linked to the induction of signaling pathways which lead to pro-inflammatory gene expression in macrophages (Brown *et al.,* 2004).

3.1. Environmental and Health Effects of Nanomaterials

Nanosized materials are generated through natural as well as anthropogenic processes. In nature the nanosized materials are found in soil and atmosphere. Soil contains nanoparticles of metal oxides and hydroxides, humic substances, allophane, imogolite and some organic nanoparticles that are produced by the natural vegetation (Theng and Yuang 2008; Xia *et al.,* 2010). Sooth and ashes that are thrown into the atmosphere during volcanic eruptions and natural fires also constitute a part of ultrafine and nanosized materials generated naturally. Some of the anthropogenic activities also lead to generation of nanomaterials unintentionally, for example, carbon black, platinum and rhodium nanoparticles from combustion byproducts, etc, (Nowack and Bucheli 2007). Nanomaterials are now being generated for various industrial and consumer applications. Metal and carbon based NPs are being explored in biological sciences including applications for biosensing, cellular imaging, drug/DNA delivery and cancer therapeutics (Hirsch *et al.,* 2003; Ma *et al.,* 2009; Nam *et al.,* 2003; Tkachenko *et al.,* 2003; Wu *et al.,* 2009). In such a scenario evaluating and understanding their effects is of utmost importance. It is well understood that the ultrafine particulate materials pose potential health hazards causing inflammation and autoimmune diseases (Oberdoster *et al.,* 2000, HEI review panel on ultrafine particles 2013). So it would be important also to evaluate the potential side effects of other engineered nanomaterials.

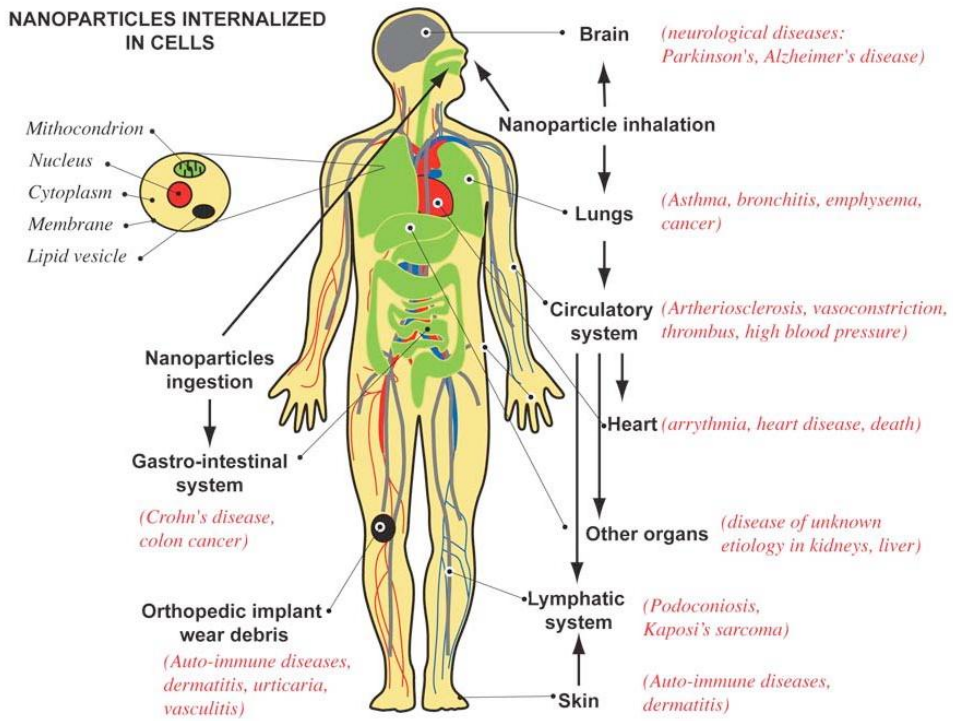

Figure 5. Modes of entry of nanoparticles and their cellular interaction
(Source: Biointerfaces volume 2)

Nanosize preparations of silver have been shown to retain antibacterial properties inherent of Ag salt solutions, a feature that has made nanosilver a promising candidate in various biomedical applications (Alt *et al.*, 2004). However, nanosilver's potential toxic effects need to be evaluated to assure the safety. Silver nanoparticles have been studied in various cell lines for their toxicological potential. Hussain *et al.*, (2005) reported the cytotoxicity of nanosilver (Ag 15 nm, 100 nm) in rat liver derived BRL3A cell line. The results in their study showed the toxicity range of nanosilver between 5-50 µg/ml, which they stated, was much lesser concentration that can induce toxicity in comparison to the other studies nanomaterials ie., iron oxide, manganese oxide, titanium oxide and aluminum nanoparticles. The effect of 7-20 nm sized silver

nanoparticles on human fibrosarcoma (HT1080) and human skin carcinoma (A431) cell lines has been studied and was reported that silver nanoparticles induced oxidative stress and induced apoptotic effects at higher doses but the lower doses that are generally used for antimicrobial action, did not have much effects (Arora *et al.,* 2008). Liu *et al.,* (2009) studied the interactions of nanosilver and BSA, where they reported the structural changes brought about by nanosilver. Their results depict that nanoparticles can interact with various proteins and bio-molecules causing alterations in their structure and function. In another study authors report that the cytotoxic effect of nanosilver varied with the surface charge, capping agent used and agglomeration of the particles (Suresh *et al.,* 2012). Asare *et al.,* (2012) have conducted a study on the primary mouse testicular cells with silver 20 and 200 nm nanoparticles and titanium oxide (TiO_2) 21 nm nanoparticles, where they found that the both nanoparticles had cytotoxic effects and also induce DNA damage. A study conducted on the human lung fibroblasts (IMR90) and human glioblastoma cells (U251) showed that the silver nanoparticles induced cytotoxicity and DNA damage (Asharani *et al.,* 2009). The authors also suggest that the observed DNA damage and cell cycle arrest could be because of the ROS generation and interruption of ATP synthesis. Silver nanoparticles have also been shown to have toxicity to aquatic organisms such as zebrafish (Asharani *et al.,* 2008), Japanese medaka (Chea *et al.,* 2009), and rainbow trout (Scown *et al.,* 2010).

Similarly, aluminum, the most abundant neurotoxic metal implicated in the etiology of several neurodegenerative disorders, is shown to induce pro-inflammatory and pro-apoptotic signaling effects (Walter *et al.,* 2005). Aluminium nanoparticles were found to be more cytotoxic compared to aluminium oxide nanoparticles. The cytotoxic effects that were observed were dose dependent and not size or surface area dependent (Wagner *et al.,* 2007). Aluminium oxide nanoparticles are also shown to induce mitochondrial oxidative stress and also change the expression of antioxidant enzymes in human mesenchymal stem cells (Alshathwi *et al.,* 2013). Oral exposure of alumina nanoparticles in mice was reported to show moderate toxicity in brain (Park *et al.,* 2011). They were also shown to decrease the expression of tight junction proteins in brain vasculature (Chen *et al.,* 2008). Tight junctions are essential for maintenance of endothelium and prevent paracellular transfer of substances from blood to the brain. Balasubramanyam *et al.,* (2009) reported the genotoxic effects of alumina nanoparticles. Nanoalumina particles are also reported to cause toxicity to algae (Pakrashi *et al.,* 2013) and retard the growth and development of N*icotiana tabacum* seedlings (Burklew *et al.,* 2012).

Although carbon based NPs are used in various industrial applications and also are highly employed in biomedical applications, they have also been reported to demonstrate some undesirable effects, including ROS generation and inflammatory responses (Koike and Kobayashi, 2006; Tian *et al.,* 2006). The induction of pro-inflammatory mediators like Interleukin 6 (IL-6), Tumor necrosis

factor (TNF-α) and Cyclooxygenase (COX-2) by titanium dioxide and silica NPs has recently been reported (Park and Park 2009; Xu *et al.,* 2009). Gold NPs, on the other hand, are proven to be non-cytotoxic, due to reduced production of reactive oxygen/nitrogen species, and pro-inflammatory cytokines, making them suitable candidates for nanomedicine (Shukla *et al.,* 2005). Many studies have focused on using various NPs for targeted drug delivery to cells and for visualizing intracellular processes (Panyam and Labhasetwar, 2003; Pitsillides *et al.,* 2003). These studies investigated NPs uptake by cells but did not address in detail on their potential toxic effects and the molecular mechanisms involved.

The foregoing studies clearly indicate ever growing increase in the application of nanoparticles in various biomedical, industrial, cosmetic and agricultural fields. As a result there is a possibility of exposure of animals and man to the nanoparticles directly or indirectly. In view of the reported undesirable side effects of many of these nanoparticles, there is need for evaluation of the potential toxic side effects before their application.

Biological systems respond to the exposure of foreign substances by various mechanisms, mainly aimed at detoxification and their elimination, a process termed as inflammation. In the present study the inflammatory responses of macrophages and cytotoxic effects on hiPSCs exposed to various NPs were evaluated *in vitro*. In addition studies were undertaken to evaluate the effects of NPs *in vivo* on mice.

Chapter 1

Biocompatibility of nanoparticles in vitro: Inflammatory responses of RAW 264.7 macrophages as a model assay

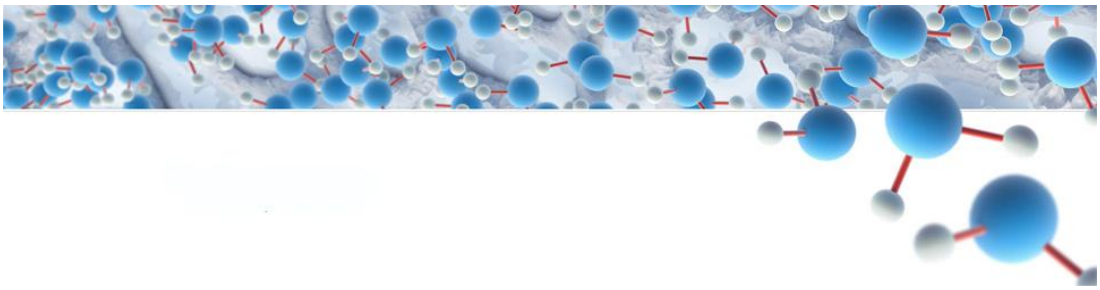

1.1. Introduction

Recent advances in particle-forming nanotechnology provided significant concern regarding their biological effects. Nanoparticles have considerably larger surface area than coarse particles, and may exhibit an associated greater propensity to produce oxidative stress and inflammatory response.

1.1.1. Inflammation

Inflammation is the body's immediate response to the damage of its tissues and cells. It is part of the innate immune system of the body and can be defined as the reaction of vascularized living tissues to local injury caused by noxious stimuli such as chemicals, biological agents such as pathogens or physical injury. It is a protective response of the organism in order to remove the injurious/foreign agent from the body. It is a complex interplay of various cellular and particulate mediators that help eliminate the noxious stimulus and clean up all the dead and dying cells in the injured region (Haworth & Levy, 2007).

Inflammation is characterized by the five basic features as described by Celus, redness (rubor), swelling (tumour), heat (calor), pain (dolor) and loss of function (functio leasa). These features of inflammation are due to vasodialtion, oedema or swelling and infiltration of fluids and cells in the affected area. Inflammation could be acute or chronic; acute inflammation is

short duration effect that lasts from a few minutes to a few days and gets resolved. Chronic inflammation lasts for few weeks, months or even years. It is the constant effort of the body to combat any pathogen or noxious foreign stimulus. Chronic inflammation is the major cause of concern in various pathologies including cancer, and is now considered one of the seven hallmarks of cancer.

1.1.2. Mediators of Inflammation

Inflammation is a complex interplay of cellular as well as particulate mediators (Roit, 1997). The cellular mediators include the macrophages/monocytes, neutrophils, T and B lymphocytes. Macrophages are generally a population of ubiquitously distributed mononuclear phagocytes responsible for numerous homeostatic, immunological, and inflammatory processes. Their primary function is to act as scavengers, roaming and engulfing foreign and potentially dangerous pathogens/materials. They are important producers of arachidonic acid and its metabolites. Upon phagocytosis macrophages release up to 50% of their arachidonic acid from membranous esterified glycerol phospholipids that is metabolized to prostaglandins and leukotrienes (Scott *et al.*, 1980). These mediators produced by the macrophages perpetuate the inflammatory reaction. So, macrophages play a very crucial role in mounting the inflammatory response to any foreign/toxic substances.

The particulate mediators of inflammation include plasma proteins, lipid mediators, cytokines and chemokines. Plasma proteins include the complement system proteins, kinins and the clotting factors. Cytokines for example are the interleukins, tumor necrotic factors and interferons. The lipid mediators are products derived from arachidonic acid (AA), synthesized by the Cyclooxygenases (COXs) and lipoxygenases (LOXs), collectively termed as eicosanoids.

1.1.3. Inflammation and Oxidative Stress

Reactive oxygen species (ROS) refer to chemically reactive oxygen and includes a variety of partially reduced metabolites of oxygen [e.g., superoxide anions (O2.-), hydroxyl radical (OH.) and hydrogen peroxide (H_2O_2)], possessing higher reactivities than molecular oxygen (Thannickal and Fanburg, 2000). A variety of processes, such as aerobic metabolism or second messengers in various signal transduction pathways lead to generation of ROS as by-product . Around 1-5% of oxygen consumed is converted to ROS. Due to the unpaired electron that reactive oxygen species have, they are extremely reactive and unstable; and in order to achieve a stable configuration they react with other molecules present in the cellular milieu. ROS can oxidize all the macromolecules in the cell including nucleic acids, which can lead to mutations (Floyd *et al.*, 2001). ROS generation is largely increased during inflammation due increased metabolic rate, locally

activated macrophages and other leukocytes, increased pressure in the inflammatory site due to edema (Whiteman *et al.,* 2002; Greenacre *et al.,* 2002). The levels of ROS are carefully controlled in normal physiological conditions by the enzymatic and non-enzymatic antioxidants present in the cells. But in inflammatory conditions this balance is lost due to increased levels of ROS, leading to a net oxidative stress (Gediminas *et al.,* 2002). This oxidative stress not only amplifies the inflammatory reaction but also tends to push the system towards other pathological conditions such as cancers (Whiteman *et al.,* 2002).

1.1.4. Role of Cyclooxygenase in Inflammation

Arachidonic acid, the most predominant polyunsaturated fatty acid in mammalian systems, is mainly acted upon by Cyclooxygenase (COX) and Lipoxygenase (LOX) pathways, which lead to the formation of prostaglandins (PGs) and leukotrienes respectively. These are potent biologically active compounds which play a key role in the initiation, progression and resolution of inflammation. Cyclooxygenase or prostaglandin H_2 synthase is the enzyme that catalyzes the biosynthesis of prostaglandins from the substrate arachidonic acid. COX-2 gene is an 'immediate early gene' that is not always present but is highly up regulated during pathological processes or inflammation. Cyclooxygenase-2, the inducible isoform of COX, is induced by several mitogenic and pro-

inflammatory stimuli including LPS, interleukin-1α (IL-1α) and IL-1β and tumor necrosis factor-α) (Diaz *et al.,* 1998; Reddy *et al.,* 2003). TNF-α is a pleiotropic cytokine primarily produced by activated macrophages and T lymphocytes that is known to stimulate COX-2 gene expression (Nakao *et al.,* 2002). Several studies have reported on the induction of COX-2 in different types of human cancers (Harris 2009). Increased expression of COX-2 has also been demonstrated in animal models and in human inflammatory bowel disease (Hendel and Nielsen 1997). This marked increase in COX-2 expression during various inflammatory processes reveals its key role in inflammation and hence is being used as a marker of progressive inflammatory processes.

1.1.5. Nanoparticles and Inflammation

The unique physicochemical properties of nanoparticles can produce chemical conditions to induce a pro-oxidant environment in the cells, causing an imbalance in the cellular energy system dependent redox potential and thereby leading to adverse biological consequences, ranging from the initiation of inflammatory pathways to cell death (Carlson et al 2008, Hsin et al 2008). Many studies have demonstrated the ability of nanoparticles to generate ROS in a cell-free environment (Brown et al 2001, Stone et al 1998). This oxidative stress may be linked to the induction of signaling pathways (Stone et al 2000) which lead to pro-inflammatory gene

expression in macrophages (Brown et al 2004). Regulation of COX-2 expression by single-walled carbon nanotubes and titanium dioxide NPs in macrophages and transgenic mouse fibroblast cells, respectively, has also been reported recently (Dutta *et al.,* 2007; Xu *et al.,* 2009). Similarly increased mRNA expression of inflammation-related genes like IL-1, IL-6, TNF-α, inducible nitric oxide synthase (iNOS), and COX-2 was observed in the cultured peritoneal macrophages of mice treated with silica NPs (Park and Park 2009). CB and silica NPs were known to induce the activation of NF-κB in A549 lung epithelial cells (Mroz *et al.,* 2007) and macrophages (Rojanasakul *et al.,* 1999) respectively. As macrophages are the front line of cells mounting inflammatory response to any foreign substances, the present study is taken up to evaluate the biocompatibility of nanoparticles on macrophages. The specific objectives of the study are:

- To evaluate the effects of size and duration of exposure of NPs such as silver, aluminum, carbon black, carbon coated silver and gold on the inflammatory responses, by employing RAW 264.7 mouse macrophage cell line.
- Understanding the role of ROS-NF-κB mediated expression of pro-inflammatory genes like TNF-α, IL-6 and COX-2 upon exposure to the nanoparticles.

1.2. Materials and Methods

1.2.1. Materials

i. Chemicals

Phosphate buffered saline (PBS), RPMI 1640, Fetal Bovine Serum (FBS), Penicillin and Streptomycin were purchased from Gibco BRL (California, USA). *Escherichia coli* lipopolysaccharide (LPS), Trypsin-EDTA, 2′,7′,-dichlorofluorescin diacetate (DCFH-DA), TMB (3,3′, 5,5′-tetramethylbenzidine)/H_2O_2 , Protease Inhibitor Cocktail and β-actin antibodies were purchased from Sigma–Aldrich company (Bangalore, India). Monoclonal antibodies of COX-2 and TNF-α were purchased from Santa Cruz Biotechnology, Inc., (CA, U.S.A). All the other chemicals and reagents were purchased from local companies and are of molecular biology grade. Ultra pure DI-water was prepared using a Milli-Q system (Millipore, Bangalore, India).

ii. Nanoparticles

Silver (Ag15 nm), nanoparticles were obtained from the Air Force Research Laboratory, Brooks AFB, TX. Silver (Ag; 10nm, 40 nm, 80nm), Aluminum nanoparticles (Al; 20 nm, 50 nm), carbon black (CB; 20 nm, 40 nm), and carbon coated silver (CAg 25 nm, 45 nm) were obtained from Nanocomposix (USA), Gold nanoparticles (Au; 20 nm, 40 nm, 80nm) were

prepared from Gold (III) chloride trihydrate (Sutherland and Winefordner, 1992), procured from Sigma (St Louis, MO).

1.2.2. Characterization and Dispersion of Nanomaterials in Solution

The size and shape of nanoparticles were confirmed by Dynamic Light Scattering (DLS) and Transmission Electron Microscopy (TEM). The dispersion test was conducted in phosphate buffer saline (PBS) or deionized water. Based on the success of homogeneous dispersion using physical mixing and sonication, stock solutions (100-1000 µg/ml) were prepared either in PBS or deionized water. The size (hydrodynamic diameter, nm) of NPs was determined by DLS from intensity size distribution. TEM samples were prepared by placing a drop of dispersed NPs solution, directly on a copper grid, and imaging was done at 100 – 200 kV. The freshly dispersed particles were then diluted to appropriate concentrations in cell culture medium and immediately applied to the cells. The zeta potential of the NPs dispersed in culture medium was obtained by using a dip cell (Nano ZS, Malvern) placed in the sizing cuvette, at 25^0C. Zeta potential average values were obtained from three independent experiments at similar conditions. The NPs dispersions were also tested for LPS contamination using the Chromo Limulus Amebocyte lysate (LAL) chromogenic kinetic assay as per the instructions in the user's manual provided with the kit.

1.2.3. Cell Culture and Nanoparticles Treatment

RAW 264.7 cells, derived from murine macrophages, were obtained from National Center for Cellular Sciences (NCCS), Pune, India. The cell line was maintained in a humidified atmosphere with 5% CO_2 at 37 °C. Medium used for culturing the cells was RPMI-1640 supplemented with 10% heat inactivated fetal bovine serum (FBS), 100 IU/ml penicillin, 100 µg/ml streptomycin and 2 mM L-glutamine. The cells were treated with graded doses of Ag, Al, CB, CAg and Au NPs and durations designated in the following study.

1.2.4. Cell Viability (MTT assay) and Cell Morphology

Mitochondrial function was determined spectrophotometrically by measuring the reduction of tetrazolium salt 3-(4,5-dimethylthiazol-2-yl)-2,5-diphenyltetrazolium bromide (MTT) to (aqueous insoluble product) formazan by succinic dehydrogenase (Carmichael et al.1987) with minor modification as described elsewhere (Hussain and Frazier 2002). Cells were seeded onto 96-well culture plates at 8×10^3 cells per well and permitted to adhere overnight at 37 ◦C. When cells reached 60% confluency, the spent medium along with the non adherent cells was removed and 150 µl fresh medium containing Ag, Al, CB, CAg and Au NPs at different concentrations (1-150 µg/ml) was added. After incubation with NPs for

various time points such as 6h, 12h, 24h, 48h, 72h, cells were treated with 20 µl of MTT solution (5 mg/ml) incubated for 3 h at 37 ◦C. Cells were treated with 100 µl of dimethylsulfoxide (DMSO) and absorbance was quantified at 570 nm using the microplate spectrophotometer system. All experiments were performed at least in triplicate on three separate occasions. Cells not exposed to the NPs served as controls in each experiment. After incubation of the cells with nanoparticles for 48h, cell morphology was assessed with a Nikon Eclipse TS-100 phase-contrast inverted microscope.

1.2.5. Localization of NPs (TEM Analysis)

RAW264.7 macrophage cells were seeded in 6 well plates and grown overnight. The cells were exposed to 5 µg/ml of various NPs for 48 h. After the specified incubation time, cells were washed thoroughly with chilled PBS, pelleted by centrifugation, and fixed with 2.5% glutaraldehyde in 0.05M phosphate buffer (pH 7.2) for 24 hrs at 4 °C and post fixed with 2% aqueous Osmium tetraoxide in the same buffer for 2 hrs. After the fixation samples were dehydrated in a series of graded acetone and infiltrated and embedded in Araldite 6005. Ultrathin sections (50-70 nm) were cut with a glass knife on a Leica Ultra cut (UCT-GA-D/E-1/00) microtome and mounted on grids and stained with saturated aqueous Uranyl acetate, counter stained with 4% lead citrate, and observed under FEI Tecnai G^2 S-Twin TEM.

1.2.6. Measurement of Intracellular ROS

The production of intracellular ROS was measured using 2',7',-dichlorofluorescin diacetate (DCFH-DA) (34). This hydrophobic non-fluorescent molecule penetrates rapidly into the cell and is hydrolyzed by intracellular esterases to give the dichlorofluorescin (DCFH) molecule which can be oxidized to its fluorescent 2-electron product 2',7',-dichlorofluorescein (DCF). Briefly, 10mM DCFHDA stock solution (in methanol) was diluted 500-fold in HBSS without serum or other additive to yield a 20μM working solution of DCFH-DA. After 24 h exposure to nanoparticles, the cells in 24-well plate were washed twice with HBSS and then incubated in 2 ml working solution of DCFH-DA at 37^{o}C for 30 min. The dye loaded samples were centrifuged at 12,500 x g for 10 min at 4^{o}C. The fluorescence measurements were performed on a Hitachi spectrofluorimeter at 485 nm excitation and 520 nm emission wave lengths. Cell-free experiments with and without nanoparticles were also conducted to determine whether there was any possible generation of ROS by direct interaction of nanoparticles. The levels are represented as fold increase or decrease from control group.

1.2.7. Reverse-Transcription PCR Analysis

RAW 264.7 cells were seeded at a density of 5 x 10^{6} in 90 mm culture dishes. Cells were treated with different NPs (5 μg/ml) for 6 h, 12 h, and 24

h. Cells were harvested and the total RNA from control and treated cells was extracted using TRI reagent. cDNA was synthesized using oligo (dT), dNTP mixture, RevertAid H Minus M-MuLV Reverse Transcriptase. A 2 µl aliquot of the 20 µl total cDNA was used for standard PCR reaction of 28 cycles using the COX-2 and TNF-α primer set Table 1.1 below.

Table 1.1 List of primers used for RT-PCR analysis

Target Gene	Primer Sequnce	Orientation	Length (bp)	Annealing Temp (°C)
COX-2	5′TGTGGGGCAGGAGGTCTTTGGTCT3′ 5′GCATCTGGCCGAGGCTTTTCTAC 3′	Sense Antisense	690	58 °C
TNF-α	5′ CAAGGAGGAGAAGTTCCCAA 3′ 5′ CGGACTCCGTGATGTCTAAG 3′	Sense Antisense	500	54°C
GAPDH	5'CTCATGACCACAGTCCATGCCATC3' 5'-CTGCTTCACCACCTTCTTGATGTC-3'	Sense Antisense	272	54°C

The PCR products were visualized on 1% agarose gels with ethidium bromide, under UV light. The GAPDH primers served as control.

1.2.8. Preparation of Whole Cell Extracts and Immunoblot Analysis

To prepare the whole cell extract, cells were washed with PBS and suspended in a lysis buffer (20 mM Tris, 1 mM EDTA, 150 mM NaCl, 1% NP-40, 0.5% sodium deoxy cholate, 1 mM β-glycerophosphate, 1 mM

sodium orthovanadate, 1 mM PMSF, 10 µg/ml leupeptin, 20 µg/ml aprotinin). After 30 min of shaking at 4 °C, the mixtures were centrifuged (10,000xg) for 10 min, and the supernatants were collected as the whole-cell extracts. The protein content was determined according to the Bradford method. An equal amount of total cell lysate was resolved on 8-12% SDS-PAGE gels along with protein molecular weight standards, and then transferred onto nitrocellulose membranes. Membranes were stained with 0.5% Ponceau *S* in 1% acetic acid to check the transfer. The membranes were blocked with 5% w/v nonfat dry milk and then incubated with the primary antibodies (for COX-2 and TNF-α) in 10 ml of antibody-diluted buffer (1X Tris-buffered saline and 0.05% Tween-20 with 5% milk) with gentle shaking at 4 °C for 8-12 h and then incubated with peroxidase conjugated secondary antibodies. Signals were detected by using peroxidase substrate TMB/H_2O_2. The blots were probed with β -actin antibodies to confirm equal loading.

1.2.9. Analysis of Proinflammatory Cytokine: IL-6

Quantitative determination of the IL-6 in the culture medium from nanoparticles exposed RAW 264.7 cells was performed using sandwich ELISA. The analyses were performed according to the manufacturer's instructions. Increase in colour intensity was quantified using an ELISA plate reader.

1.2.10. Preparation of nuclear extracts for NF-kB estimation

The cells were treated with or without 10 mM NAC and exposed to NPs and LPS. To prepare the nuclear extracts for ELISA of NF-kB, the cells were washed twice with cold PBS, lysed in 350 ml of cold buffer A [HEPES 10 mM pH 7.9, KCl 10 mM, EDTA 1 mM, EGTA 1 mM, dithiothreitol (DTT) 1 mM, aprotinin 1 mg/l, leu-peptin 1 mg/l, and pepstatin A 1 mg/l]. After 15 min incubation on ice, 0.1% NP-40 was added to the homogenates and the contents were mixed vigorously for 1 min. Then, the homogenates were centrifuged (10,000*g*, 5 min) at 4°C. The supernatant (cyto-plasmic extracts) was collected and stored in aliquots at 70°C. The nuclear pellets were washed once with cold buffer A, then suspended in 50 ml of cold buffer B (HEPES 20 mM, pH 7.9, NaCl 420 mM, EDTA 1 mM, EGTA 1 mM, DTT 1 mM, aprotinin 1 mg/l, leupeptin 1 mg/l, and pepstatin A 1 mg/l) and mixed vigorously by intermittent vortexing for 45 min. This was then centrifuged at 10,000 *g* for 5 min, and the supernatant (nuclear extract) was used for NF-kBp65 immunoassay. The NF-kB activation and translocation was determined by immuno kit assay (according to the manufacturer's instructions).

1.2.11. Statistical Analysis

All experiments were done in triplicate, unless otherwise stated, and the results were presented as mean ± standard deviation. Statistical analysis of differences was carried out by one-way analysis of variance (ANOVA). A *P*-value of less than 0.05 was considered to indicate significance.

1.3. Results

1.3.1. Characterization and Dispersion of Nanoparticles

TEM and DLS analysis were employed to assess shape and particle size distribution of all the NPs. These studies showed fine dispersion of NPs, ranging in their specified sizes as shown in Figure 1.1. Silver-15 ± 3 nm, 40 ± 4 nm; Aluminium-20 ± 4 nm, 50 ± 5 nm; Carbon black-20 ± 6 nm, 40 ± 6nm and Gold-20 ± 3 nm, 40 ± 4 nm NPs are discoid or spherical. The Carbon coated silver-25 ± 6 nm, 45 ± 7 nm in the cluster were loosely arranged and individual NPs showed dumbbell or spherical characteristics. The size distribution of NPs was determined by DLS and the dispersion of the NPs was analyzed by zeta potential (Table 1.2).

Table 1.2. Zeta potential and size distribution of nanoparticles*

S.No.	Type of Nanoparticle	Zeta potential (mV)	Size (nm) #
1.	Silver (15nm)	-39.5 ± 3.5	15 ± 3
2.	Silver (40nm)	-34.5 ± 3.7	40 ± 4
3.	Aluminum (20nm)	-33.5 ± 2.8	20 ± 4
4.	Aluminum (50nm)	-28.4 ± 2.6	50 ± 5
5.	Carbon black (20nm)	-25.0 ± 2.3	20 ± 6
6.	Carbon black (40nm)	-27.4 ± 2.1	40 ± 6
7.	Carbon coated Ag (25nm)	-29.2 ± 2.7	25 ± 6
8.	Carbon coated Ag (45nm)	-27.8 ± 2.1	45 ± 7
9.	Gold (20nm)	-37.5 ± 2.0	20 ± 3
10.	Gold (40nm)	-41.1 ± 3.8	40 ± 4

#Hydrodynamic diameter (size, nm) of NPs was determined from intensity size distributions.
*Each value represents the mean ± SD (n=3).

The average zeta potential of various NPs was in the range of -20mV to -40mV. The surface charge of all the NPs employed in the present study was consistently negative.

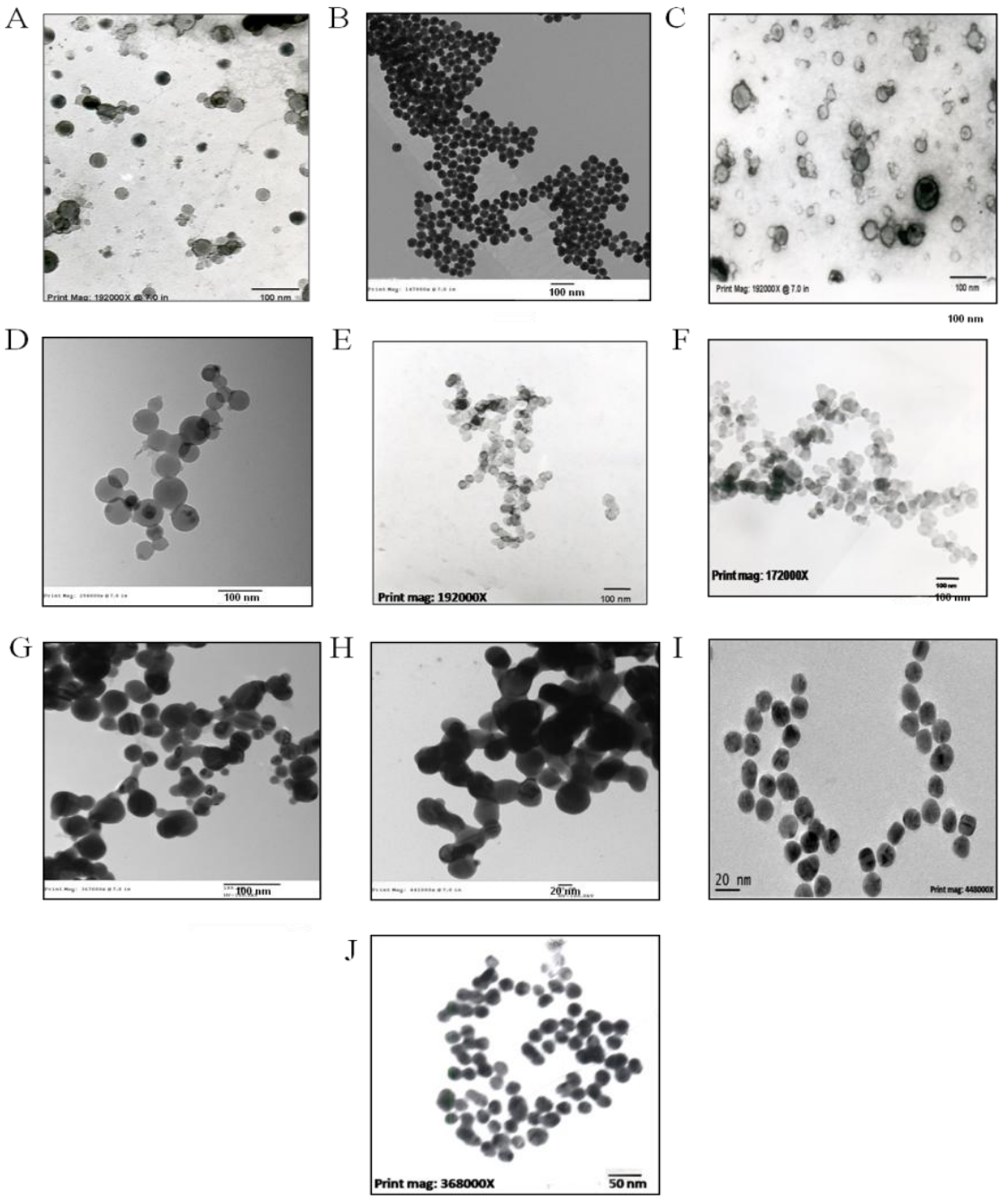

Figure 1.1. Transmission electron micrographs of nanoparticles: A and B, Silver NPs (Ag-15 nm and 40 nm); C and D, Aluminum NPs (Al-20 nm and 50 nm); E and F, Carbon black NPs (CB-20 nm and 40 nm); G and H, Carbon coated silver NPs (CAg-25 nm and 45 nm); I and J, Gold NPs (Au-20 nm and 40 nm).

1.3.2. Effect of Nanoparticles on Cell Viability

To determine an effective concentration range, we tested the effects of dosage (1 – 50 µg/ml Ag, Al, CB, CAg NPs; 1- 200 µg/ml Au NPs) and duration of exposure (6 h – 72 h) of NPs on RAW 264.7 cells using MTT assay. Cell viability by MTT assay after 48 h NPs exposure is shown in Table 1.3. After determining the EC_{50} of all NPs a fixed concentration of 5 µg/ml (less than half of the EC_{50} value) was employed for evaluating inflammatory responses. In addition, the morphology of the RAW 264.7 cells incubated with NPs (5 µg/ml) was observed under phase-contrast microscope (Figure 1.2).

Table 1.3. Cell viability of RAW264.7 cells upon exposure to nanoparticles*

S.No.	Type of nanoparticles	EC_{50} (µg/ml) #
1.	Silver 15 nm	14 ± 0.8
2.	Silver 40 nm	15 ± 1.0
3.	Aluminium 20 nm	15 ± 1.4
4.	Aluminium 50 nm	19.5 ± 1.8
5.	Carbon black 20 nm	20 ± 0.8
6.	Carbon black 40 nm	23 ± 1.2
7.	Carbon coated silver 25 nm	22 ± 1.4
8.	Carbon coated silver 45 nm	24 ± 1.8
9.	Gold 20 nm	91 ± 8.5
10.	Gold 40 nm	132 ± 11.4

These data are expressed as mean ± SD of five independent experiments.

* Each value represents the mean ± SD (n=5).

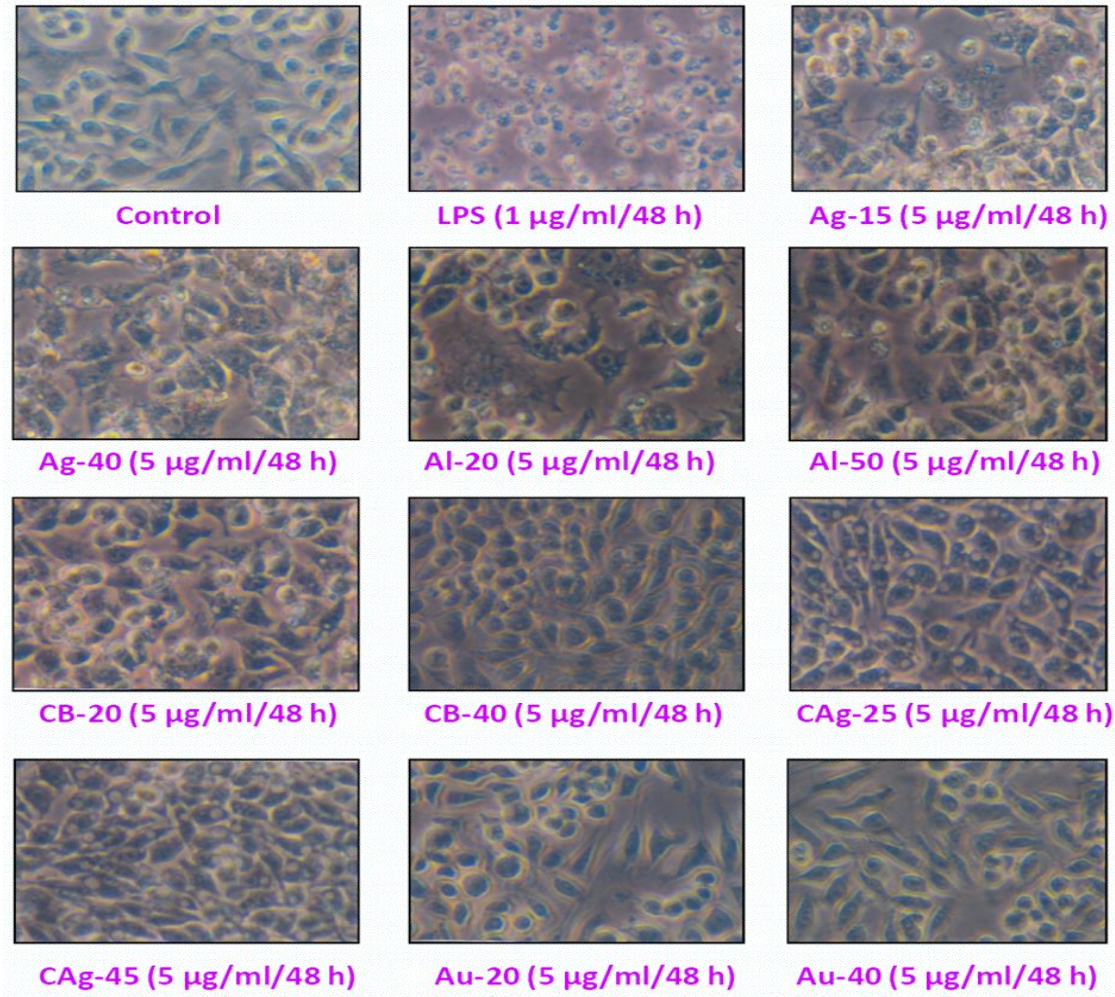

Figure 1.2. Phase contrast images of RAW 264.7 macrophage cells: Cells observed at 40X upon exposure to various nanoparticles at 5µg/ml for 48 hrs.

1.3.3. Localization of Nanoparticles

The transmission electron microscopic (TEM) micrographs have clearly indicated the intracellular localization of NPs. They were distinctly present in vacuoles, cytoplasm and even in the nucleus. Further the NPs were well dispersed within the cell, without any considerable aggregation (Figure 1.3).

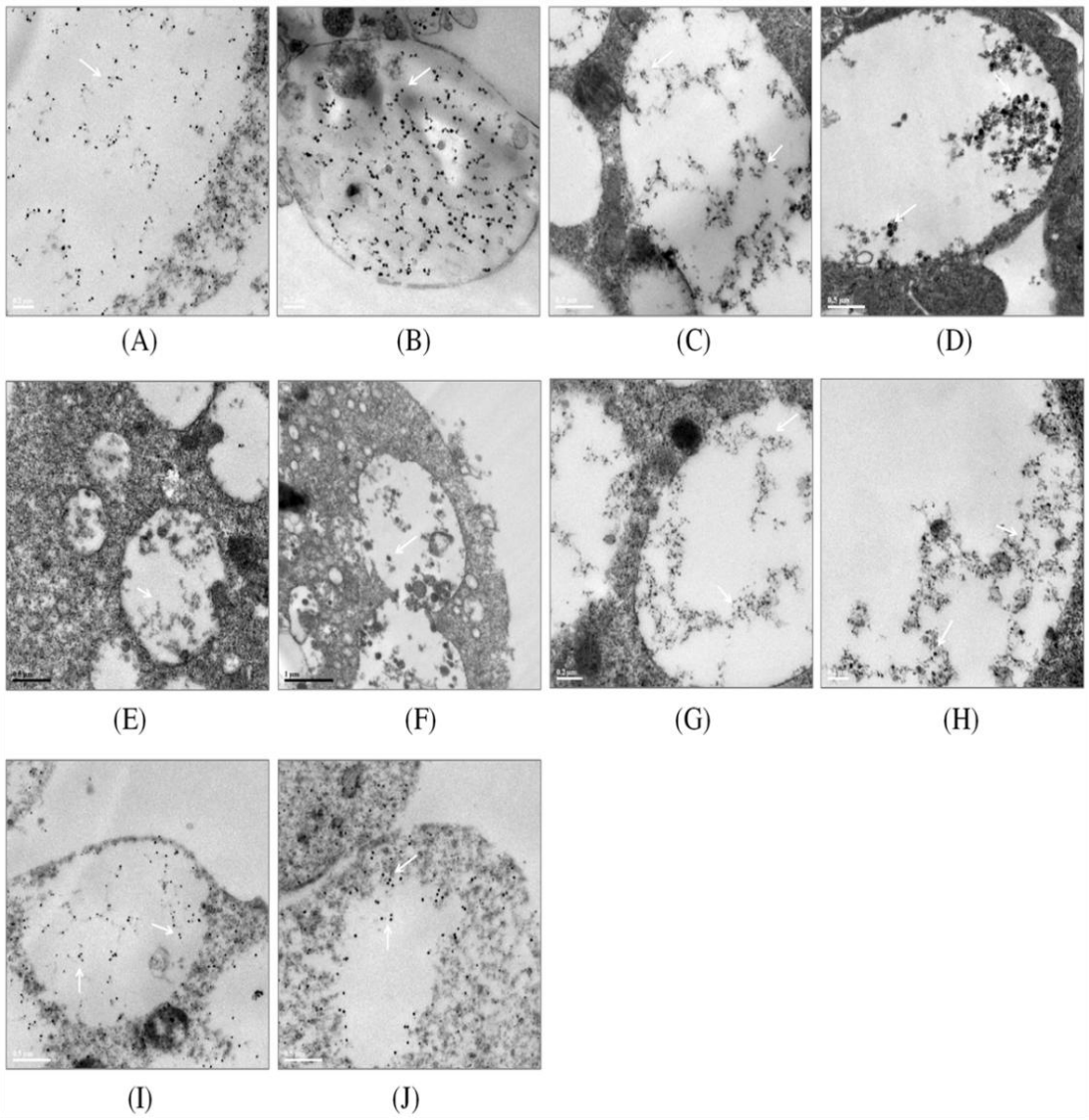

Figure 1.3. Transmission electron micrographs of RAW 264.7 cells upon exposure to nanoparticles: A and B, Silver NPs (Ag-15 nm and 40 nm); C and D, Aluminum NPs (Al-20 nm and 50 nm); E and F, Carbon black NPs (CB-20 nm and 40 nm); G and H, Carbon coated silver NPs (CAg-25 nm and 45 nm); I and J, Gold NPs (Au-20 nm and 40 nm).

1.3.4. Effect of Nanoparticles on Intracellular ROS

The mechanism underlying induction of inflammation by NPs may be through the generation of ROS. Therefore, we have measured the generation of ROS using DCFH-DA fluorescence in RAW 264.7 cells in

response to NPs (5 µg/ml) exposure (Figure 1.4). Exposure of macrophages to Ag-15 and Ag-40 NPs resulted in 3.80 ± 1.12 and 3.24 ± 0.98 fold increase in ROS generation, respectively, over control levels. Exposure to Al-20 and Al-50 NPs resulted in 3.12 ± 0.93 and 2.22 ± 0.85 fold increase in ROS generation, respectively. Similarly CB-20 and CB-40 particles showed 3.44 ± 1.12 and 3.10 ±1.04 fold higher ROS generation, respectively. Exposure of cells to CAg-25 and CAg-45 NPs showed 2.52 ± 0.76 and 2.12 ± 0.70 fold increase in the ROS generation, respectively. Incubation of macrophages to Au-20 and Au-40 NPs, however, resulted in 0.66 ± 0.12 and 0.73 ± 0.09 fold decrease in ROS generation over control macrophage levels.

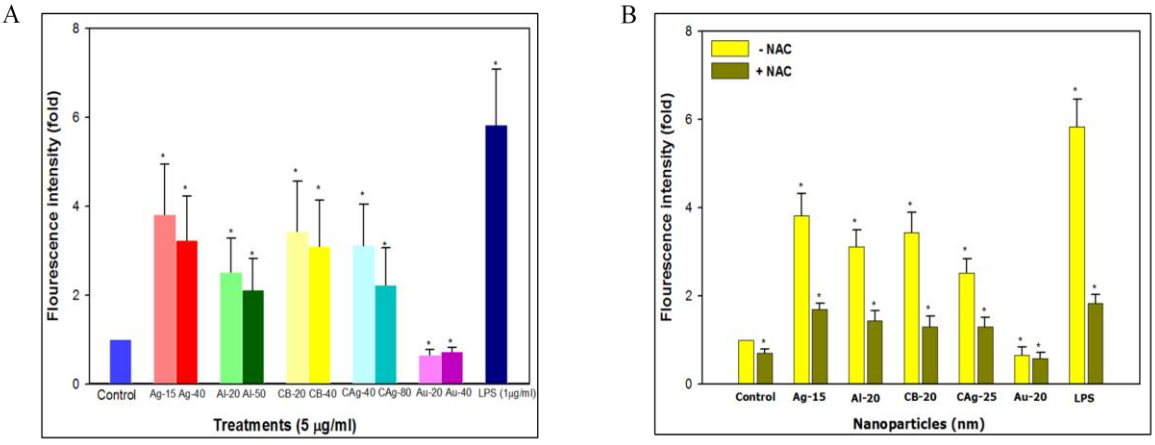

Cells treated with NPs *Cells treated with NPs + NAC*

*Figure 1.4. Effect of NPs on intracellular ROS generation: Cells were treated with 5 µg/ml of NPs (Ag-15, 40 nm; Al-20, 50 nm; CB-20, 40 nm; CAg-25, 45 nm and Au-20, 40 nm) and LPS at concentration of 1 µg/ml for 24h with and without NAC pretreatment. * Denotes statistical significance over untreated controls.*

Incubation of macrophages with LPS (1 µg/ml), a known strong ROS inducer in macrophage cell lineages, showed a drastic (5.83 ± 1.25 fold) increase in ROS generation. Pre-incubation of macrophages with a well-

known inhibitor of ROS, N-acetyl-L-cysteine (NAC), followed by exposure to NPs, resulted in a significant decrease in the ROS generation.

1.3.5. Effect of Nanoparticles on NF-κB Nuclear Translocation

NF-κB, a mammalian transcription factor is known to control the expression of cell survival genes as well as induction of pro-inflammatory enzymes and cytokines. In the present study, LPS and NPs induced nuclear translocation of NF-κB p65, as revealed by ELISA analyses (Figure 1.5).

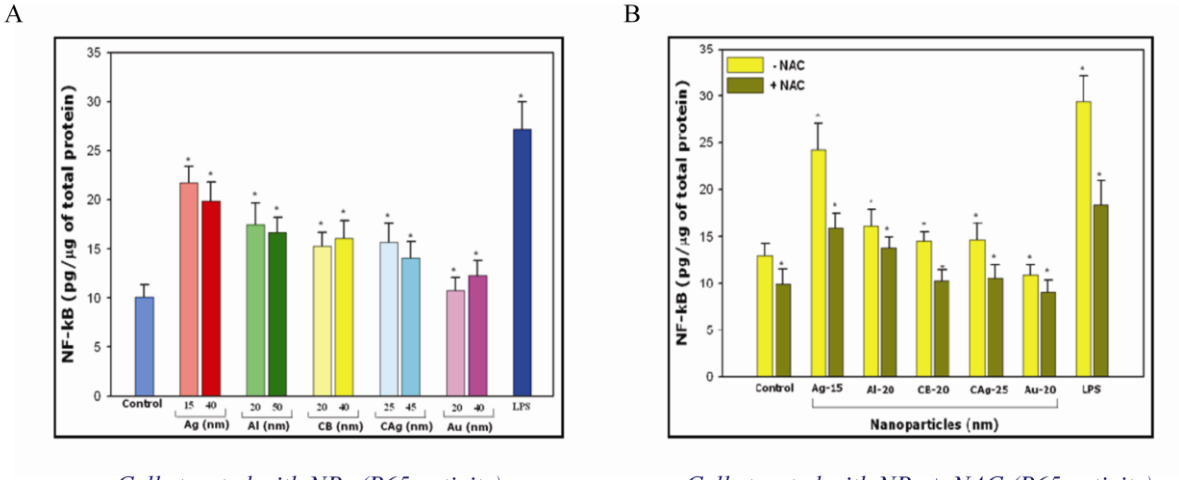

*Figure 1.5.ELISA analysis of NF-κB activity: (A) Cells were treated with 5 µg/ml of NPs (Ag-15, 40 nm; Al-20, 50 nm; CB-20, 40 nm; CAg-25, 45 nm and Au-20, 40 nm) and LPS at concentration of 1 µg/ml for 3h without NAC and (B) Cells were treated with 5 µg/ml of NPs (Ag-15nm; Al-20 nm; CB-20 nm; CAg-25 nm and Au-20 nm) and LPS at concentration of 1 µg/ml for 3h with and without NAC pretreatment and checked for NF-κB activity in the nuclear extracts. * Denotes statistical significance over untreated controls.*

Ag and Al NPs showed significant induction of NF-κB translocation, followed by CB and CAg NPs. The NF-κB activation induced by NPs and LPS was repressed by the treatment with NAC, a known antioxidant,

suggesting the role of ROS in NF-κB activation. Au NPs, on the other hand, showed lower activation of NF-κB in comparison to all other nanoparticles tested.

1.3.6. Effect of Nanoparticles on COX-2 and TNF-α mRNA and Protein Expression

To verify whether there is any pro-inflammatory effect of NPs on macrophages, the expression of COX-2, a major mediator of inflammation and TNF-α, a traditional cyclooxygenase-2 inducer were analyzed by RT-PCR and Western blot analysis. The results presented clearly suggest the induction of COX-2 and TNF-α gene expression in macrophages expressed to various NPs and LPS.

i. Induction of COX-2 and TNF- α with Ag and Al NPs: RAW 264.7 cells were exposed to Ag and Al NPs at a concentration of 5 µg/ml for 6-48 h, and the induction of COX-2 and TNF-α was monitored. A significant induction of COX-2 and TNF-α expression was observed with both Ag and Al NPs at mRNA (Figure 1.6A) and protein (Figure 1.6B) levels, which was dependent on the size of NPs and duration of exposure. While increase in the size of NPs showed a slight decrease in the induction of COX-2 and TNF-α, the increase in exposure time showed gradual increases in COX-2 and TNF-α mRNA and protein induction up to 24 h and 48 h observation, respectively.

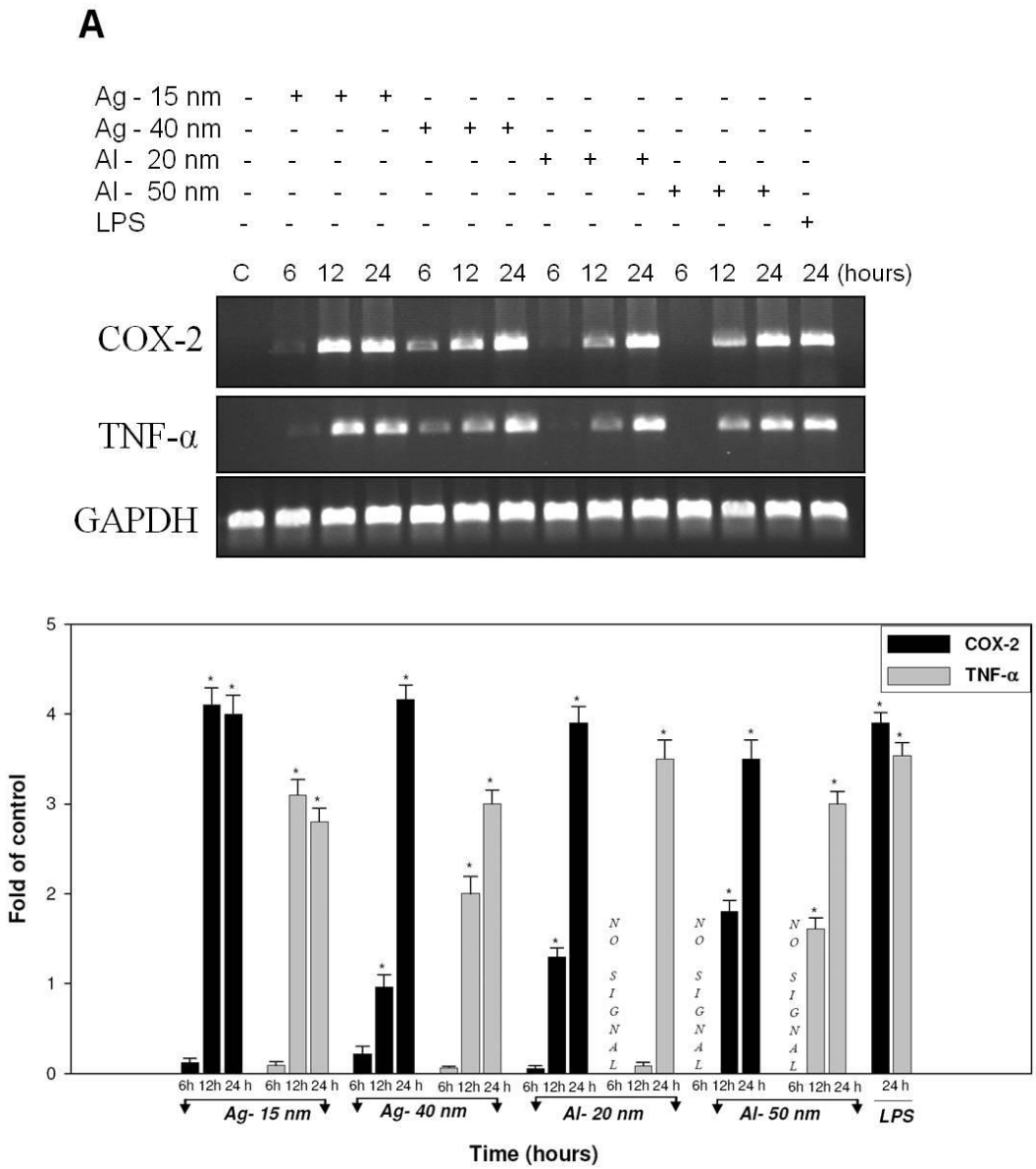

Figure 1.6A. Effect of Ag and Al NPs on RAW 264.7 cells: Cells were treated with 5 µg/ml Ag-15 nm, 40 nm and Al-20 nm, 50 nm nanoparticles. Total RNA was isolated at 6h, 12h and 24h after treatment and subjected to RT-PCR analysis using COX-2 and TNF-α specific primers as described in the methodology. GAPDH was used as an internal control. Bar graph represents densitometric values of COX-2 and TNF-α level.

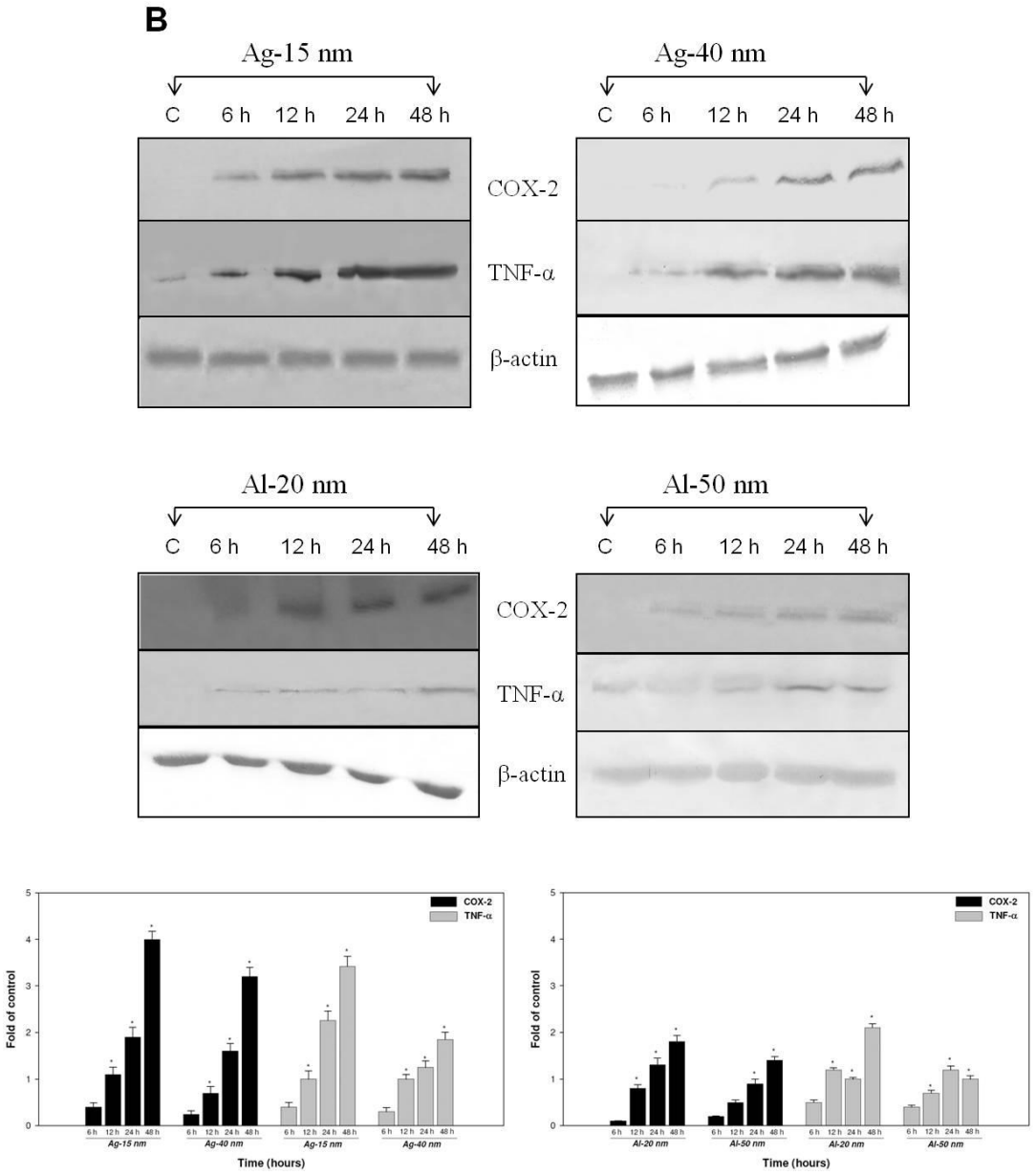

Figure 1.6B. Effect of Ag and Al NPs on RAW 264.7 cells: Cells were treated with 5 µg/ml Ag-15 nm, 40 nm and Al-20 nm, 50 nm nanoparticles. Aliquots of cell lysates prepared after 6-48h exposure were resolved by SDS-PAGE and analyzed for COX-2 and TNF-α protein expression by Western blotting. β-actin was used as an internal control to monitor equal loading. Bar graph represents densitometric values of COX-2 and TNF-α level.

ii. Stimulation of COX-2 and TNF-α with CB and CAg NPs: Induction of COX-2 and TNF-α was studied upon exposure of RAW cells to CB and CAg NPs. Since carbon NPs showed less toxicity or higher cell viability

compared to silver NPs, we checked if the carbon coating of the silver NPs would reduce the pro-inflammatory effects.

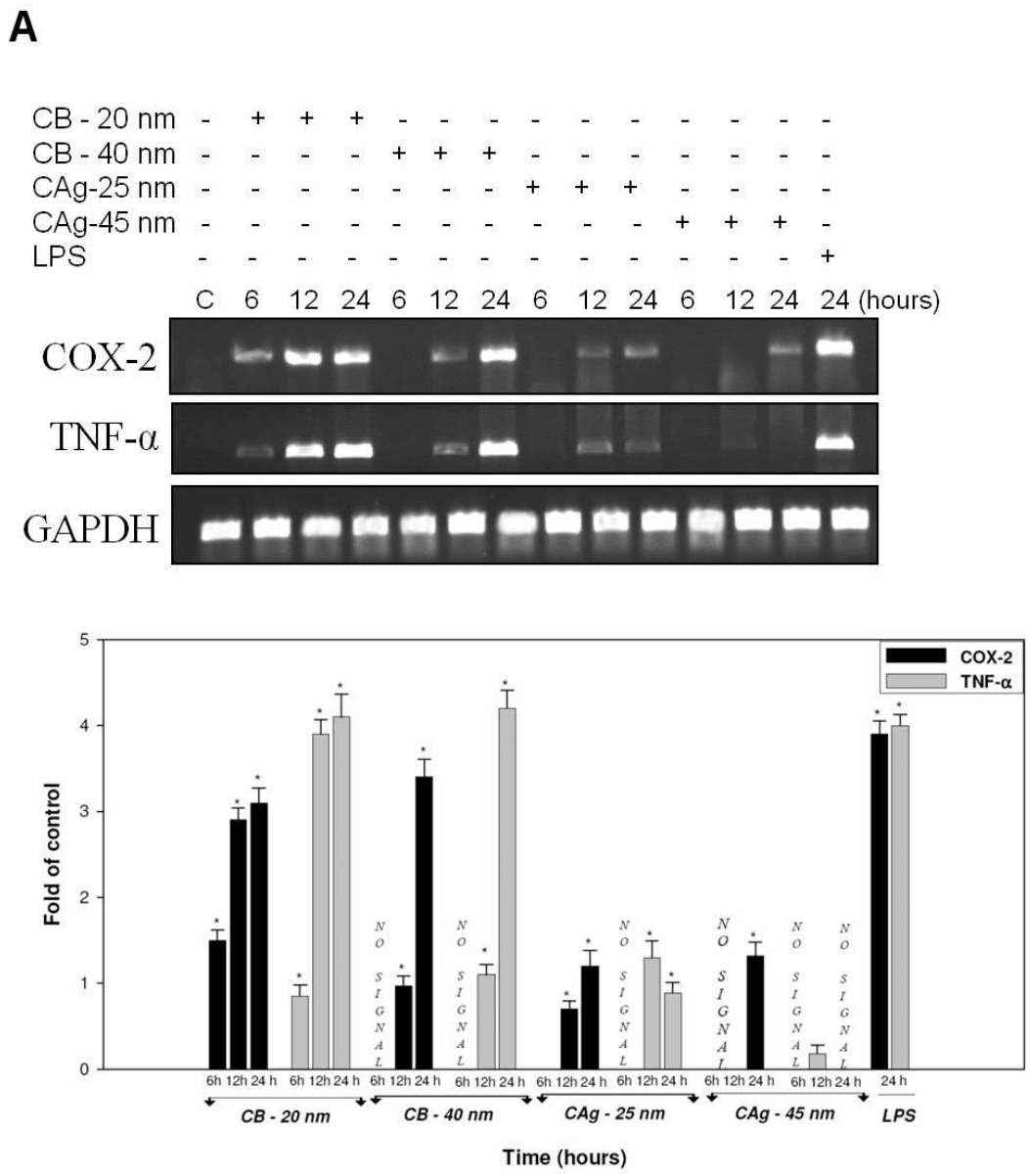

Figure 1.7A. Effect of CB and CAg NPs on RAW 264.7 cells: Cells were treated with 5 µg/ml CB-20 nm, 40 nm and CAg-25 nm, 45 nm nanoparticles. Total RNA was isolated after 6h, 12h and 24h of exposure and subjected to RT-PCR analysis using COX-2 and TNF-α specific primers as described in the methodology. GAPDH was used as an internal control. Bar graph represents densitometric values of COX-2 and TNF-α level.

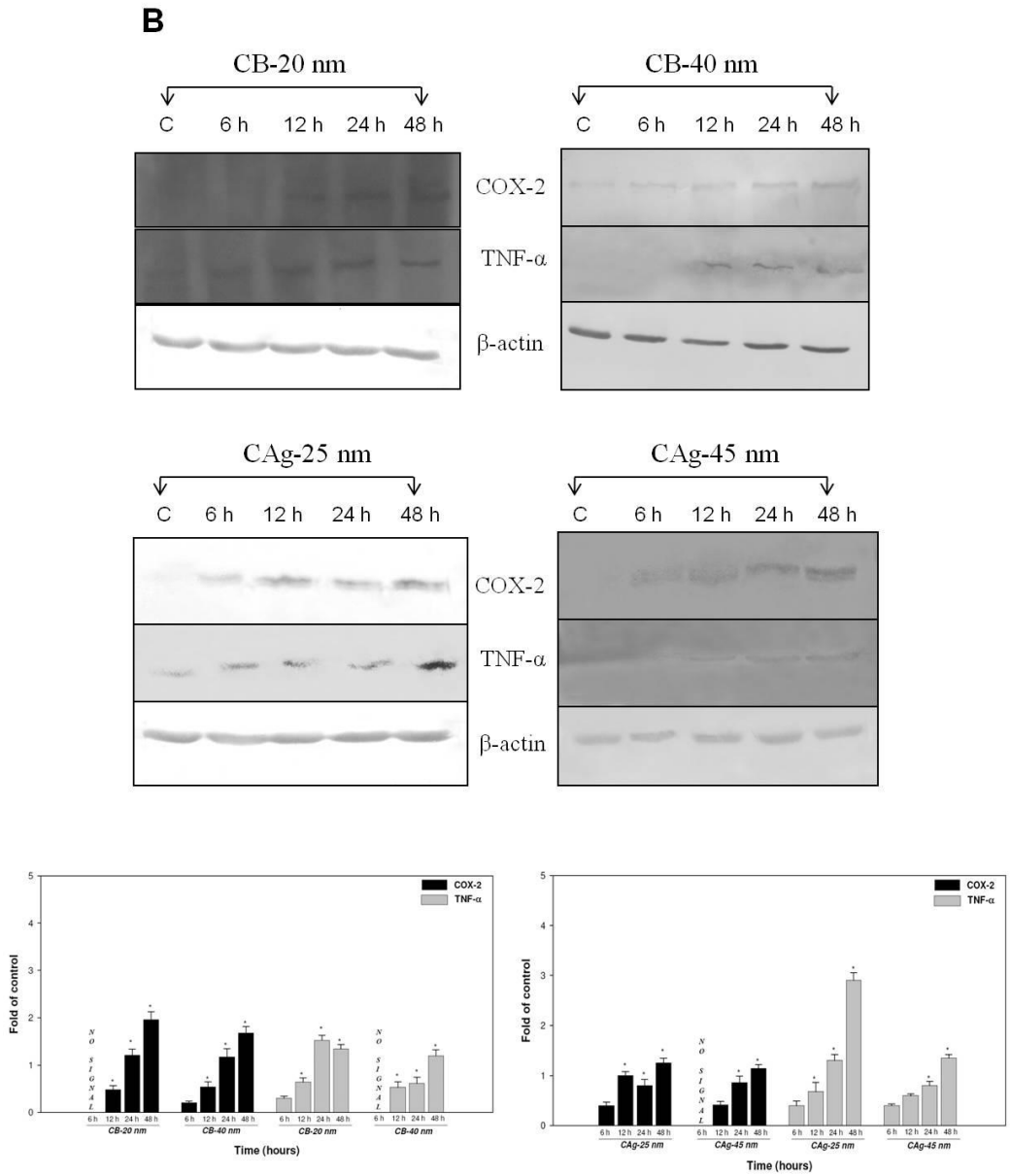

*Figure 1.7B. Effect of CB and CAg NPs on RAW 264.7 cells: Cells were treated with 5 µg/ml CB-20 nm, 40 nm and CAg-25 nm, 45 nm nanoparticles. Aliquots of cell lysates prepared after 6-48h exposure were resolved by SDS-PAGE and analyzed for COX-2 and TNF-α protein expression by Western blotting. β-actin was used as an internal control to monitor equal loading. Bar graph represents densitometric values of COX-2 and TNF-α level. * Denotes statistical significance (P<0.05) over untreated controls.*

These studies showed maximum induction of COX-2 and TNF-α expression at mRNA (Figure 1.7A) and protein (Figure 1.7B) levels upto 24 h and 48 h, respectively. However, the induction of COX-2 and TNF-α in CAg and CB

NPs was much lower when compared to Ag (without carbon coating) and Al NPs. When compared, carbon coated silver NPs showed a significant degree of difference in COX-2 and TNF-α induction; where uncoated silver NPs showed the higher level of induction compared to carbon coated silver nanoparticles.

iii. Effects of Au NPs and LPS on COX-2 and TNF-α expression: Interestingly, when RAW 264.7 cells were exposed to Au NPs (20 nm and 40 nm) at concentration of 5 µg/ml for 6-48 h, there was no considerable induction of COX-2 and TNF-α at both mRNA (Figure 1.8A) and protein (Figure 1.8B) levels at initial time points, but a slight induction was observed at 24 h (mRNA) and 48 h (protein) of exposure.

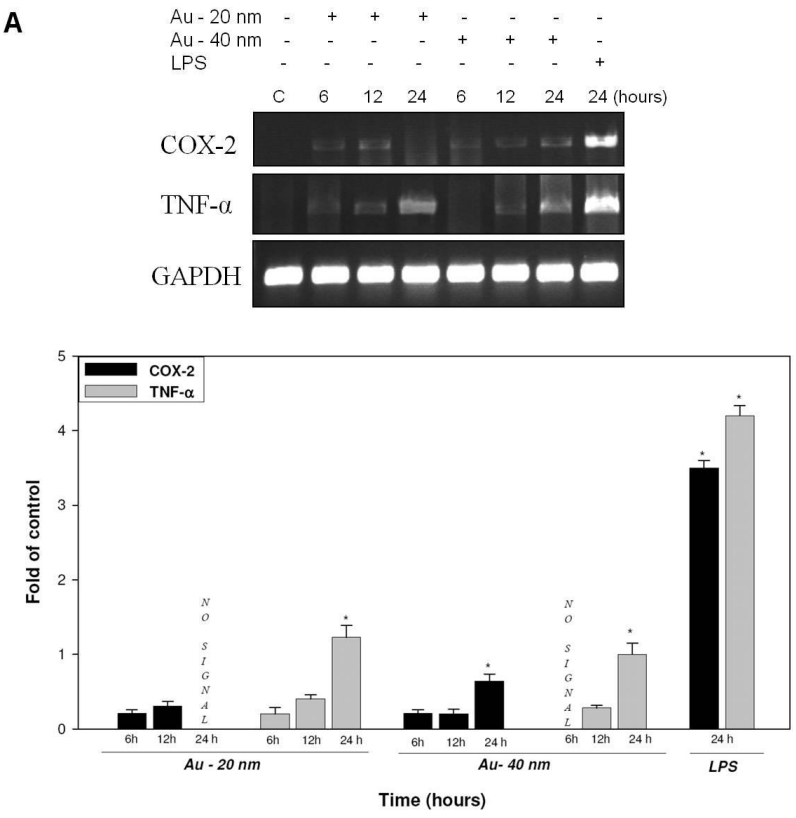

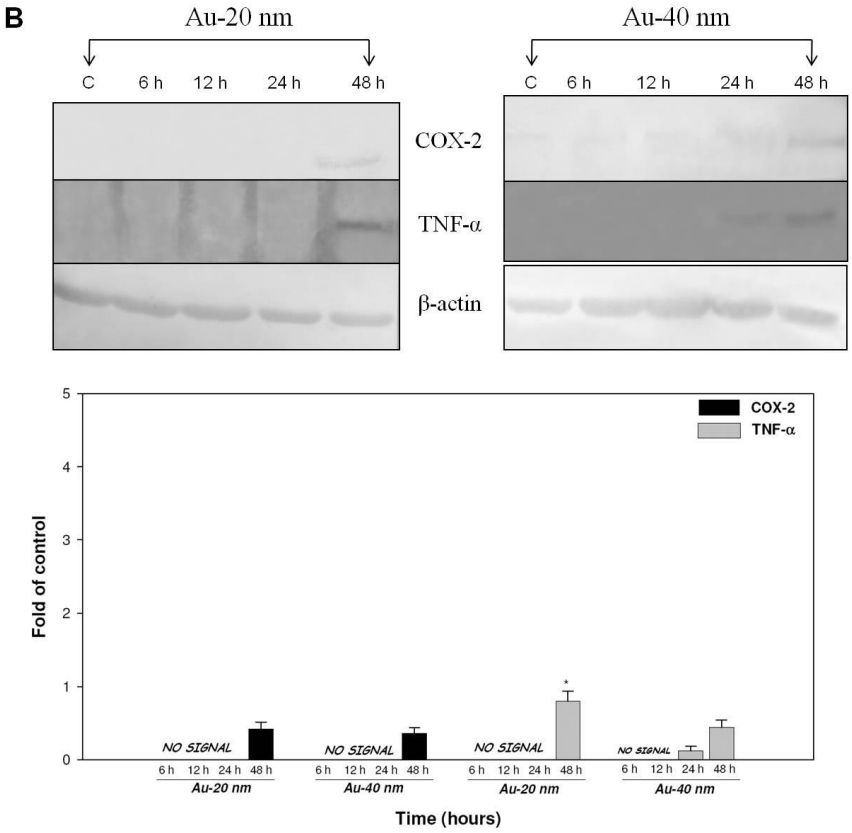

Figure 1.8AB. Effect of Au NPs and LPS on RAW 264.7 cells: Cells were treated with 5 µg/ml Au-20 nm, 40 nm nanoparticles. (A) Total RNA was isolated after 6h, 12h and 24h exposure was subjected to RT-PCR analysis using COX-2 and TNF- α specific primers as described in the methodology. GAPDH was internal control. (B) Aliquots of cell lysates were resolved by SDS-PAGE and analyzed for COX-2 and TNF-α protein expression by Western blotting. β-actin was internal control to monitor equal loading. Bar graph represents densitometric values of COX-2 and TNF- α levels upon Au NPs treatment.
** Denotes statistical significance (P<0.05) over untreated controls.*

Exposure of macrophages to LPS (1 µg/ml), a known pro-inflammatory agent, showed a dramatic time dependent induction of COX-2 expression (Figure 1.8C). In order to rule out the possibility of bacterial LPS contamination which could be responsible for the observed pro-inflammatory responses, an endotoxin detection assay was done (LAL chromogenic assay kit). The NPs employed in the present study showed very low to negligible LPS level, ruling out such a possibility.

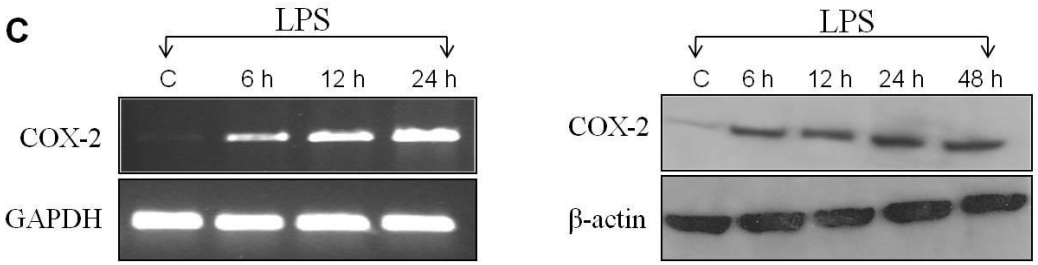

Figure 1.8C. Effect of LPS on RAW 264.7 cells: Macrophages were treated with 1 µg/ml LPS for 6–48 h. COX-2 mRNA and protein expression was checked using RT-PCR and Western blot analysis.

1.3.7. Induction of Pro-inflammatory Cytokine IL-6 by Nanoparticles

Macrophages are able to secrete inflammatory mediators like cytokines upon stimulation by various agents. In the present study the cellular release of the cytokine IL-6 into the culture medium was measured when macrophages were exposed to various NPs at 5 µg/ml concentration (Figure 1.9). Ag (15, 40 nm) and CAg (25, 45 nm) NPs showed a significant release of IL-6 from RAW 264.7 macrophages after 48 h. Similarly, Al (20, 50 nm) and CB (20, 40 nm) NPs also induced the release of IL-6 in to the medium but not to the extent recorded with Ag and CAg NPs. Au (20, 40 nm) NPs, however, showed no appreciable release of IL-6 from RAW 264.7 cells. The positive control bacterial endotoxin, LPS (1 µg/ml) showed a significant induction of IL-6.

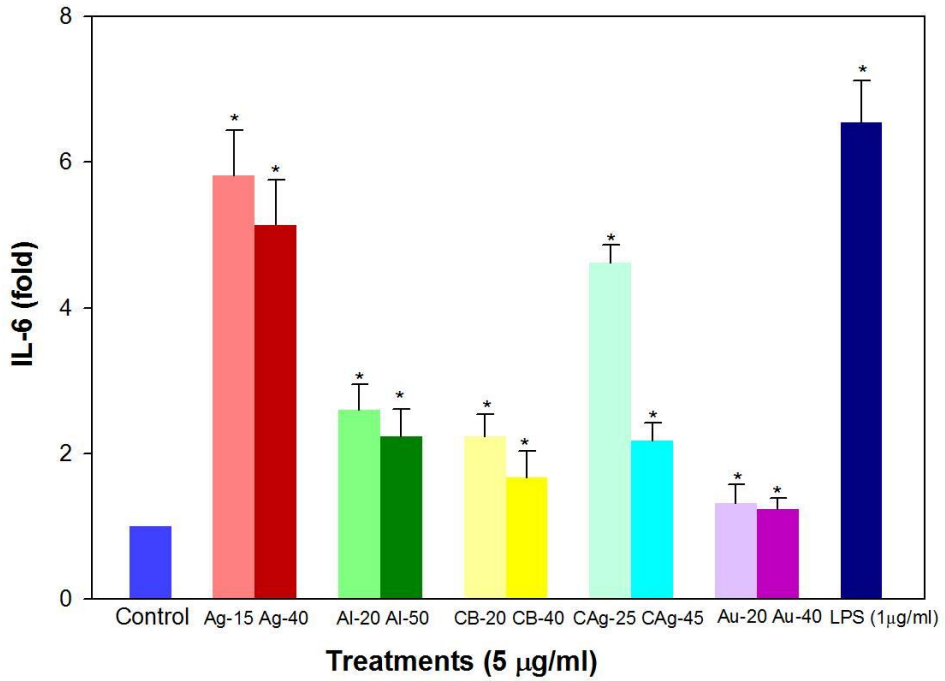

*Figure 1.9. Effect of NPs on the release of IL-6 from mouse macrophage cells RAW 264.7: Cells were treated with 5 μg/ml of NPs (Ag-15, 40 nm; Al-20, 50 nm; CB-20, 40 nm; CAg-25, 45 nm and Au-20, 40 nm) and LPS at concentration of 1 μg/ml for 48 h and the culture supernatant was analyzed for the IL-6 concentration. Results are the mean ± SD (n = 3). * Denotes statistical significance (P<0.05) over untreated controls.*

1.4. Discussion

There is growing importance of nanotechnology to improve the quality of human life through its impact on medicine, discovery of disease state biomarkers, *in vivo* molecular diagnostics and drug delivery systems (Medina *et al.,* 2007). In view of their growing use in varied areas, there is need to understand the adversities of exposure to nanomaterials. Available evidences suggest that many of the metal NPs that are being used have cytotoxic effects. Recent studies have also suggested the pro-inflammatory effects of metal and carbon based NPs in animals and cultured cell systems (Braydich-Stolle *et al.,* 2005**;** Hussain *et al.,* 2005; Magrez *et al.,* 2006). Hence, there is an immediate need for a framework to understand the impact of these novel nanomaterials on human health and environment and to evaluate the molecular mechanisms involved, so as to develop reliable methods for their risk assessment.

In the present study we have used mouse macrophage RAW264.7 cells to assess the inflammatory response of various NPs. Macrophages represent a primary line of defense to foreign materials. The macrophage phenotype generates reactive oxygen or nitrogen species as well as a plethora of inflammatory cytokines that facilitate killing of invading pathogens and cancer cells. We have employed LPS, a known inflammatory activator of macrophages as a standard pro-inflammatory mediator. Induction of COX-2 and other pro-inflammatory genes by LPS through ROS

and NF-κB mediated pathway is a well established mechanism (Lu and Wahl, 2005). The pro-inflammatory effects elicited by the Ag and Al NPs were observed to be similar to the effects of LPS. Although there have been studies showing that NPs provoked ROS generation is responsible for the cytotoxicity, there are only a few reports suggesting the induction of pro-inflammatory markers such as TNF-α and COX-2. In a recent study it has been shown that vehicular exhaust particulates generated from incomplete fuel combustion upregulate COX-2 and PGE_2 through ROS generation in exposed rat vascular smooth muscle cells (Tzeng *et al.,* 2007). The production of ROS, induction of inflammation and ensuing cytotoxicity has been described for many different forms of fine, ultrafine and nanosized particles (Brown *et al.,* 2004**;** Hiura *et al.,* 1999). The oxidative stress induced redox signaling is known to involve the activation of transcription factors (NF-κB/AP-1), which in turn induce the expression of various pro-inflammatory genes like COX-2, TNF-α and IL-6 (Castranova, 2004; Hashimoto *et al*., 2013). Among these COX-2, the regulatory enzyme involved in the production of pro-inflammatory prostaglandin E_2 (PGE_2), forms a key marker of inflammation.

In the present study, mouse macrophages in culture were incubated with different NPs and analyzed the effects of size and duration of exposure. The NPs were well dispersed within the cell, without any considerable aggregation, suggesting that the pro-inflammatory effects

observed are mediated by the finely dispersed NPs. The NPs employed in the present study were found to be free from LPS, also suggesting the role of NPs in eliciting inflammatory responses. Thus the finely dispersed NPs which are free from contaminating LPS showed induction of pro-inflammatory gene expression, which was dependent on the nature and size of NPs and duration of exposure. Results showed induction of COX-2, which was the highest in cells exposed to silver NPs followed by aluminum, carbon black and carbon coated silver NPs. The induction of COX-2, TNF-α and IL-6 decreased with the increase in the size of NPs, but increased gradually with increasing duration of exposure up to 48 h. As ROS mediated redox signaling is a well known mechanism to induce COX-2 expression (Lu and Wahl, 2005**;** Tzeng *et al.,* 2007), the generation of ROS was measured in NP exposed macrophages. These studies showed a trend similar to COX-2 expression, with the highest ROS levels in cells exposed to Ag NPs followed by Al, CB, CAg NPs, suggesting a key role of ROS in COX-2 induction. These pro-inflammatory effects of NPs may have been mediated by the NF-κB activation and subsequent pro-inflammatory genes expression. Hence in the present study we have investigated NF-κB as an upstream event of NP initiated oxidative stress that induces expression of pro-inflammatory genes. Compared to the untreated cells Ag NPs showed a significant increase in the translocation of NF-κB 65 and 50 kDa subunits to nucleus, followed by Al, CB, CAg nanoparticles. When macrophages were

treated with NAC, the known antioxidant, prior to NPs exposure, NF-κB activation was diminished, suggesting a possible role for ROS in the activation of NF-κB by NPs.

Gold nanoparticles, on the other hand, provided interesting results showing negligible effects at 6h and 12 h time points and low expression of the pro-inflammatory genes at 24 h (mRNA) and 48h (protein) as compared with the other NPs and LPS. The ROS generation was in fact quenched upon exposure of macrophages to these NPs, equivalent to NAC pretreatment. Correlating well with the ROS generation, gold NPs showed neither NF-κB activation (p65) nor NF-κB translocation (p65/p50). And there was also no appreciable IL6 release. These observations are not conclusive that gold NPs are completely safe, but supports the earlier reports on gold NPs being not acutely cytotoxic (Patra *et al.*, 2007). Further work will be required to determine if phenotypic or cytotoxic chronic changes occur with long term exposures to gold NPs.

In conclusion silver NPs showed a greater degree of pro-inflammatory effects, when incubated with the mouse macrophage cell line, RAW 264.7, by inducing pro-inflammatory markers like COX-2, TNF-α and IL-6 through ROS- NF-κB signaling pathway. This pro-inflammatory response pattern was similar, but progressively less intense in case of Al, CB and CAg NPs. The induction of pro-inflammatory markers decreased with increase in the nanoparticle size, and increased with increasing

duration of exposure. In addition, carbon- coating of the NPs appear to down regulate the pro-inflammatory effects of silver NPs. In contrast, macrophages did not show remarkable inflammatory responses with two nanosizes of Au particles compared to other particles used in the study. In summary, four important factors – elemental nature, size, duration of exposure and surface coating of NPs seem to play a vital role in the inflammogenicity of NPs. These studies also suggest the potential use of monitoring the expression of COX-2 in a macrophage-based *in vitro* system for evaluating the inflammatory responses of the metal and carbon based nanoparticles. In order to further understand the other protein players that would be involved in the effects of nanoparticles, the changes in the global proteome were investigated.

Chapter 2

Evaluation of responses of RAW 264.7 macrophages upon exposure to the nanoparticles: A proteomics approach

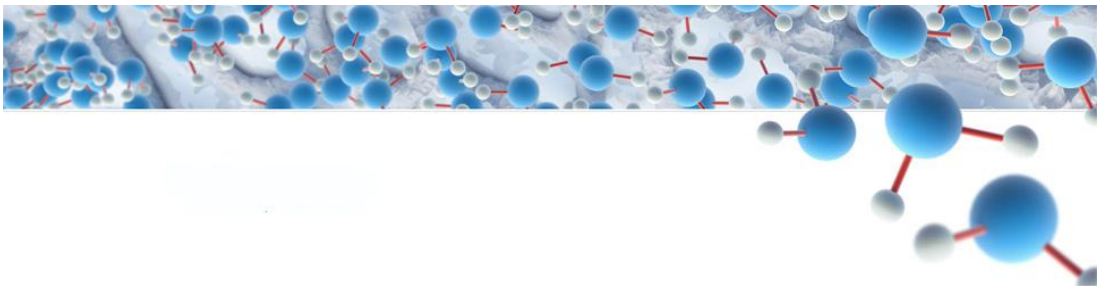

2.1. Introduction

The increasing understanding that nanoparticles and nanomaterials can have adverse effects on the environment and human and animal health, calls for a mechanistic study on their adverse effects and biocompatibility. It would be essential to look at not just one or two parameters but to understand the effects globally or in totality. By studying the global pattern of proteins and analyzing how these change during development or in response to external environmental changes, will boost our understanding of systems-level cellular behavior. A proteomics approach would be the most suitable way to do so. It would help us gain better insights into the pharmacological, toxicological and pathophysiological effects of the nanoparticles and also helps identify new protein markers.

2.1.1. Global Proteome Profile

The term proteome refers to the protein equivalent of the genome. It comprises the complete set of gene products that are synthesized by the genome, and the analysis of these gene products has been termed proteomics (Yarmush and Jayaraman, 2002). Proteome is a very dynamic and complex entity that defines the cellular behavior and function. Although every cell in an organism carries the same genome, the proteome seems to vary largely and this variation is what defines a particular cell type. The dynamics of the proteome in a cell are generally influenced and

altered by the function and environment that the cell is in. It is thus, a demand and supply situation of the cell that dictates the expression of the static genome as the dynamic proteome. And since, proteins are the effector molecules; the study of the proteome has been the classical approach in understanding the cellular function and behavior (Aebersold and Goodlett, 2001). There are several post translational protein modifications (e.g., phosphorylation, glycosylation, ubiquitination, and methylation) that influence the behavior of the proteins. The studies on mRNA expression at the transcriptional level can only partly serve the purpose of understanding the cellular behavior during various biological processes. The cellular events such as localization of proteins to certain organelles, sequestration and recycling cannot be understood by simple transcriptional analysis. This emphasizes the need to study the proteome of the cell at given variable conditions (de Hoog and Mann, 2004).

2.1.2. Two-dimensional Electrophoresis

There are several analytical methods including two-dimensional gel electrophoresis (2DE) and amino acid sequencing which are being used for the identification and characterization of proteins. Two-dimensional electrophoresis was popularized with the advent of the idea of proteomics and proteome analysis. Two-dimensional gel electrophoresis was an extension of 1-D SDS-PAGE, that increased the number of proteins resolved

on an electrophoresis gel by separating the proteins based on their native charge and molecular mass. The first attempt to separate the serum proteins using a 2-D combination of paper and starch gel electrophoresis was made by Smithies and Poulik in 1956. Later, in the year 1975 O'Farrell and Klose introduced the basic method of 2-DE that now is a crucial technology in the field of proteomics. Combining isoelectric focusing (IEF) for the first dimension separation with SDS-PAGE in the second dimension resulted in a 2-D method in which proteins were being distributed across the two-dimensional gel profile (Dunn and Gorg, 2001). 2DE followed by mass spectrometry and bioinformatics has now become a well established approach for any proteomics study. Advancements in mass spectrometry to allow higher image quality, sensitivity and resolution, as well as development of better software for more efficient data mining provides more and detailed information of the proteome. Thus, this state-of-the-art technology involves separation, identification and quantification of proteins. It also offers several advantages which include the identification of marker proteins amongst a large protein pool of cell or tissue extracts, provide a greater level of the purified protein for subsequent characterization using mass spectrometry (Westermeier, 2005).

2.1.3. MALDI- MS/MS for Protein Identification

There have been some major developments in the analytical methods due to the improvement of mass spectrometric (MS) methods (Bantscheff *et al.,* 2007). MS for protein identification relies on the digestion of protein samples into peptides by a sequence-specific protease such as trypsin. Peptides are much more amenable to MS analysis than the whole proteins (Steen *et al.,* 2004). After the proteins are digested, the peptides are often delivered to a mass spectrometer for analysis via chromatographic separation coupled online to electrospray ionization (LC-MS for liquid chromatography mass spectrometry). Matrix-assisted laser desorption/ionization (MALDI) is an alternative ionization method. When MALDI is used, the samples of interest are solidified within an acidified matrix, which absorbs energy in a specific UV range and dissipates the energy thermally. This rapidly transferred energy generates a vaporized plume of matrix and thereby simultaneously ejects the analytes into the gas phase where they acquire charge. A strong electrical field between the MALDI plate and the entrance of the MS tube forces the charged analytes to rapidly reach the entrance at different speeds based on their mass-to-charge (*m/z*) ratios. A significant advantage of MALDI-TOF is that it is relatively easy to perform protein or peptide identification with moderate throughput i.e., 96 samples at a time (Van Bramer, 1998). MALDI-MS provides a rapid way to identify proteins when a fully decoded genome is available because

the deduced masses of the resolved analytes can be compared to those calculated for the predicted products of all of the genes in the genomes of an organism.

Proteomics technologies, such as 2D gel electrophoresis (2-DE) and analytical techniques like MALDI give a momentary snapshot of the proteome of a cell or tissue and identification of selective proteins, respectively (Rubakhin *et al.,* 2005). A proteomics map derived from 2-DE provides data on the charge, mass and abundance of approximately 2000 individual proteins or spots consisting of similar proteins. The number of proteins that can be visualized using a proteomics map will increase as the detection technology advances. The management of such vast amounts of information, and the recognition of the subset of proteins that play a critical role in a particular physiological, pharmacological or toxicological situation, is a daunting task.

Earlier we have screened various nanoparticles (silver, aluminium, carbon, carbon coated silver and gold) for their inflammatory responses in a typical cell line- mouse macrophage cell line, RAW264.7 (Nishanth *et al.,* 2011). These studies revealed the induction of inflammatory responses in macrophages by silver, aluminium, carbon black and carbon coated silver nanoparticles. Gold nanoparticles, on the other hand had no inflammatory effects on the macrophage cell line. This prompted us to further understand and identify the other marker proteins that could play a role in the effects

brought about by the nanoparticles. The present study is aimed to understand the global changes in the protein profile of the macrophage cells RAW 264.7 exposed to the various nanoparticles. Macrophages being the first immune cells to counter any foreign material entering the circulation we have chosen to study the effect of nanoparticles on these cells. The specific objectives are:

- Understanding the differential global proteome of the macrophages after exposure to silver and gold nanoparticles.
- Identification of key protein players involved in the effects of nanoparticles.

2.2. Materials and Methods

2.2.1. Materials

Phosphate buffered saline (PBS), RPMI 1640, Fetal Bovine Serum (FBS), Penicillin and Streptomycin were purchased from Gibco BRL (California, USA), Bio-lyte ampholytes were procured from Bio-Rad (Hercules, CA). All the other chemicals and reagents were purchased from Sigma Aldrich and are of molecular biology grade. Ultra pure DI-water was prepared using a Milli-Q system (Millipore, Bangalore, India). Silver (Ag-10 nm and 40 nm) nanoparticles were purchased from nanocomposix and Gold NPs (Au; 10 nm, 40 nm) were prepared from Gold (III) chloride trihydrate, procured from Sigma (St Louis, MO), by citrate reduction of $HAuCl_4$.

2.2.2. Cell Culture and Sample Preparation

Mouse Macrophage cells (RAW. 264.7) were grown in RPMI 1640 medium supplemented with 10% heat inactivated FBS, 100 IU/ml penicillin, 100 µg/ml streptomycin and 2mM L-glutamine. The cells were maintained in a humidified atmosphere with 5% CO_2 at 37°C. The cells were exposed to 5µg/ml nanoparticles at 60% confluence and harvested after 24hrs. Cells were washed with PBS and suspended in a lysis buffer (20 mM Tris, 1 mM EDTA, 150 mM NaCl, 1% NP-40, 0.5% sodium deoxy cholate, 1 mM β-glycerophosphate, 1 mM sodium orthovanadate, 1 mM

PMSF, 10 µg/ml leupeptin, 20 µg/ml aprotinin). After 30 min incubation at 4 °C, the mixtures were centrifuged (10,000 x g) for 10 min, and the supernatants were collected as the whole-cell extracts. The proteins were then precipitated by cold acetone with 10% trichloroacetic acid overnight. After centrifugation, the protein pellet was washed with cold acetone followed by air drying, and then resuspended in the rehydration buffer containing 7 M urea, 2 M thiourea, 4% CHAPS, 2% Bio-Lyte 3/10 and 50 mM dithiothreitol (DTT) (Sigma, St. Louis, MO). Protein concentration was assessed using a Bio-Rad detergent compatible kit as per the manufacturer instructions.

2.2.3. Two-dimensional Gel Electrophoresis

For the first-dimension IEF, pH 4-7 non-linear range IPG strips (7 cm) were rehydrated with 125 µl of solubilized sample (130 µg protein amount) for 12 h before the sample was separated by IEF at 50 V for 10 h, 500 V for 30 min, 5000 V for 2h30 min, 5000 V for 25000Vh, and finally 500 V for 10 h. Prior to the second dimension SDS-PAGE, the IPG strips were equilibrated with 2 ml of equilibration buffer consisting of 0.375 M Tris, 6 M urea, 2% SDS, 20% glycerol and 0.02 g/ml DTT at 25°C for 15 min followed by equilibration in 0.375 M Tris, 6 M urea, 2% SDS, 20% glycerol and 0.025 g/ml iodoacetamide (IAA) at 25°C for 15 min. For the second dimensional SDS-PAGE a 12.5% separating gel was used and performed without a

stacking gel. The equilibrated IPG gel strip was placed on top of the SDS-PAGE gel and was sealed with 0.5% low-melting temperature agarose with 0.01% bromophenol blue. Electrophoresis was carried out at 75-150 V until the tracking dye reached the bottom of the gel. After 2-DE, proteins in gel were stained with Commassie Brilliant Blue G-250.

2.2.4. Quantitative Analysis of the Proteins in the 2-DE

Protein pattern images in 2-DE SDS-PAGE were obtained using a high-resolution Image scanner GE healthcare and the amount of protein in each spot was estimated using ImageMaster 2D Platinum software (v6.0, GE Healthcare Bio-Sciences AB). The volume report was generated and to correct quantitative variations in the intensity of protein spots, spot volumes were normalized as a percentage of the total volume of all the spots present in each gel.

2.2.5. Protein Identification by Mass Spectrometry

The protein spots were manually excised from 2-DE gels, destained, washed and in-gel digested. The gel pieces were dehydrated and dried by SpeedVac concentrator, the dried gel pieces were rehydrated with 20 ng of modified trypsin (sequencing grade, Promega, Madison, WI, USA) in 25 mM ammonium bicarbonate (pH 8.5) at 37°C for 16 h. The tryptic peptide mixture was concentrated and immediately redissolved for protein

identification. Matrix assisted laser desorption ionization time-of-flight mass spectrometer (MALDI-TOF MS) (Autoflex III, Bruker Daltonics, Bremen, Germany) was employed for peptide mass fingerprinting (PMF) analysis. We subsequently searched all peak lists against Mascot engine with Swiss- Prot database. The search parameters allowed for one missed cleavage tryptic peptides, oxidation of methionine, carbamidomethylation of cysteine and at least 50 ppm mass accuracy.

2.3. Results

2.3.1. Differential Protein Expression Pattern

The 2DE gel images of the whole cell lysates of RAW 264.7 marophage cells either exposed to 5 µg/ml for 24 h or unexposed were analyzed using the Image Master Platinum 6.0 (Figure 2.1) and the spot intensities have been represented here below in the form of a heat map (Figure2.2). The differentially expressed spots were categorized into four groups based on the differences in the spot intensity compared to the control.

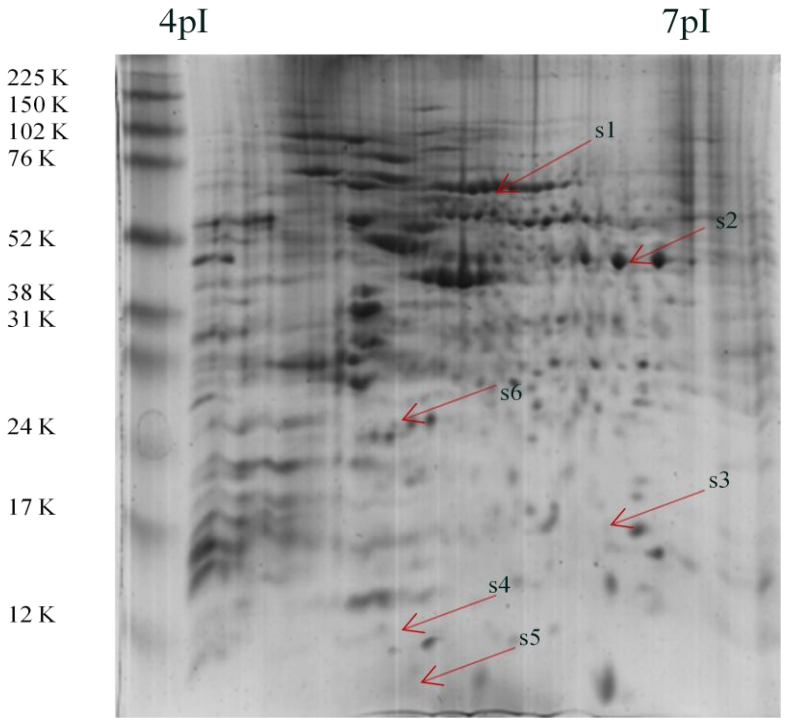

(A) Control

Figure 2.1 2DE gel images of the cell lysates of RAW 264.7 cells: (A) Untreated cells were used as control. The IEF was carried out in pI range 4-7.

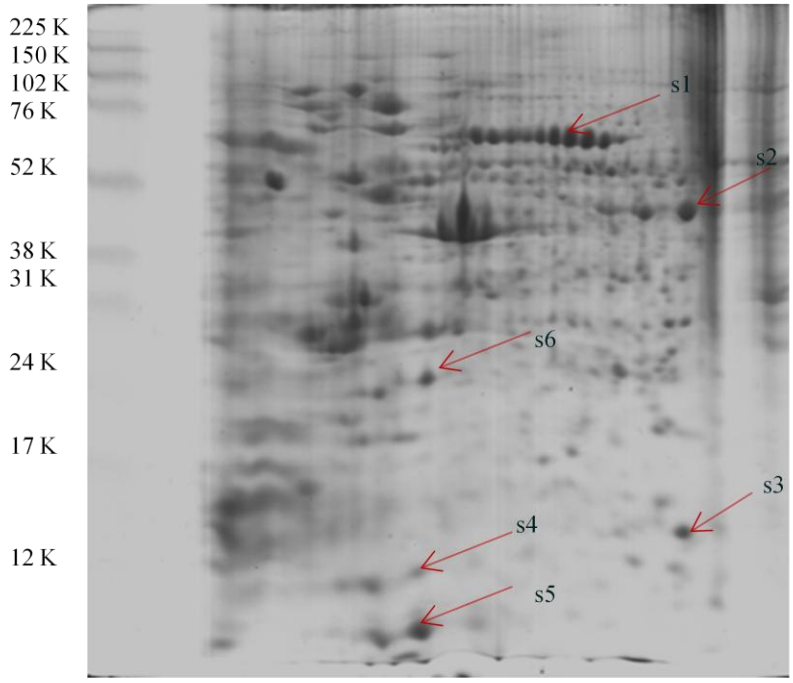

(B) Ag 10

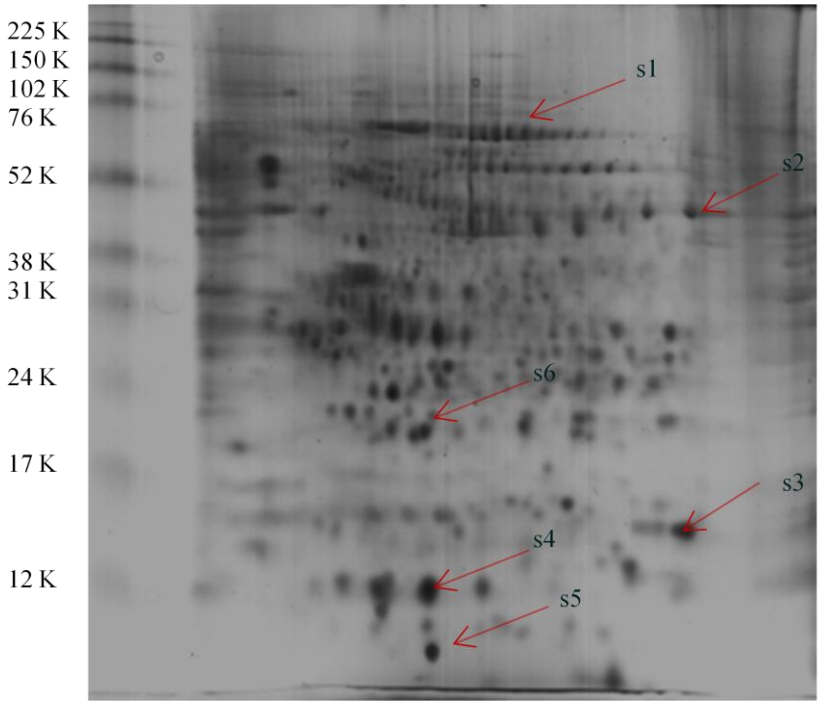

(C) Ag 40

Figure 2.1 2DE gel images of the cell lysates of RAW 264.7 cells: (B,C) Cells were treated with 5 µg/ml of Ag 10 and 40 nm NPs for 24 h. The IEF was carried out in pI range 4-7.

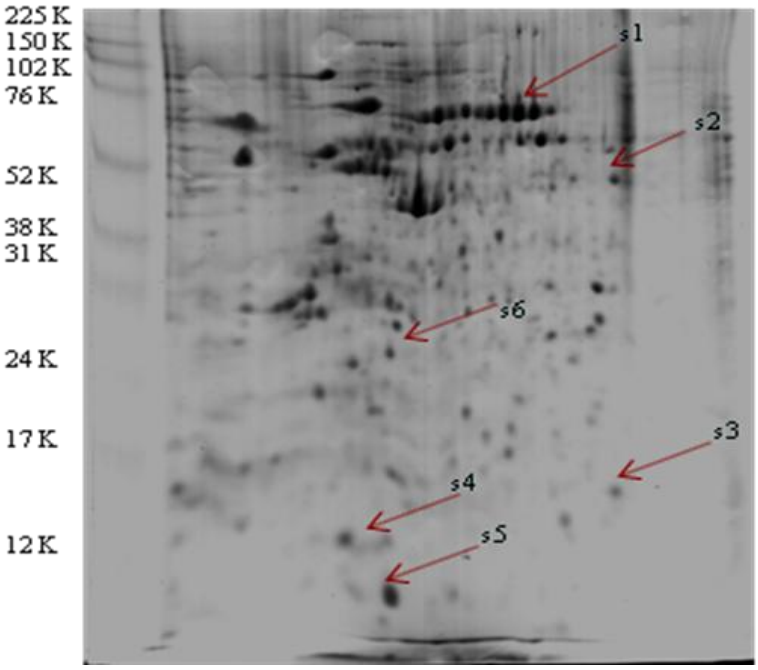

(D) Au 10

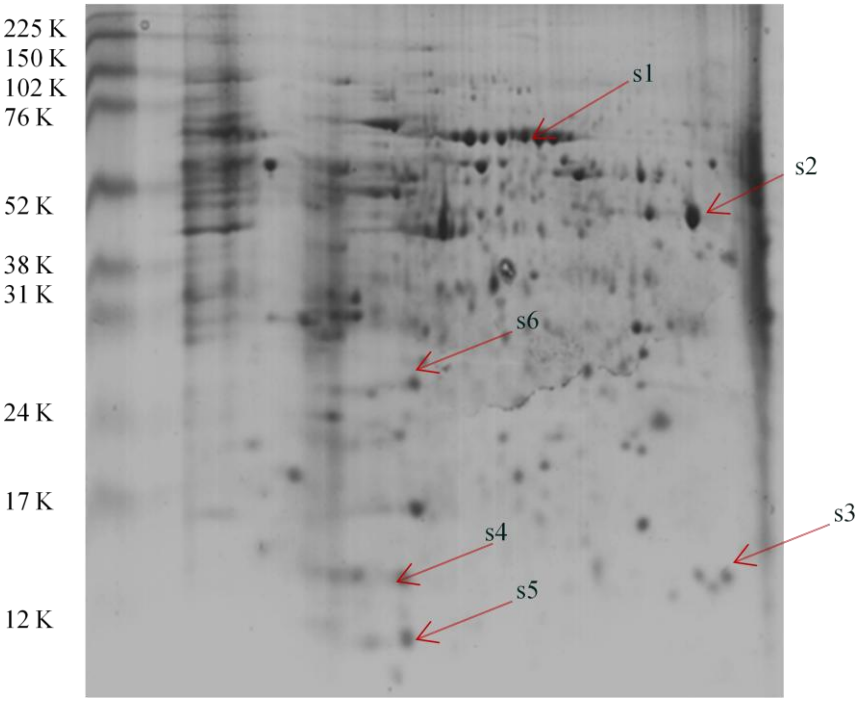

(E) Au 40

Figure 2.1 2DE gel images of the cell lysates of RAW 264.7 cells: (D, E) Cells were treated with 5 µg/ml of Au 10 and 40 nm NPs for 24 h. The IEF was carried out in pI range 4-7.

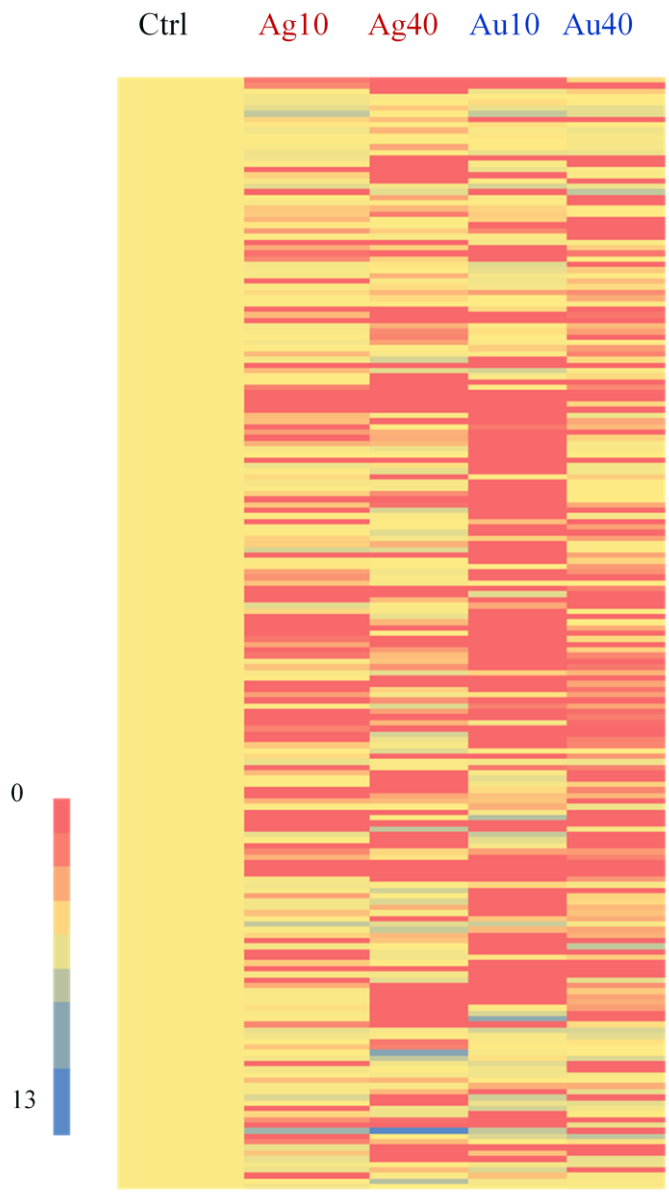

Figure 2.2 Heat map of the spot intensities of the proteins extracted from RAW 264.7 cells: Cells were exposed to 5 µg/ml Ag and Au 10 and 40 nm NPs for 24hrs. Spot intensities as compared to the untreated control.

Spots that showed 2 fold or more increased intensity compared to the control were considered upregulated and 2 fold or more decreased intensity compared to the control have been considered down regulated. Anything below the 2 fold intensity difference were considered as having no change.

There were a group of spots that were not detected by the software and these were grouped under the non detectable category (Table 2.1).

Table 2.1. Differentially expressed spots upon exposure to silver and gold nanoparticles

Treatment	Upregulated	Downregulated	No change	Not detected in treated	Total
Ag10	44	66	36	53	199
Ag40	44	28	62	65	199
Au10	40	37	23	99	199
Au40	34	80	20	65	199

2.3.2. Identification of the Proteins using MALDI-MS/MS

The spots that showed maximum differential expression with Ag NPs and Au NPs were picked up for identification and the list is presented in the table 2.2 and table 2.3 below, respectively. In case of exposure of macrophages to Ag NPs there were two spots which showed marked upregulation. One among them that showed a 12 fold increase was identified by the Mascot database search as Chloride intracellular channel (CLIC-1). It has been implicated in oxidative stress conditions (Stefania *et al.,* 2010).

Table 2.2. List of differentially expressed proteins identified in RAW 264.7 cells upon exposure to silver nanoparticles.

Protein name	Fold change	Mol wt KDa	pI	Score	% Seqence match
Cathepsin B	7 ↑	38	5.57	249	9
Chloride intracellular channel-1 (CLIC-1)	12 ↑	27	5.09	57	12
Macrophage simulating factor 1 receptor (MSt1R)	3 ↑	152	6.71	28	0.2
Patatin like phospholipase protein	2.9 ↑	151	6.47	28	1
ATP synthase subunit D (ATP5H)	2 ↑	18	5.52	77	13
Galectin	2.75 ↓	15	5.32	19	23
Map 3 Kinase 13 (M3K13)	Not detected *	108	6.27	26	1

** Not detected in cells exposed to Ag NPs*

The spot which was 7 fold upregulated upon exposure to Ag NPs was identified as Cathepsin B, a lysosomal protease that is involved in autophagy, protein post translational modification and trafficking (Ha *et al.*, 2008).

In case of macrophages exposed to Au NPs one of the spots that showed a notable down-regulation corresponded to Enolase-1 or α-Enolase, which is an auto antigen that aggravates the inflammation in rheumatoid arthritis. The down regulation of this protein in Au NPs treated samples could be of some significance in therapy.

Table 2.3. List of differentially expressed proteins identified in RAW 264.7 cells upon exposure to gold nanoparticles.

Protein name	Fold change	Mol wt KDa	pI	Score	% Sequence match
α-Enolase	2.69 ↓	47	6.37	127	6
Heat Shock cognate 70	2 ↑	71	5.3	92	5
T-cp1 theta T-complex protein 1	3.6 ↑	60	5..44	57	3
M3K13 Map 3 Kinase 13	Detected in Au	108	6.27	26	1

Map3 Kinase 13 was detected in control and Au NPs treated cells but not detected in Ag NPs treated cells. This probably could be due to the phosphorylation and ubiqutinylation following the signal transduction, in case of Ag NPs treated cells.

2.4. Discussion

The Chloride intracellular channel (CLIC-1) is an evolutionarily conserved protein of the Metazoa, and structurally similar to Glutathione S-transferase fold superfamily. The biological role and the significance of its structural conservation are not well understood, but there is increasing evidence that it is involved in maintaining the redox homeostasis of the cells (Averaimo *et al.,* 2010, Littler *et al.,* 2010). Reports suggest that in oxidative stress conditions, expression of CLIC-1 is increased. CLIC-1 is shown to be localized in phagosomal membranes and has a role in phagosomal acidification as well (Jiang *et al.,* 2012). The CLIC-1 expression in microglial cells is consistently upregulated in the presence of Aβ-amyloid protein, leading to the chronic inflammatory conditions in Alzhimers Disease where there is increase in proinflammatory cytokines like TNF-α production (Novarina *et al.,* 2004). CLIC-1 has also been upregulated in several other pathophisiolgical conditions such as arthritis, gastric cancer, heptocellularcarinoma. CLIC-1 has also been implicated in cell cycle regulation, apoptosis, cellular adhesion and motility. It has also been speculated that CLIC-1 expression may be involved in cellular transformation due to its involvement in the cell cycle regulation (Chen *et al.,* 2007). The results of the present study in accordance with the earlier reports reiterate the fact that CLIC-1 could me an important marker to be studied in nanoparticle induced inflammatory responses.

Cathepsin B, a lysosomal protease involved in the degradation and processing of the lysosomal proteins (McGrath, 1999), is upregulated in cells exposed to Ag NPs. It has been reported that Cathepsin B is associated with inflammosome formation and vesicle trafficking. Ha *et al* (2008) demonstrated in macrophages, the involvement of Cathepsin B in trafficking the tumour necrosis factor-α (TNF-α) containing vesicles to the plasma membrane. There are some reports showing the involvement of Cathepsin B in inflammosome formation stimulated by the silica crystals and aluminium salts (Hornung *et al.*, 2008).

Enolase is a glycolytic pathway enzyme that catalyses the conversion of 2-phosphoglycerate to phosphoenolpyruvate in the last but one reaction. It is one of the very highly conserved proteins across species from bacteria to humans. It exists in three isoforms in vertebrates: α-enolase (ENO-1), β-enolase (ENO-2) and γ- enolase (ENO-3). Although enolases have been thought to have only enzymatic function, of late there is increasing evidence of their role in various physiological functions, especially α-enolase is involved in the plasminogen mediated monocyte and macrophage activation. Its surface expression on monocytes and macrophages is also reported in induction of inflammation in rheumatoid arthritis (Bae *et al.,* 2012). The down regulation of α-enolase in the presence of Au NPs may be of therapeutic importance as there are some Ayurvedic formulations that contain gold colloids which are used for treating arthritis.

Galectins are a family of β-galactoside binding proteins with 14KDa molecular weight. There are a group of 15 different isoforms that have been identified which may be in monomeric or homodimeric states. Among these Galectin-1 and Galectin-3 are known to be antagonistic in their activities. Galectin-1 is mostly anti-inflammatory in its effects (Rabinovich *et al.*, 2000). In the present study the expression of Galectin-1 is decreased in case of Ag NPs treated samples which may indicate that its decrease may promote the pro-inflammatory responses by the Ag NPs.

Mitogen activated protein 3 kinase 13 (M3K13) is an upstream protein in the MAP kinase pathway and is involved in the signal transduction pathways of inflammation and cell survival (Masaka, 2003). The presence of M3K13 in control and gold NPs treated cells and its absence in the silver NPs treated cells may be due to the fact that the silver NPs could generate the signal, convert it to the phospho form that triggers the NF-κB and then could have been ubiquitinylated. This correlates well to the findings of NF-κB mediated COX-2 induction by silver NPs and not by gold NPs. These studies explain the mechanism behind activation of pro-inflammatory signals observed in cells exposed to Ag NPs and no such activation in cells exposed to Au NPs.

A recent study by Lim *et al.*, 2012 reported the induction of HO-1, IL-8, HSP-70 expression upon exposure to Ag NPs. In our present study these have not been identified but other pro-inflammatory markers such as CLIC-1 and Cathepsin B over-expression was noticed. In conclusion, CLIC-1 and Cathepsin

B could be used as good markers along with COX-2, in evaluating the biocompatibility of nanoparticles.

Chapter 3

Biocompatibility of nanoparticles in vitro: Effect on stem cells proliferation and differentiation

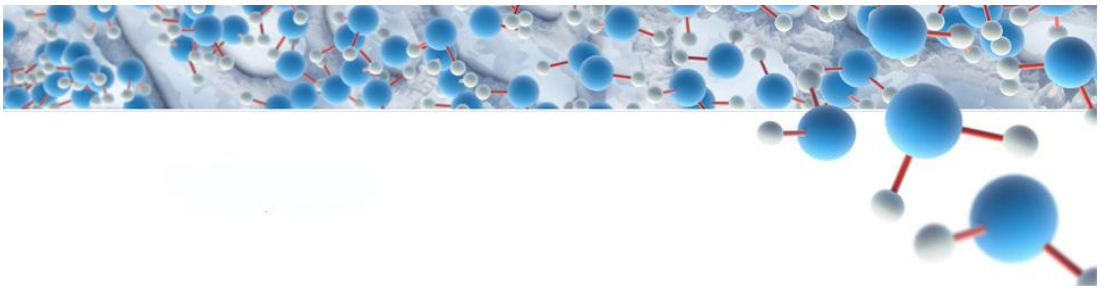

3.1. Introduction

Nanomatertials have been exploited for innumerable number of applications in industry, health care, and basic research. Engineered nanomaterials especially silver and gold nanoparticles have been attracting the attention of industry and the research community due to their unique physicochemical properties. Silver nanoparticles are used as antimicrobials in wound healing, sterilization of surgical instruments and catheters, nanosilver coatings on implantable devices like heart valves, neurological catheters, in bone cement and dental fillings (Salata, 2004). Gold nanoparticles are being used in drug delivery, cancer therapy and tumor ablation by photo thermal excitation, for stem cell tracking within the organism (Brown *et al.,* 2010, Cai *et al.,* 2008, Nagesh *et al.,* 2007). This increase in use also calls for the development of evaluation methods and safety parameters not only on various tissue somatic cell types but also on stem cells. There have been lot of reports throwing light on the adverse effects of the nanomaterials *in vitro* and *in vivo* but there are very limited studies on their effects on stem cells (both embryonic or adult). The understanding and development of stem cell technology has opened up the vistas at establishing the screening systems to study the embryotoxicity and effects on embryonic as well as adult stem cells.

3.1.1. Stem Cells

Stem cells are undeveloped cells capable of self-renewal, proliferation and differentiating into any cell type in the complex tissues present in the body of a multicellular organism. Stem cells are critical to both embryogenesis and postnatal life (Tuch, 2006). The term stem cells was first coined in 1908 by the Russian histologist Alexander Maksimov in relation to hematopoietic pluripotent cells. But it was much later, in the 1960s that there was more evidence of stem cell existence in adult neurogenesis which was a controversial revelation. Followed by this there were several reports suggesting that self-renewing cells do exist. The Nobel Prize winning work by Prof. Martin Evans and his colleagues on embryonic stem cells was an important development in using and understanding the stem cells.

3.1.2. Types of Stem Cells

Embryonic stem cells (ESCs)

Stem cells can be embryonic or non embryonic ie., adult stem cells in nature. Embryonic stem cells are derived from the inner cell mass of a blastocyst. Embryonic stem cells are totipotent and capable of differentiating into all cell types. Mouse embryonic stem cell lines were the first to be established in the cell culture by Evans *et al.*, in 1981 followed by establishment of human embryonic stem cells in 1998. Thus far at least 225 human ESCs have been established (Tuch, 2006).

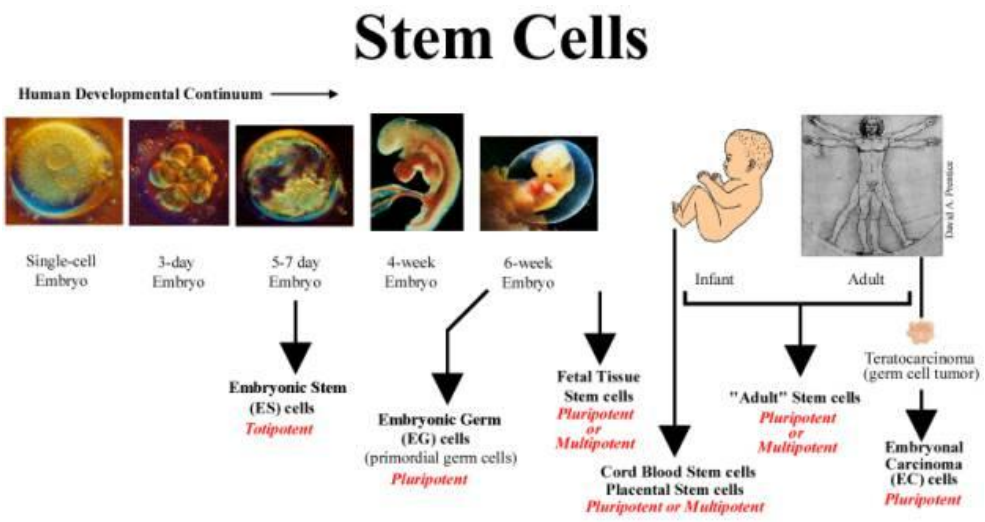

Figure 3.1 Types of Stem cells; source: www.cyhsanatomy1.wikispaces.com

Embryonic stem cells require co-culturing with feeder layer of fibroblasts. These fibroblasts are known to secrete the factors that help in maintaining the undifferentiated state. Scientists have been able to identify that the mouse ESCs require leukemia inhibitory factory (LIF) in order to remain undifferentiated in the culture conditions and removal of the same would instantly lead to the differentiation of the ESCs (Fuchs and Segre, 2000).

Adult stem cells

Adult or non embryonic stem cells are pluripotent cells that are capable of differentiating into several cell types of a particular organ system. They help maintain the integrity and function of the organs by replenishing the cells lost due to regular wear and tear. In the last twenty years it is becoming increasingly evident that every tissue has a repository of pluripotent stem cells, and that these cells help in the regular regeneration, repair and self renewal of the tissues, for example

mesenchymal stem cells, hematopoietic stem cells, neural stem cells, keratinocyte stem cells, etc., (Sell, 2005).

Induced pluripotent stem cells (iPSCs)

Recent advances in stem cell generation and culturing lead not only to the isolation and culturing of ESCs and adult stem cells but also reprogramming the somatic cells to function as stem cells. Such cells have been called induced pluripotent stem cells (iPSCs) and the stemness of these cells is conferred by expression of some of the transcription factors such as OCT4, SOX2, c-Myc, KLF4, NANOG, and LIN28 etc., (Fontes *et al.,* 2013, Yu *et al.,* 2007). The expression of a combination of any of the above mentioned factors by transfection reprograms the somatic cells to attain the de-differentiated state. So far there have been different viral vectors and episomal vectors used for reprogramming somatic cells to form induced pluripotent stem cells (Yu *et al.,* 2009). Induced pluripotent stem cells are being considered for various applications and one among them is the use of these in the safety evaluation. In the present study iPSCs have been used to look at the effects that the nanoparticles might cause on.

As is known, every tissue in an organism has some niches of stem cells, and that there would be every possibility of these cells being exposed to NPs if they are used for drug delivery, cancer therapy, stem cell tracking *in vivo*, it would be important to see how these cells are affected when they are exposed to NPs (Fereira *et al.,* 2008). Silver and gold are

being considered as candidates in stem cell tracking *in vivo* based on the Surface Enhanced Raman spectroscopy imaging (Nagesh *et al.,* 2007, Bankapur *et al.,* 2012). But, the isolation and propagation of these stem cells in itself has been a challenging task as the numbers of these cells are very low and their propagation in large numbers in cultures has also been difficult. The iPSCs provide a promising candidature in such a situation, especially in case of humans, where acquiring the various organ specific stem cells would be very difficult. The iPSCs can also be used as a replacement for ESCs as well and avoid the ethical issues. They have also been found to show similar properties as ESCs, so they can be used for *in vitro* embryotoxicity screening studies too. This helps the development of rapid and comprehensive screening system for screening various nanoparticles *in vitro*. So, in this preliminary study we have checked the effect of nanoparticles on human induced pluripotent stem cells (hiPSCs) proliferation and observed the effects of nanoparticles on the morphology and growth of randomly differentiating embryoid bodies of hiPSCs. The specific objectives of the present study are:

- Study the effect of nanoparticles on human induced pluripotent stem cells (hiPSCs) proliferation
- Studying the effects of nanoparticles on the randomly differentiated embryoid bodies of hiPSCs.

3.1. Materials and Methods

3.1.1. Materials

Phosphate buffered saline (PBS), DMEM F12, Knockout serum supplement, Fetal Bovine Serum (FBS), Penicillin and Streptomycin, non essential amino acid mix, L-glutamine, beta mercaptoethanol were purchased from Gibco BRL. Human bFGF was acquired from Peprotech Inc. and Matrigel matrix from BD biosciences. All other cell culture ware was acquired from Corning Inc. Silver nanoparticles (Ag; 10nm, 40 nm) were obtained from Nanocomposix (USA) and gold NPs (Au; 10 nm, 40 nm) were prepared from Gold (III) chloride trihydrate, procured from Sigma (St Louis, MO), by citrate reduction of $HAuCl_4$ (Sutherland and Winefordner, 1992).

3.2.2. Culturing Human Induced Pluripotent Stem Cells (hiPSCs)

The hiPSCs were derived from foetal foreskin cells and maintained as a cell line. They were co-cultured conventionally on mouse embryonic fibroblasts (MEFs) using DMEM F12 medium with 20% knockout serum, 1% Non essential amino acids, 1mM L-Glutamine, 0.1mM beta mercaptoethanol, 100ng/ml bFGF and 10,000 U/ml Pen Strep. Media was changed every day and the cells were passaged every fifth day by manual cutting. Prior to setting any experiment the cells were propagated in feeder free conditions on matrigel coated plates.

3.2.3. Cell Viability Assay

Ninetysix-well cell culture tested flat bottom plates were coated with matrigel and 2.5 x 10^3 single cell hiPSCs were seeded per well using culture

medium, supplemented with 100 ng·mL-1 bFGF. After 48 h, medium was removed completely and fresh medium containing the nanoparticles at various concentrations was added. Three days later, 20 µl of MTS and phenazine methosulphate solution was added to the medium as per the manufacturer's instructions. After 1–2 h incubation at 37°C the absorbance was measured with a TECAN spectrophotometer at 490 nm.

3.2.4. Random Differentiation for Embryoid Body Formation

Colonies were manually detached from culture plates and about 50–60 hiPSC clumps, each clump containing approximately 100–150 cells, were added onto 5% pluronic-F127 (Sigma, Steinheim, Germany)-coated V-bottom 96-well tissue culture grade plates and centrifuged. The clumps were centrifuged at 400xg for 4 min at 4°C. EBs were maintained in differentiation media containing DMEM F-12 , 20% KO-SR, 1% Non-essential amino acids, 1mM L-glutamine 0.1mM β-mercaptoethanol 10,000 U/ml Pen Strep. On day 4, EBs were picked manually transferred to pluronic (5%) coated bacteriological dishes. The embryoid bodies were maintained for 7 days on a horizontal shaker in differentiation medium containing the nanoparticles.

3.3. Results

3.3.1. Morphology and Differentiation of hiPSCs

The human induced pluripotent stem cells appear as well defined colonies with tight thick as shown in the figure 3.2. They reach full confluence in about five days and can be transferred from MEF co-cultures on to matrigel coated dishes.

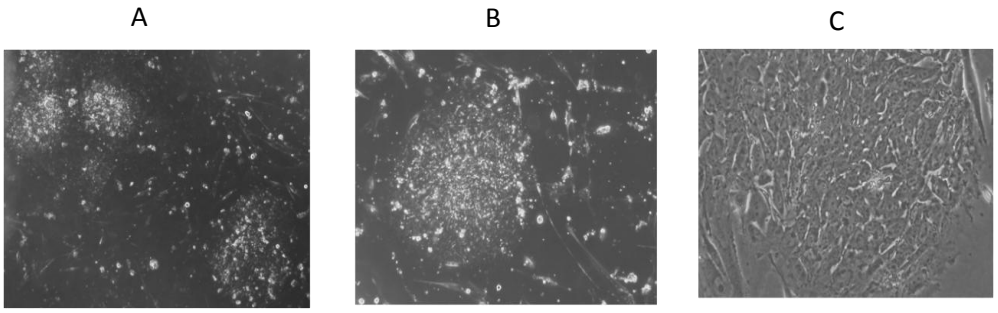

Figure 3.2. Morphology of hiPSCs at various magnifications: Colonies were observed at 2.5x (A), 4x (B) and 10x (C).

These were then maintained for 3 to 4 days before setting up further experiments. The cells showed similar morphology on the matrigel dishes but the colonies spread to form a more confluent and monolayer like appearance. The feeder free iPSCs were then used for embryoid body formation in the v-shaped 96 well dishes. These were spherical loosely formed structures that have been carefully collected manually on day2 into a 10cm perti dishes. These EBs were either unexposed and served as control or exposed to nanoparticles.

3.3.1. Effect of Nanoparticles on Proliferation of Stem Cell

The hiPSCs were exposed to silver and gold nanoparticles to determine the effect on the cell viability. The concentrations used were 0.1 – 50 µg/ml for a period of 72 hrs. The EC_{50} values for the nanoparticles treated cells after 72 h of incubation are presented in the table 3.1 below.

Table 3.1 Cell viability of hiPSCs upon exposure to nanoparticles

S.No.	Type of particle	Effective concentration 50 (EC_{50})
1.	Silver 10nm	4.5 µg/ml
2.	Silver 40nm	6.4 µg/ml
3.	Gold 10nm	26.7 µg/ml
4.	Gold 40nm	44.3µg/ml

3.3.2. Effect of Nanoparticles on Embryoid Body Formation

The size of the unexposed embryoid bodies (EBs) increased with increasing number of days and appeared intact and healthy (Figure 3.3). The embryoid bodies exposed to silver nanoparticles showed no increase in size but showed disintegration at 10 µg/ml concentration as compared to 1

µg/ml concentration. The EBs exposed to gold nanoparticles, on the other hand, showed very little change as compared to the control (Figure 3.4).

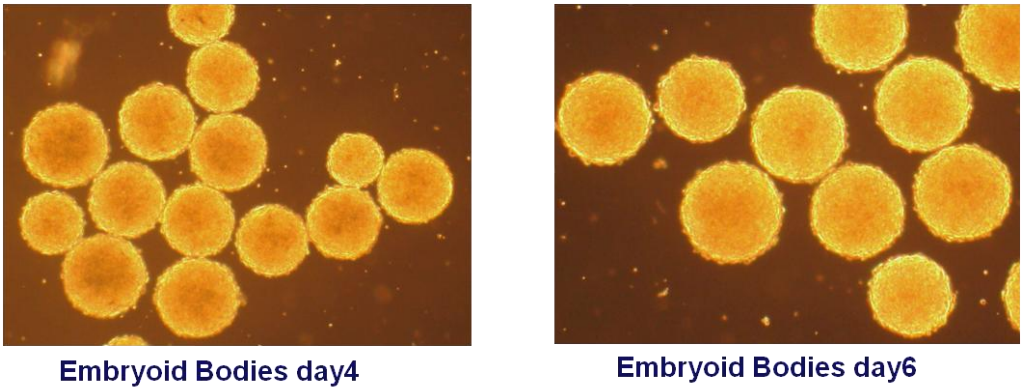

Figure 3.3. Control embryoid bodies of hiPSCs: EBs as observed on day 4 and day 6 of incubation at a magnification of 2.5X

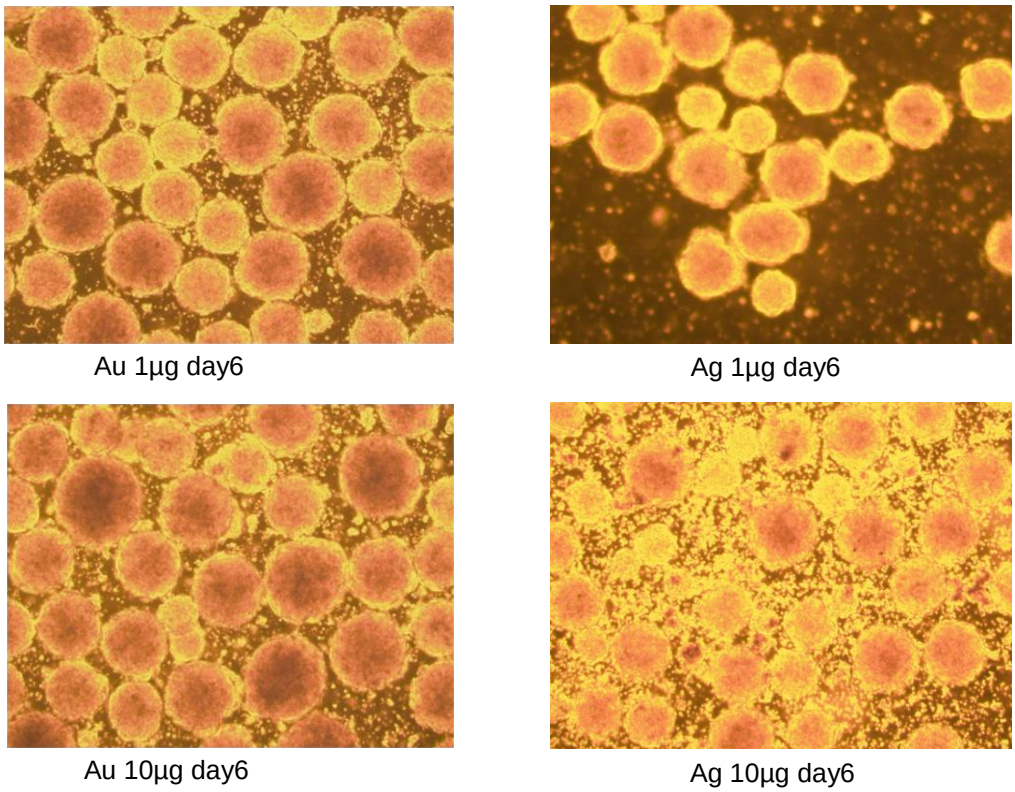

Figure 3.4. Effect of Ag and Au NPs on embryoid bodies of hiPSCs: EBs as observed on day 6 in the presence of Ag10 and Au10 NPs at 1 µg/ml and 10 µg/ml at a magnification of 2.5X.

3.4. Discussion

Nanoparticles are capable of entering the organism through various routes and can penetrate deep into the tissues. They have been shown to reach the tissues like liver, lung, blood and bone marrow (Jani *et al.,* 1990). Nanoparticles are also known to cross the blood brain barrier and blood testicular barrier as well (Takenaka *et al.,* 2001). These reports prompt that nanoparticles can penetrate into the tissues and have a greater chance of interacting with stem cells too. The interactions of the nanoparticles with the stem cells may affect the self renewal and regeneration capacities of the various tissue and organ systems, leading to the decreased viability and vigour of the organism as such. Therefore there is a need to check the effects of the nanoparticles on stem cells and the iPSCs could be a good model system.

In the present study the cell proliferation assay on iPSCs showed that silver nanoparticles have a lower IC_{50} compared to gold nanoparticles indicating that they have more cytotoxicity. Further when the embryoid bodies were exposed to the nanoparticles, silver showed more deleterious effects as compared to gold. There was increased debris in the plates containing Ag NPs at a concentration of 1 µg/ml as well and at 10 µg/ml it was much higher and kept increasing as the number of days increased. The size of the EBs had decreased with the increase in concentration as well as with time as seen in figure 3.4. On the other hand the EBs upon exposure to

gold NPs showed very little effect on size of the EBs and the EBs appeared almost normal with less debris. Gold nanoparticles are more biocompatible compared to the silver. These observations are in close agreement with the earlier reports on the silver nanoparticles showing embryotoxicity and developmental toxicity in zebrafish (Asharani *et al.,* 2008). There has been a study on human mesenchymal stem cells (hMSCs) showing that silver nanoparticles induce cytotoxicity and genotoxicity (Hackenberg *et al.,* 2011) The silver nanoparticles also had been demonstrated to have some toxicological effect on mouse embryonic stem cells (Park *et al.,* 2011).

Although the IC_{50} concentration of the silver and gold nanoparticles was much less when exposed to the stem cells, the concentration that causes the embryoid body disintegration seems to be slightly higher. This could be due to the compact mutlicelluar, multilayer structures of EBs. The nanoparticles might be affecting the outer layers of the EBs and leading to the layer by layer disintegration of the cells. The transmission electron microscopic studies would further help understand this. The effects of the nanoparticles also need to be studied at the molecular level for further detailed understanding.

Chapter 4

Biocompatibility of Nanoparticles In vivo: Studies on Mice Model

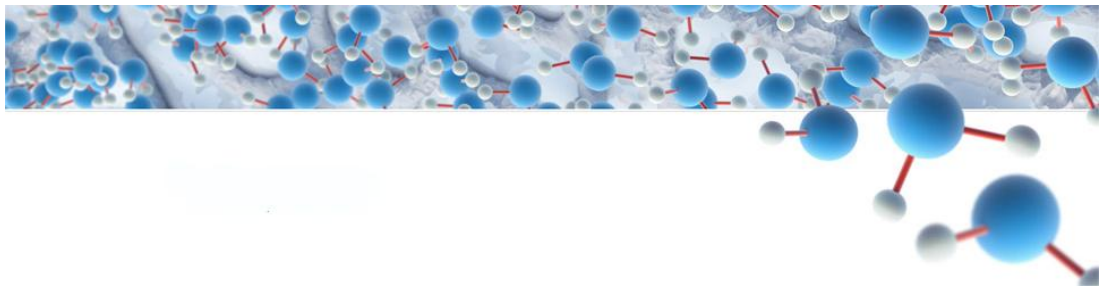

4.1. Introduction

Nanoparticles are extensively being used in a range of applications to improve the quality of the products. These include the electrical and electronic applications, bioengineered prosthesis, food packaging, sterilization of medical equipment and also in drug delivery and diagnostics. Although there has been exposure of humans to ambient ultrafine particles in the environment, the possibility was much lesser. But, with the advent of technology for synthetic and chemical methods of nanoparticles preparation and their increased use, makes it essential to understand the risks associated. In such a scenario there is a need to understand the effects that these nanomaterials might bring about when they interact with the biological systems and whole organisms. The routes of entry, the pathophysiology and the molecular mechanisms of any associated toxicity need to be well understood. Nanoparticles find their way into the body through the skin, lungs or intestinal tract, and accumulate in several organs causing adverse biological reactions by modifying the physiochemical properties of living matter (Oberdorster *et al.,* 2005). There have been several studies *in vivo* that indicated the toxicological and pathophysiological changes that are brought about by the micro and nano sized particulates (Oberdorster *et al.,* 2001).

Among the metal nanoparticles that are being used for various applications in biomedical and health care products, silver and gold top the

list. With this wide spread use of Ag and Au NPs in various applications there is a need to understand the effects they would cause to human health. There are only limited reports available on studies carried out *in vivo* and more studies need to be carried out to understand their effects so as to define the safe levels of use of these nanoparticles. Reports on the inhalation exposure of rats to silver nanoparticles for 0-7 days suggested that the nanoparticles could reach various organs including brain olfactory portion (Takenaka *et al.,* 2001). Hyun *et al.,* reported that the inhaled silver nanoparticles (13-15 nm) caused an increase of neutral mucins in the nasal mucosa in rats (Hyun *et al.,* 2008). The prolonged exposure of rats to Ag NPs (18-19 nm) brought about inflammatory response and also altered the pulmonary tissue function as reported by Sung *et al.,* (2009). There have also been reports of severe argyria that was observed in a patient who received the Ag NPs containing Acticoat wound dressing (Trop *et al.,* 2006) and upon ingestion of colloidal silver (Kim *et al.,* 2009a). There has also been a study carried out for 28 days to assess the effects of Ag NPs upon oral exposure at 30, 300 and 1000 mg/Kg body weight, where the authors report the systemic distribution of the silver nanoparticles in the rats and damage to the hepatic tissue with inflammatory cell infiltration (Kim *et al.,* 2008). An *ex vivo* study on tracheal smooth muscle cells upon exposure to Ag NPs suggested the increase in the contractile function through iNOS induction.

The study also emphasized that the Ag NPs through NO generation could cause hyper-activity and toxicity to bronchial tissues (Gonzales *et al.,* 2011).

The findings of Sonnavane *et al.,.,* 2008 revealed that intravenous injection of various sizes of gold nanoparticles showed differential organ distribution with smaller 15 nm size particles having higher bio-distribution capabilities and also were seen localising in the brain. In another study, the authors reported that Au NPs were able to cross the blood retinal barrier upon intravenous administration, but they did not find any retinal toxicity (Kim *et al.,* 2009b). Acute toxicity studies of 13 nm PEG coated Au NPs *via* intravenous administration showed induction of inflammatory genes at the transcriptional level in the liver tissue (Cho *et al.,* 2009). The same group also reported that the gold nanoparticles caused induction of phase-I xenobiotic metabolising enzymes in the liver (Cho *et al.,* 2010). The study conducted by Mironava *et al.,* (2010) showed that the cellular detrimental effects caused upon exposure of dermal fibroblasts to gold nanoparticles could be reversed by their removal.

Most of the above mentioned studies did not give a detailed insight into the effects that the silver and gold nanoparticles caused. So in the present study an attempt has been made to evaluate the effect of Ag and Au NPs of different sizes and dosages on the mice hepatic and pulmonary tissues. In the earlier studies carried out *in vitro* it is evident that the silver nanoparticles had a higher toxicological effect at low doses and they also

had a pro inflammatory effect too. They also affected the stem cell proliferation and survival of the embryoid bodies. Gold nanoparticles at the same dosage showed no induction of inflammatory effects and their effect on the stem cells was lesser compared to the silver nanoparticles. Taking into consideration of the results obtained *in vitro* the study was extended to evaluate their effects *in vivo*.

4.2. Materials and Methods

4.2.1. Materials

Nitrocellulose membrane was from Millipore (Bangalore, India). TMB/H_2O_2 and protease inhibitor cocktail were purchased from Sigma-Aldrich (Bangalore, India). Primary antibodies to COX-2, Hsp70 were from Santa Cruz Biotechnology (California, USA). All the other chemicals and reagents were purchased from local companies and are of molecular biology grade. Silver nanoparticles (Ag; 10nm, 80 nm) were obtained from Nanocomposix (USA) and gold NPs (Au; 10 nm, 80 nm) were prepared from Gold (III) chloride trihydrate, procured from Sigma (St Louis, MO), by citrate reduction of $HAuCl_4$.

4.2.2. Animals and Treatment Regimen

Adult albino mice, 5-6 week old and weighing 25–35 g were procured from National Institute of Nutrition (NIN), India. They were fed standard mice chow and water *ad libitum* in individual stainless steel wire bottom cages. The animals were kept under controlled conditions of 12-h light:dark cycle, 72° ± 5° F and 50 ± 20% relative humidity in central animal facility at the University of Hyderabad. All animal protocols for the research described here were approved by the Institutional Animal Ethics Committee. The animals were acclimatized to this environment for 4-7 days prior to the start of the study. Mice were randomly assigned in to 13 groups

of five animals each. Group I received vehicle (PBS). Group II, III, IV, V, received Ag10 nm, Ag80 nm, Au10 nm and Au80 nm respectively. Each group was further divided into three subgroups based on the dosages 0.5 mg/kg body weight, 1.0 mg/kg body weight, 2.0 mg/kg body weight, administered daily for twenty eight days. The route of administration in all the above groups was through oral gavages. The dosages of nanoparticles were chosen based on a pilot dose response study conducted in the laboratory. Animals were continuously monitored for general health. The mice were sacrificed humanely, after 28 days of treatment.

4.2.3. Tissue Collection and Storage

Following treatment, animals were humanely scarified using diethyl ether anesthesia, liver and lung specimens were dissected out and fixed in Bouin's solution and stored in 70% ethanol. For Western blot analysis and RT-PCR analysis tissues were first snap-frozen in liquid nitrogen and stored at -80 ^{o}C. The ROS, nitrite and antioxidant enzymes assays were performed immediately.

4.2.4. Estimation of ROS

The levels of ROS were determined by the method described elsewhere (Montoliu *et al.*,., 1994). An appropriate volume of freshly prepared tissue homogenate was diluted in 100 mM potassium phosphate

buffer (pH 7.4) and incubated with final concentration of 5 µM dichlorofluoroscein diacetate for 60 min at 37 °C. The dye loaded samples were centrifuged at 12,500 x g for 10 min at 4 °C. The fluorescence measurements were performed on a Hitachi spectrofluorimeter at 488 nm for excitation and 525 nm of emission wave lengths. The levels were represented as fold increase or decrease from control group.

4.2.5. Nitrite Estimation

Nitric oxide (NO) was measured in terms of Nitrite levels. Nitrite levels were determined in the freshly collected tissue lysates. Briefly, 100 µl of tissue lysate was mixed with 100 µl of Griess reagent (equal volumes of 1% (w/v) sulfanilamide in 5% (v/v) phosphoric acid and 0.1% (w/v) naphtylethylenediamine-HCl), and incubated at room temperature for 10 min. Absorbance was then measured at 540 nm using microtiter plate reader (Bio-Tek Instruments). Tissue lysis buffer was used as blank in the experiments. Nitrite levels in samples were determined using a standard sodium nitrite curve.

4.2.6. Catalase Activity Assay

The assay mixture consisted of 50mM phosphate buffer (pH 7.0), 19 mM hydrogen peroxide, and 40 ug protein containing tissue lysate in a final volume of 1.0 ml per measurement. Changes in absorbance were recorded

at 240 nm. Catalase activity was calculated in terms of nmol of hydrogen peroxide consumed/mg of protein/min. (Claiborne, 1985)

4.2.7. Peroxidase Activity Assay

The endogenous catalase activity was assayed as described by Franz *et al.*, 1999 with slight modification. Briefly, 40 µg of protein (tissue lysate) was taken in a microtitre plate well and made upto 100 µL with 100 mM phosphate buffer. To this 100 µL of 1X 30% TMB/H_2O_2 in 50 mM citrate buffer was added. The plate was incubated at room temperature for 15 minutes. Reaction was stopped with 100 µL of 1.5 N H_2SO_4 and absorbance recorded at 415 nm in an ELISA plate reader.

4.2.8. Preparation of Tissue Extracts and Immunoblot Analysis

Tissues from 13 treated groups were minced and homogenized in lysis buffer (20 mM Tris, 1 mM EDTA, 150 mM NaCl, 1% NP-40, 0.5% sodium deoxycholate, 1 mM β-glycerophosphate, 1 mM sodium orthovanadate, 1 mM PMSF, 10 µg/ml leupeptin, 20 µg/ml aprotinin and phosphatase inhibitor cocktail 1 and 2 with 100 fold dilution). After 30 min of shaking at 4 ^oC, the mixtures were centrifuged (10,000 x g) for 10 min, and the supernatants were used as the whole-cell extracts. The protein content was determined according to the Bradford method (Bradford, 1976). 70 µg of protein from each treatment was resolved on 8-12% SDS-PAGE gels

along with protein molecular weight standards, and then transferred onto nitrocellulose membranes. Membranes were stained with 0.5% Ponceau *S* in 1% acetic acid to check the transfer. The membranes were blocked with 5% w/v nonfat dry milk and then incubated with the primary antibodies in 10 ml of antibody-diluted buffer (1X Tris-buffered saline with 1% milk powder) with gentle shaking at 4 ^{o}C for 8-12 h and then incubated with peroxidase conjugated secondary antibodies. Signals were detected by using peroxidase substrate, TMB/H_2O_2. Equal protein loading was detected by probing the membrane with β-actin antibodies.

4.2.9 Histopathology and Ultra-structural Observations

Tissue histology studies were carried out in the thirteen groups of mice. Small pieces of liver tissue fixed in Bouin's solution and stored in 70% ethanol were dehydrated in graded ethanol, and embedded in paraffin. After embedding in paraplast, the excess paraplast was trimmed off and the blocks were fixed on the microtome and 5 μm sections were cut using a rotary microtome. The sections were stained with haematoxylin-eosin and observed under a light microscope at various magnifications to verify the structural integrity. The samples were fixed in 2.5% gluteraldehyde for the TEM ultrastructural studies. The tissue samples were sectioned into 50-70 nm ultramicrotome slices stained and observed under the FEI Technai G Transmission Electron Microscope.

4.2.10. Statistical analysis

Data reported as the mean +/- SE of three independent experiments. Statistical analysis of differences was carried out by one-way analysis of variance (ANOVA). A P-value less than 0.05 was considered to indicate significance.

4.3. Results

4.3.1. ROS and Nitric Oxide Levels in Hepatic and Pulmonary Tissues of Animals Exposed to Ag and Au NPs.

The hepatic and pulmonary tissue lysates of animals exposed to Ag and Au NPs of different sizes and concentrations were estimated for ROS. The ROS generation in the hepatic tissues was observed to be dose dependent both in case of Ag as well as Au NPs treated animals (Figure 4.1A). There was a 7 fold increase compared to the control in the animals exposed to Ag80 NPs at a concentration of 2 mg/Kg body weight.

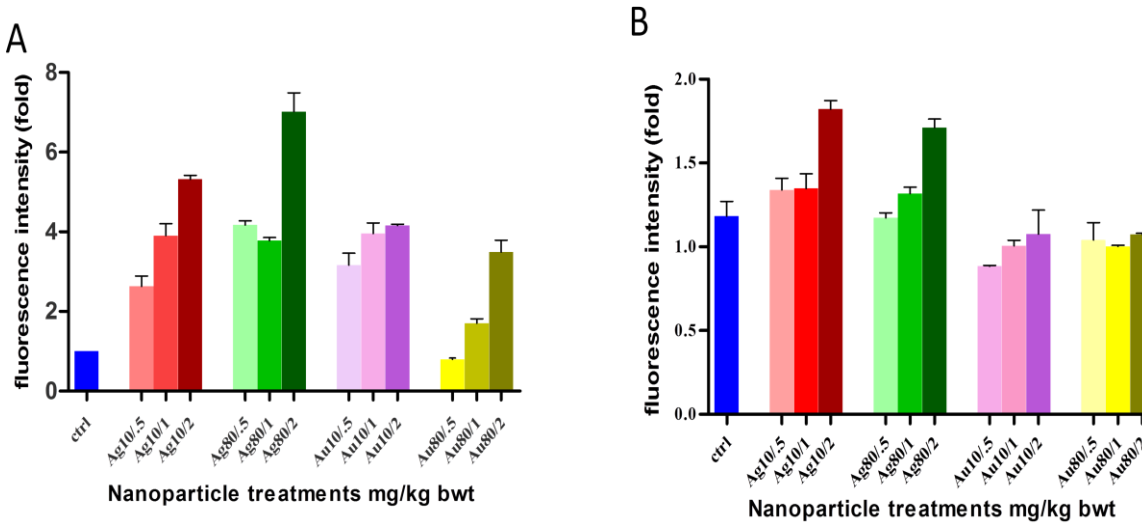

Figure 4.1. Effect of Ag and Au NPs on intracellular ROS. Fold change of ROS levels in the (A) Hepatic and (B) Pulmonary tissues of animals exposed to Ag10, Ag80, Au10 and Au80 NPs at different dosages.

ROS levels in the pulmonary tissue lysates also increased in a dose dependent manner (Figure 4.1B). In this case the fold change was not observed to be as high as was seen in case of hepatic tissue. And also the Au

NPs treated animals did not have a notable change in the ROS levels compared to the control. The NO levels as determined by the nitrite concentration in the hepatic and pulmonary tissue lysates were altered only mildly in both hepatic and pulmonary tissues (Figure 4.2). The higher doses of Ag 10 and Ag 80 NPs treatment showed a notable level of NO induction in both hepatic and pulmonary tissues. The hepatic and pulmonary tissue lysates of animals treated with Au 10 showed a slight induction of NO at the higher concentration of treatment but the ones treated with Au 80 NPs did not induce NO production.

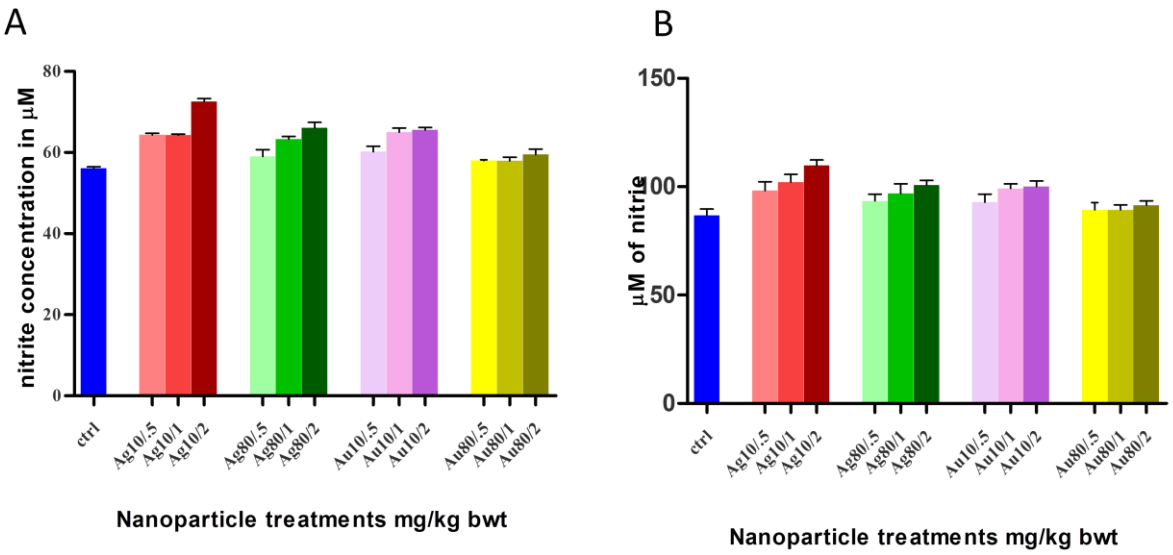

Figure 4.2. Effect of Ag and Au NPs on nitric oxide generation: Nitrite levels in (A) Hepatic and (B) Pulmonary tissues of animals exposed to Ag10, Ag80, Au10 and Au80 NPs at different dosages

4.3.2. Effect of Silver and Gold Nanoparticles Exposure on the Antioxidant Enzyme Activities

The catalase and peroxidase enzyme activities were assayed in the hepatic and pulmonary tissue lysates. The activity of the catalase decreased slightly in both hepatic as well as pulmonary tissues. The decrease was dose dependent in case of Ag10 and Ag80 NPs treated animals (Figure 4.3). Au 10 and Au 80 NPs, on the other hand, did not cause a change in the activities of catalase and peroxidase as compared to the control.

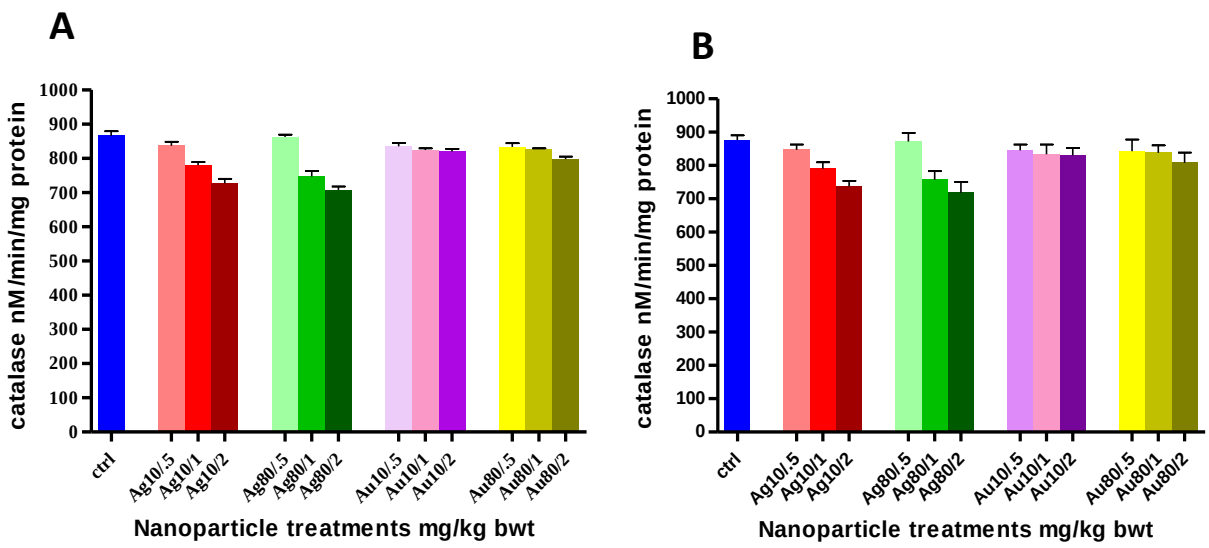

Figure 4.3. Effect of Ag and Au NPs on Catalase activity: Catalase enzyme activities in the (A) Hepatic and (B) Pulmonary tissue lysates of animals exposed to Ag10, Ag80, Au10 and Au80 NPs at different dosages.

The peroxidase activity showed a slight dose dependent decrease in the hepatic tissue of Ag10 and Ag80 treated animals. In the pulmonary tissue the peroxidase enzyme activities showed a decrease but not in dose dependent manner. However size dependent effect was observed. The Ag10

NPs showed a slightly higher drop in the enzyme activities as compared to the Ag80 NPs (Figure 4.4). Au 10 and Au 80 exposure did not cause any alteration of the peroxidase activity in both hepatic and pulmonary tissues.

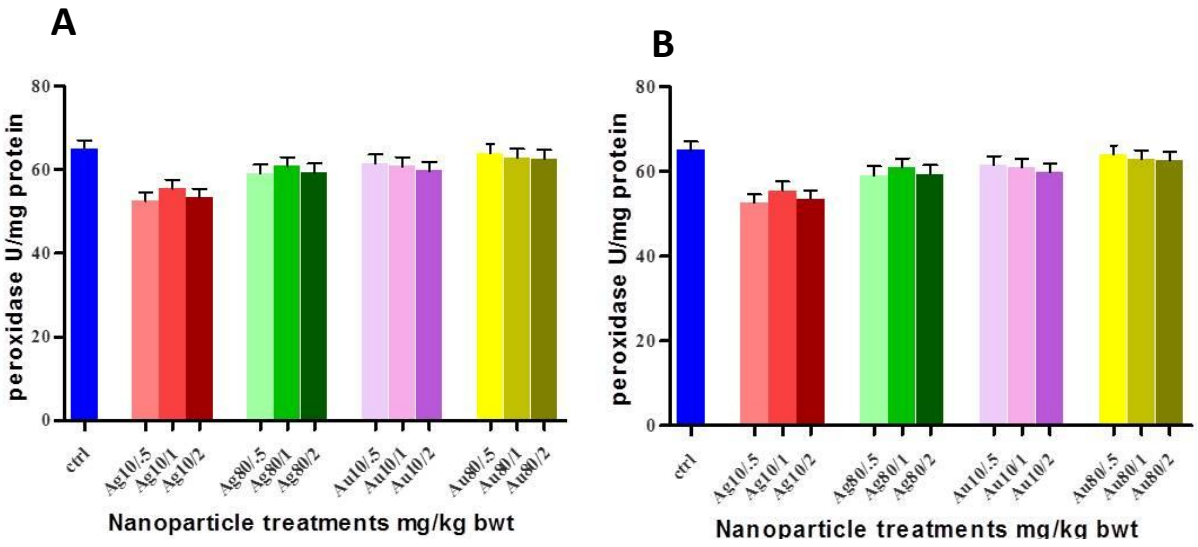

Figure 4.4. Effect of Ag and Au NPs on Peroxidase activity: Peroxidase enzyme activities in the (A) Hepatic and (B) Pulmonary tissue lysates of animals exposed to Ag10, Ag80, Au10 and Au80 NPs at different dosages.

4.3.3. Effect of Ag and Au NPs on the COX-2 and Hsp70 Expression in Hepatic Tissue

The Ag NPs treated animals showed an induction of COX-2 and Hsp70 starting at the 0.5 mg/Kg body weight in the hepatic tissue. There was a dose dependent increase in the effects observed in the animals exposed to Ag NPs. The size dependent effects were not very prominent. Au NPs treatment, on the other hand, did not induce COX-2 but there was a slight increase in Hsp70 in the animals exposed to Au10 NPs at 1 mg/Kg body weight and 2mg/Kg body weight (Figure 4.5).

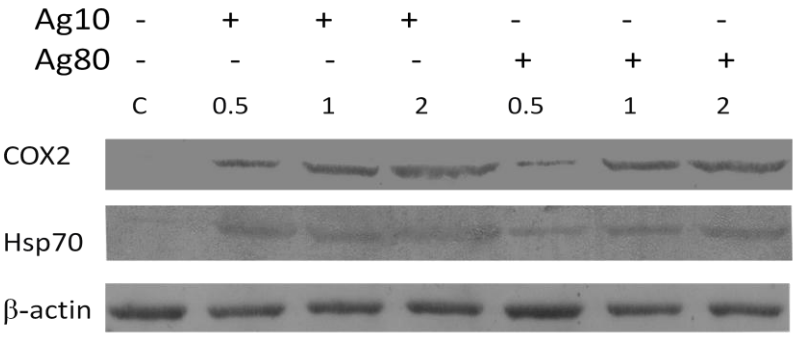
Ag10 - + + + - - -
Ag80 - - - - + + +
C 0.5 1 2 0.5 1 2
COX2
Hsp70
β-actin

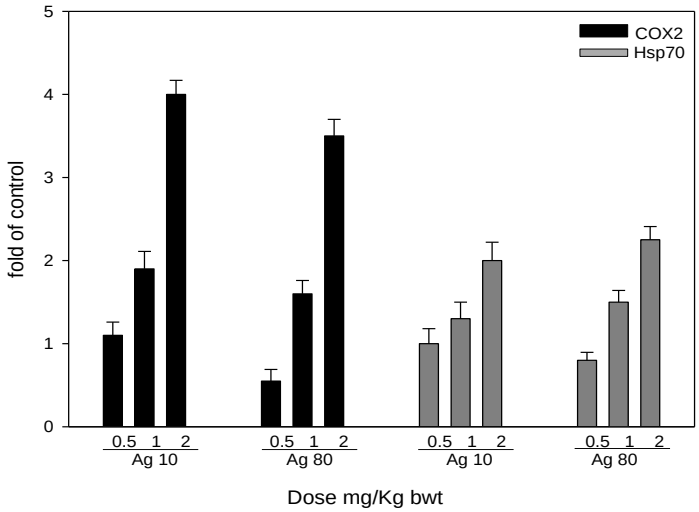
COX2
Hsp70
fold of control
0 1 2 3 4 5
0.5 1 2
Ag 10
Ag 80
Dose mg/Kg bwt

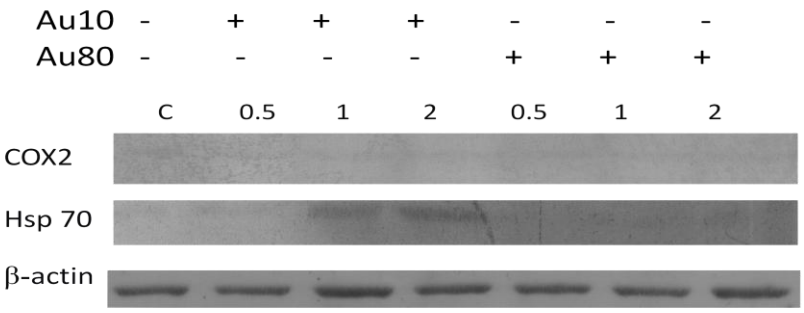
Au10 - + + + - - -
Au80 - - - - + + +
C 0.5 1 2 0.5 1 2
COX2
Hsp 70
β-actin

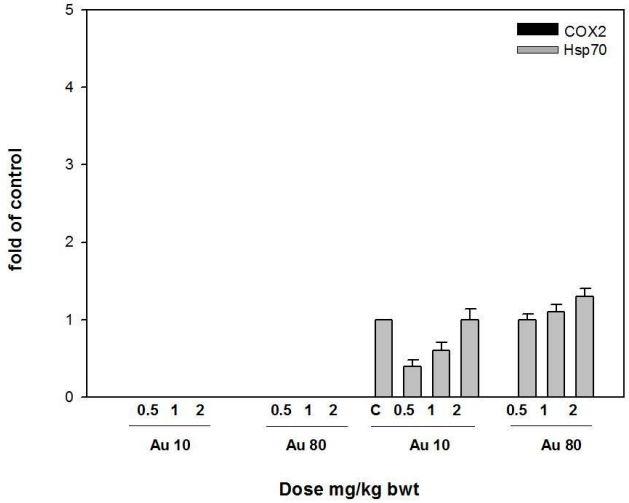
COX2
Hsp70
fold of control
0 1 2 3 4 5
0.5 1 2
Au 10
Au 80
C 0.5 1 2
Dose mg/kg bwt

Figure 4.5. Effect of Ag and Au NPs on expression of COX-2 and Hsp70 in hepatic tissue: Western blot analyses of COX-2 and Hsp70in the hepatic tissue lysates of animals exposed to Ag10, Ag80, Au10 and Au80 NPs. Bar graphs represent the densitometric values corresponding to the COX-2 and Hsp70 expression.

4.3.4. Effect of Ag and Au NPs on the COX-2 and Hsp70 Expression in Pulmonary Tissue

The COX-2 and Hsp70 expression was induced in the pulmonary tissues in a dose dependent manner. The induction in the expression of COX-2 and Hsp70 was observed in the three dosages used in case of animals exposed to Ag NPs. In animals exposed to Au NPs there was no induction of COX-2 but there was a slight increase in Hsp70 in Au80 NPs treated animals (Figure 4.6).

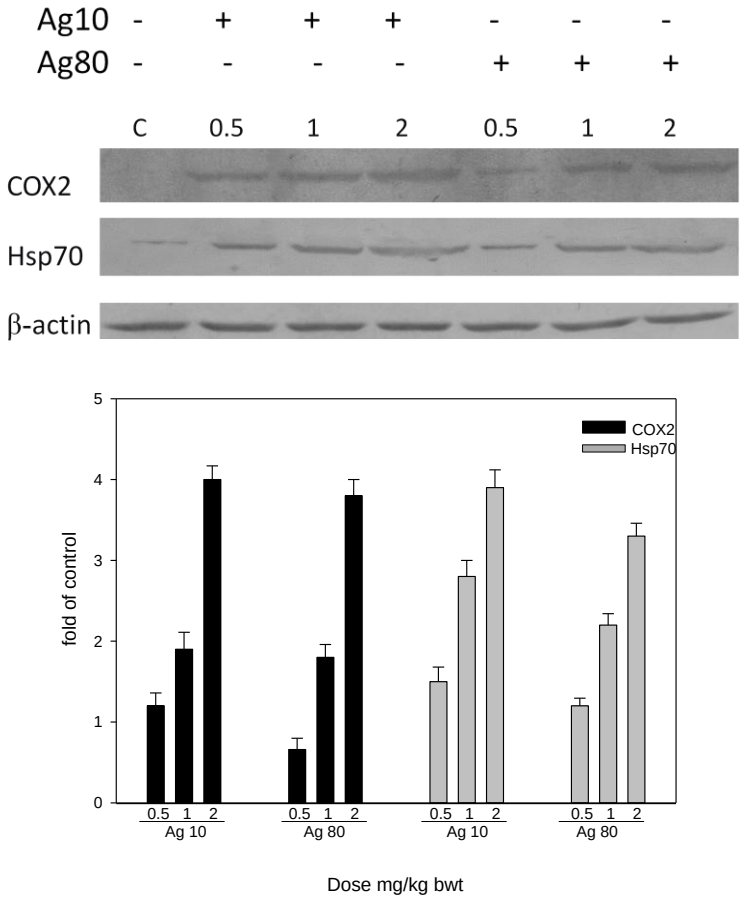

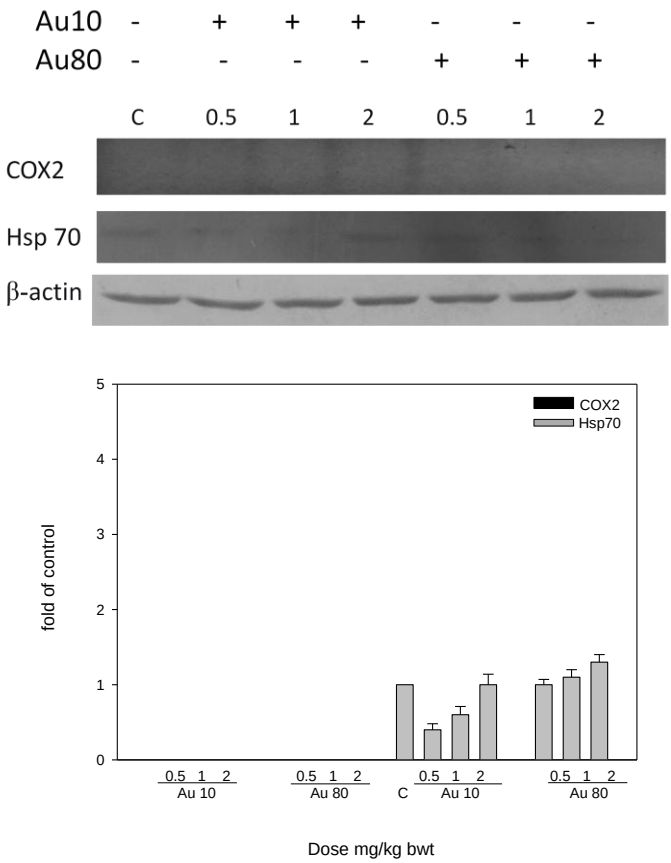

Figure 4.6. Effect of Ag and Au NPs on expression of COX-2 and Hsp70 in pulmonary tissue: Western blot analyses of COX-2 and Hsp70in the pulmonary tissue lysates of animals exposed to Ag10, Ag80, Au10 and Au80 NPs. Bar graphs represent the densitometric values corresponding to the COX-2 and Hsp70 expression.

4.3.5. Histopathological and Ultra Structural Changes in Hepatic Tissue of Animals Exposed to Ag and Au NPs

The hepatic tissues of animals exposed to Ag NPs showed centrizonal necrosis and large infiltration of cells. The inter-cellular gaps also had increased and these spaces were filled with inflammatory cells (Figure 4.7). The ultra structural observations showed a massive distortion in the morphology of the hepatocytes and loss of cellular organelles (Figure 4.8).

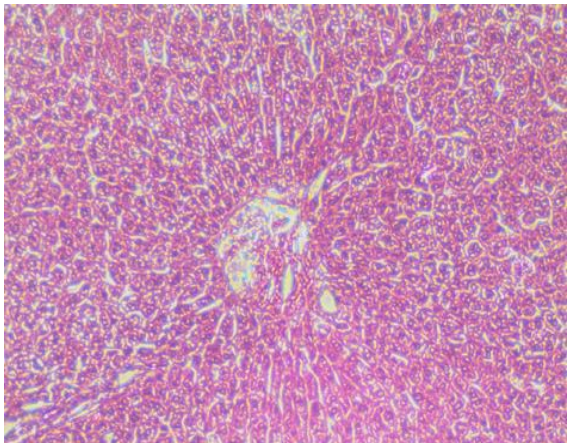

Control

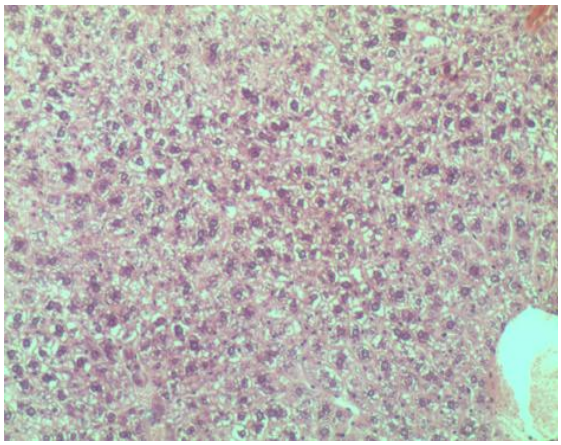

Ag 10

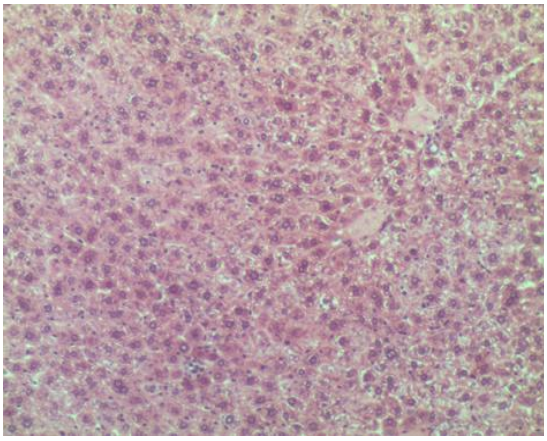

Au 10

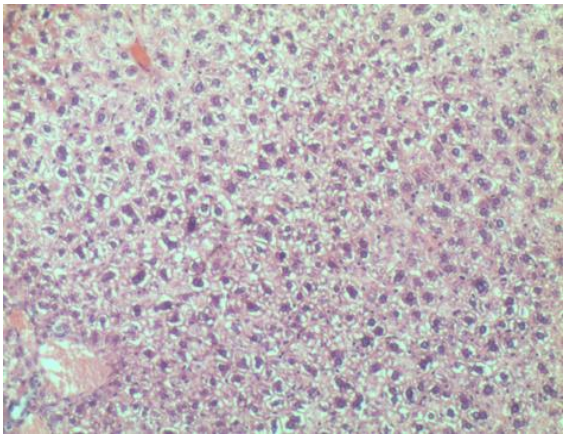

Ag 80

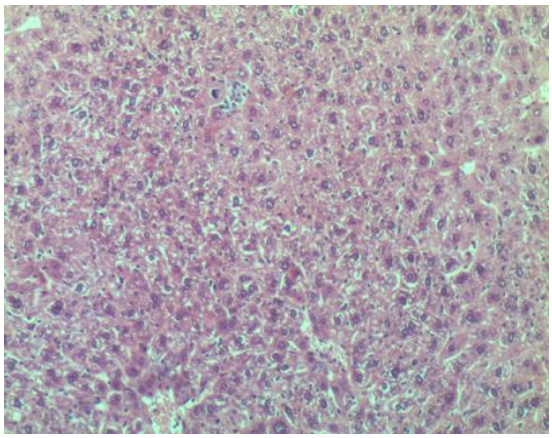

Au 80

Figure 4.7. Effect of Ag and Au NPs on the histology of hepatic tissue. *Histopathology of hepatic tissues of animals exposed to Ag10, Ag80, Au10 and Au80 NPs. Untreated animal tissue was considered as control. Images were obtained at 20X magnification.*

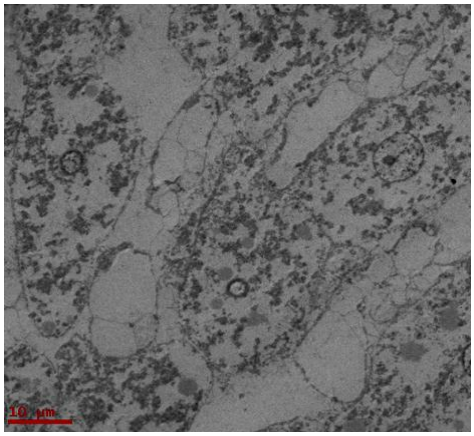

Control

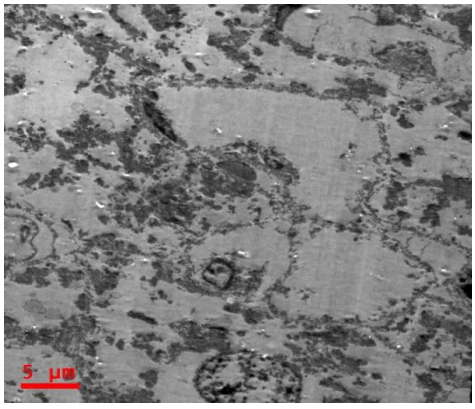

Ag 10

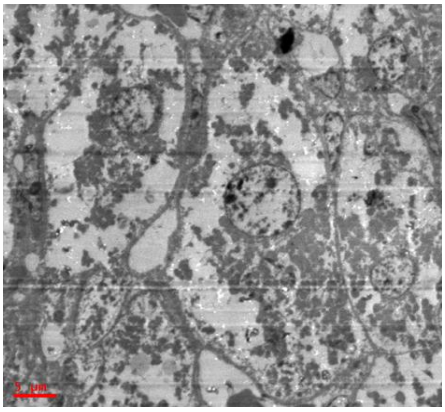

Au 10

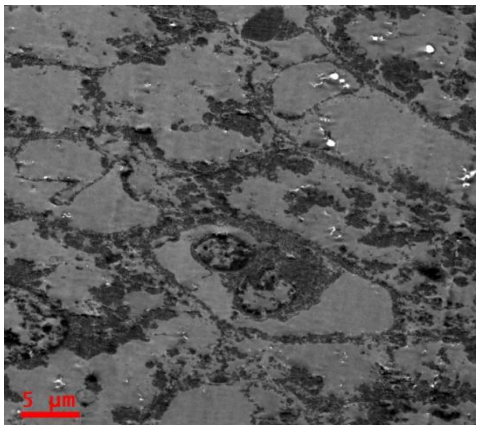

Ag 80

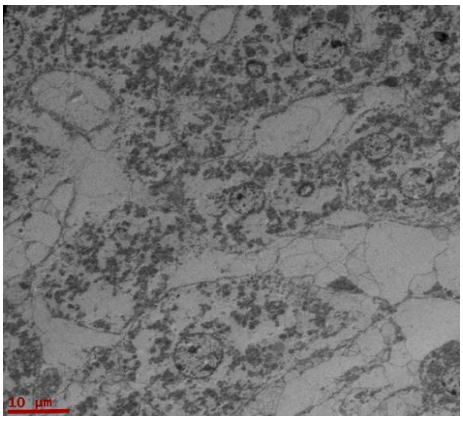

Au 10

Figure 4.8. Effect of Ag and Au NPs on the cellular ultrastructure of hepatic tissue. TEM micrographs of hepatic tissues of animals exposed to Ag10, Ag80, Au10 and Au80 NPs. Untreated animal tissue was considered as control. Images acquired at 100kV resolution

These effects were more drastic with the increasing dosages. There was also a size dependent effect where the lower sizes of nanoparticles showed more drastic effects compared to the higher sizes. The hepatic tissues of animals exposed to Au NPs, on the other hand, showed no changes compared to the control.

4.3.6. Histopathological and Ultra Structural Changes in Pulmonary Tissue of Animals Exposed to Ag and Au NPs

The pulmonary tissues of animals exposed to Ag NPs showed peribronchial infiltration of cells. The alveolar lining appeared to have collapsed with a decrease in the alveolar space. There was nodal accumulation of inflammatory cells (Figure 4.9). The ultra structural observations showed substantial deformation in the morphology of the pneumocytes and loss of cellular organelles (Figure 4.10). These effects were more drastic with the increasing dosages. There was also a size dependent effect where the lower sizes of nanoparticles showed more drastic effects compared to the higher sizes. The pulmonary tissues of animals exposed to Au NPs, on the other hand, showed no changes compared to the control.

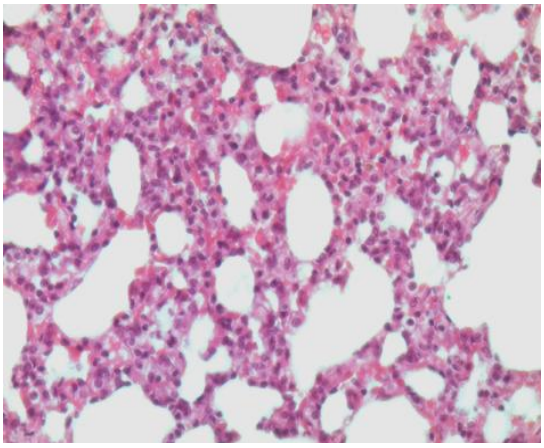

Control

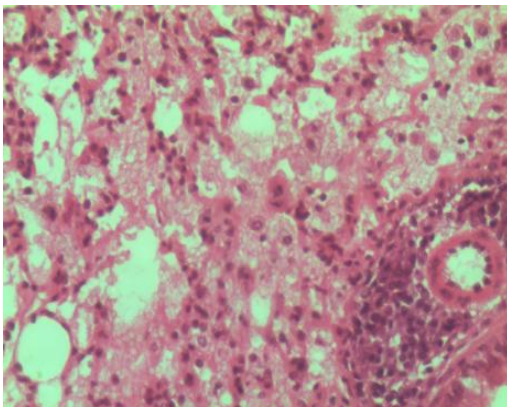

Ag 10

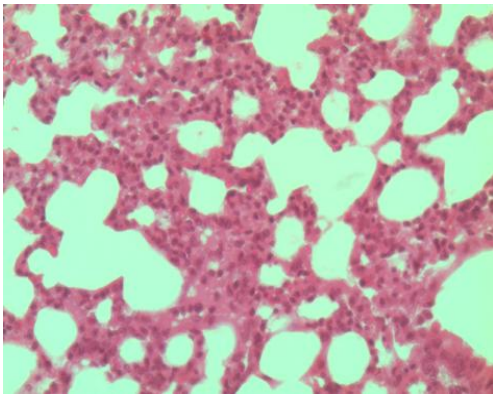

Au 10

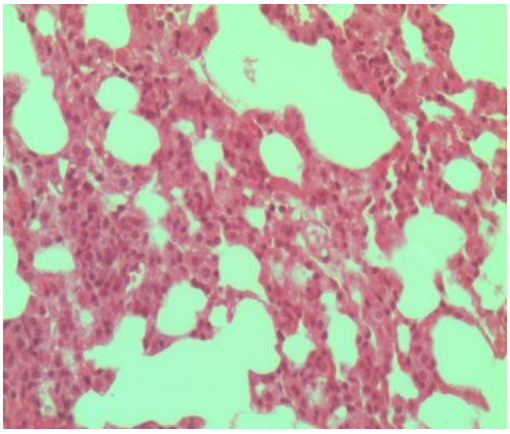

Ag 80

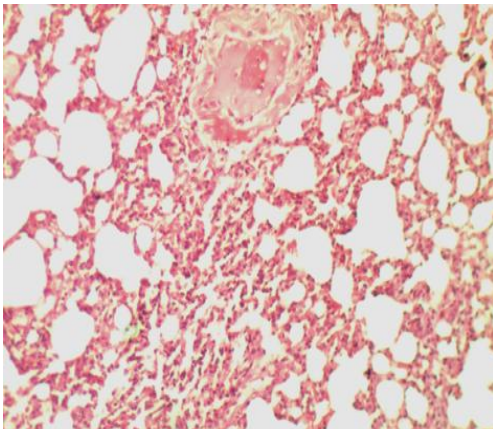

Au 80

Figure 4.9. Effect of Ag and Au NPs on the histology of pulmonary tissue: *Histopathology of pulmonary tissues of animals exposed to Ag10, Ag80, Au10 and Au80 NPs. Untreated animal tissue was considered as control. Images taken at 20X magnification*

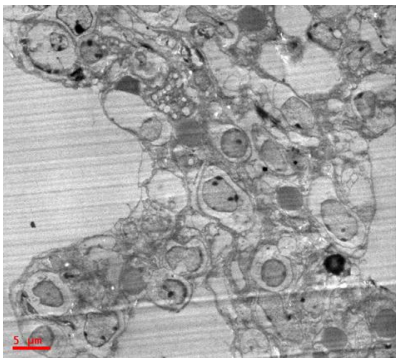

Control

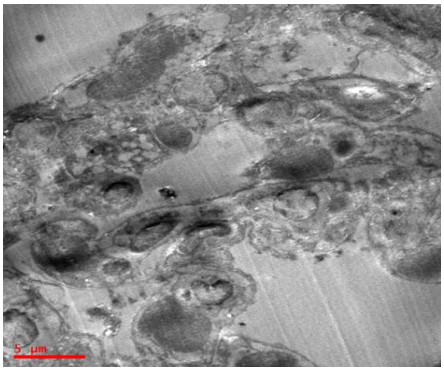

Ag 10

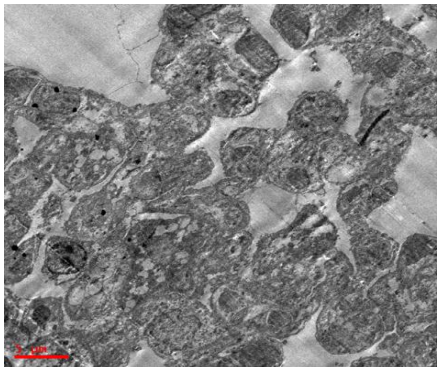

Au 10

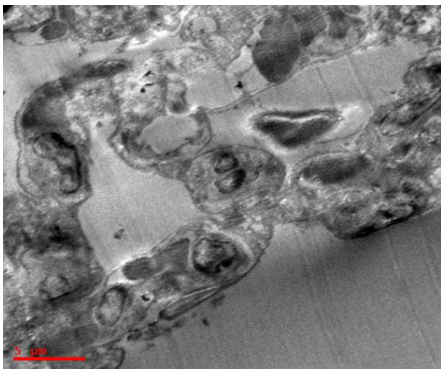

Ag 80

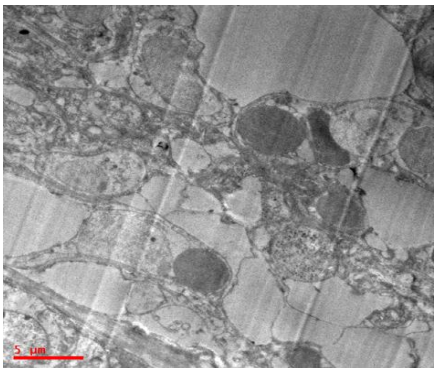

Au 80

Figure 4.10. Effect of Ag and Au NPs on the cellular ultrastructure of pulmonary tissue: TEM micrographs of pulmonary tissues of animals exposed to Ag10, Ag80, Au10 and Au80 NPs. Untreated animal tissue was considered as control. Images acquired at 100 kV resolution.

4.4. Discussion

Nanoparticles have the capacity to enter the organism through various routes and bio-distribute themselves systemically, also crossing the blood brain barrier (Takenaka *et al.,* 2001). They were also seen causing histopathological changes in liver (Kim *et al.,* 2008). In our present study, there was a significant increase in ROS, and decrease in antioxidant enzyme activities in the tissues of animals exposed to Ag NPs. The nitric oxide levels also increased in Ag NPs treated animals that seem to correlate with the earlier reports by Kim *et al.,* (2008). But in the present study these effects were observed at much lower concentrations of exposure to Ag NPs as opposed to the earlier reports. In addition, the expression of one of the major inflammatory markers, Cyclooxygenase-2 (COX-2), was induced in the hepatic and pulmonary tissue of mice exposed to 0.5 mg/kg bodyweight of Ag NPs treatment. The expression levels of COX-2 increased in a dose dependent manner. In a study on the effects of silica nanoparticles the authors reported that there was induction of oxidative stress mediated COX-2 expression (Park and Park, 2009). Studies on different forms of ultrafine nanoparticles also caused the ROS generation and induction of inflammatory conditions leading to cytotoxic effects (Brown *et al.,* 2004, Hiura *et al.,* 1999). Similarly, the stress responsive protein Hsp70 had also been induced in animals treated with Ag NPs (Grodzik *et al.,* 2009). Further, the histopathological and ultrastructural observations also revealed that

there was extensive damage in both hepatic and pulmonary tissues with inflammatory cell infiltration, in animals exposed to Ag NPs. There was a complete loss of cellular morphology of hepatocytes at the higher concentration of Ag NPs exposure. The nanoparticles were seen to localise in all the cellular organelles. These observations correlate well with our earlier studies on macrophages *in vitro* (chapter1). It was observed that the effects of Ag NPs were much higher in hepatic tissue compared to that on the pulmonary tissues, firstly, because of the route of administration which was oral and secondly because hepatic tissue is the sight of xenobiotic metabolism. Gold nanoparticles, on the other hand, showed no or very minimal effects compared to silver nanoparticles, tested under same conditions. Exposure to Au NPs did not bring about any notable change in the antioxidant activities although they caused only a slight induction of ROS and Hsp70.

Although there have been reports of number of *in vitro* studies, they do not give a complete picture of the physiological changes that the nanoparticles might bring about in the whole organisms. It is also important to evaluate the effects of these nanoparticles *in vivo* so as to find a better correlation to the effects they would cause in humans. Several studies *in vivo* on mice and rat models so far looked at the toxicological effects that the silver and gold nanoparticles might bring about. But these studies have used very high concentrations of the nanoparticles which may not be

regularly encountered, be it as drug delivery agents or in sterilizing and food packaging industries. As it would be more appropriate to look at the effects of sub-lethal doses of nanoparticles we used dosages ranging from 0.5 mg/Kg body weight to 2 mg/Kg body weight. The present study also provides evidence for the mechanisms for NPs induced tissue damage, in terms of inflammatory markers, ROS generation and impaired antioxidant defences. The oral route of administration of nanoparticles was chosen for the study; as there could be every chance of accidental ingestion of these nanoparticles. And also since gold and silver nanoparticles are considered as candidates for drug delivery and the most facile, often used route of administration of any drug would be giving it orally in the form of capsules or tablets.

In conclusion, the effects of Ag and Au nanoparticles *in vivo* in the present study correlate well with the *in vivo* studies (chapter 1). The results obtained in the present study indicate that the Au NPs have better biocompatibility with no or minimal side effects at the similar doses tested in comparison to Ag NPs.

Summary & Conclusions

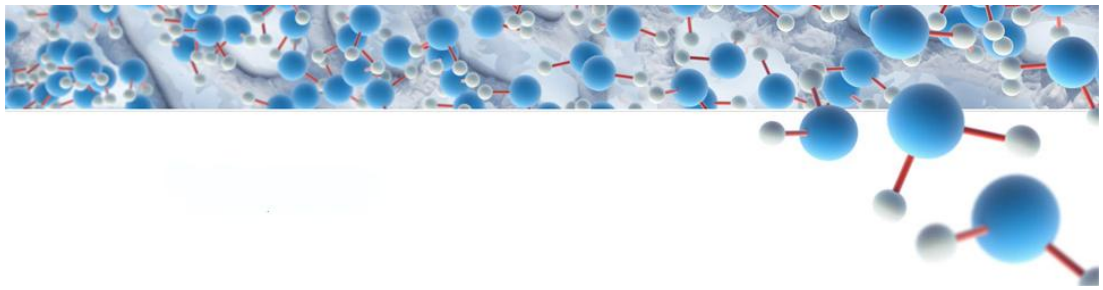

Summary and Conclusions

Nanomaterials have unique physicochemical properties that result from the combination of their small size, chemical composition, surface structure, solubility, shape, and aggregation. As we recognize new uses for materials with these special properties, the number of products containing such nanomaterials and their promising applications continue to grow exponentially. Nanomaterials are already being used or tested in a wide range of consumer products such as sunscreens, composites, medical and electronic devices, and are also being used as chemical catalysts. In addition the metal nanoparticles are being explored in biological sciences as well which include biosensing (Nam *et al.,* 2003), cellular imaging (Tkachenko *et al.,* 2003), drug/DNA delivery and cancer therapeutics (Hirsch *et al.,* 2003). However, some of the same special properties that make nanomaterials useful can also cause some side effects to humans and may have impact on the environment (Brown *et al.,* 2001).

While it is likely that most of the nanomaterials are safe, the unique properties of nanomaterials and how they may interact with living cells created considerable attention recently. Importantly, the substances that are inert in bulk form may be toxic at nanosize, due to their altered chemical and physical properties (Nel *et al.,* 2006; Oberdorster *et al.*, 2005), arguing that most

of the nanomaterials must be methodically evaluated for their toxic potential. The NPs have been reported to induce a pro-oxidant environment in the cells, causing an imbalance in the cellular energy system dependent redox potential and thereby leading to adverse biological consequences, ranging from the initiation of inflammatory pathways to cell death (Braydich-Stolle, *et al.,* 2005; Carlson *et al.,* 2008; Hsin *et al.,* 2008; Hussain *et al.,* 2005). Many studies have demonstrated the ability of nanoparticles to generate reactive oxygen species (ROS) in a cell-free environment (Brown *et al.,* 2001; Stone *et al.,* 1998; Wilson *et al.,* 2002). This oxidative stress may be linked to the induction of signaling pathways (Stone *et al.,* 2000) which lead to pro-inflammatory gene expression in macrophages (Brown *et al.,* 2004).

As it is increasingly evident that every tissue in an organism has some niches of stem cells, there would be every possibility of these cells being exposed to NPs if they are used for drug delivery, cancer therapy, stem cell tracking *in vivo*, it would be important to see how these cells are affected when they are exposed to NPs (Fereira *et al.,* 2008). Silver and gold nanoparticles are being considered as candidates in stem cell tracking *in vivo* based on the Surface Enhanced Raman spectroscopy imaging (Nagesh *et al.,* 2007, Bankapur *et al.,* 2012). But, the isolation and propagation of these stem cells in itself has been a challenging task as the number of these cells is very low and their propagation in large numbers in cultures has also been difficult. The iPSCs

provide a promising candidature in such a situation, especially in case of humans, where acquiring the various organ specific stem cells would be very difficult. The iPSCs can also be used as a replacement for ESCs as well and avoid the ethical issues. They have also been found to show similar properties as ESCs, so they can be used for *in vitro* embryotoxicity screening studies too. This helps the development of rapid and comprehensive screening system for screening various nanoparticles *in vitro*. So, in this preliminary study we have checked the effect of nanoparticles on human induced pluripotent stem cells (hiPSCs) proliferation and observed the effects of nanoparticles on the morphology and growth of randomly differentiating embryoid bodies of hiPSCs.

Recently, a number of studies have shown nanoparticles induced toxicity in different organs of animal models (Chen *et al.,* 2006; Donaldson *et al.,* 2006; Hussain *et al.,* 2006; Lam *et al.,* 2004). These studies at large addressed the toxicological effects, so we took up the studies on the mouse model to see the effects of nanoparticles at lower concentrations, especially, on the inflammatory parameters. The following are the objectives of the present study.

- Evaluation of inflammatory effects of nanoparticles on the macrophage cell line, RAW. 264.7.

- Understanding the global differential proteome expression of macrophages (RAW 264.7) upon exposure to silver and gold nanoparticles and identification of other key players involved.
- Effect of silver and gold nanoparticles on human induced pluripotent stem cells (hiPSCs).
- Evaluation of the effects of silver and gold nanoparticles *in vivo*.

i. Nanoparticles Induce Inflammatory Responses and Oxidative Stress

Macrophages the front line of immune cells that are involved in the inflammatory responses of an organism were chosen for the study. The macrophages were exposed to nanoparticles at various concentrations and for different time points. The nanoparticles were characterized using TEM, DLS and zeta potential and found that they were uniformly dispersed, ranging in their specified sizes and were discoid or spherical. The nanoparticles were well dispersed and had no aggregations as evidenced by the zeta potential results.

The effective concentrations (EC_{50}), of all the nanoparticles were calculated at 48 hours time point. Silver nanoparticles (Ag) showed lowest EC_{50} of 13.5 µg/ml, followed by Aluminium (Al), carbon black (CB) and carbon coated silver (CAg). Gold nanoparticles (Au NPs), on the other hand, were

least toxic with EC_{50} approximately 100 µg/ml. Upon exposure to Ag, Al, CB and CAg NPs, marked changes were also observed, where cells became more swollen, with vacuoles, irregular membrane integrity, and loss of adherence capability. The morphological changes induced were more intense in cells exposed to silver NPs when compared to Al, CB and CAg NPs. Exposure to gold nanoparticles did not bring about such changes. The TEM micrographs have evidently indicated the intracellular presence of nanoparticles. They were distinctly present in vacuoles, cytoplasm and some nanoparticles were seen dispersed in nucleus too. It was observed that the nanoparticles were well dispersed within the cell. There was no considerable aggregation of the particles observed, which suggests that the pro-inflammatory effects elicited were certainly due to finely dispersed nanoparticles and not the aggregates.

The mechanism underlying nanoparticles induced inflammation is believed to be the generation of reactive oxygen species (ROS), therefore, intracellular ROS levels were measured. Exposure of macrophages to Ag nanoparticles induced highest ROS generation followed by exposure to Al, CB and CAg nanoparticles. Au NPs resulted in slight decrease in ROS generation over control levels. A well-known inhibitor of ROS, NAC, significantly decreased the ROS generated by NPs and LPS. NF-κB, a mammalian transcription factor is known to control the expression of cell survival genes as well as pro-inflammatory enzymes and cytokines such as, COX-2, TNF- α, and

IL-6. In the present study, LPS and NPs induced nuclear translocation of NF-κB/p65 and p50 proteins is clearly evident from ELISA and Western blot analyses. Ag and Al NPs showed significant induction of NF-κB translocation. It was found that NF-κB activation induced by NPs and LPS was repressed by the treatment of NAC, a known antioxidant, confirming the role of ROS mediated NF-κB activation. Au NPs, on the other hand, did not show any significant NF-κB activation, compared to untreated control cells.

The expression of COX-2, a major mediator of inflammation and TNF-α, a traditional cyclooxygenase-2 inducer was analyzed by RT-PCR and Western blot analysis from cells exposed to nanoparticles of different sizes and at varying exposure times.RAW 264.7 cells were exposed to Ag, Al, CB, and CAg NPs at a concentration of 5 µg/ml for 6-48 h, and the induction of COX-2 and TNF-α was monitored. A significant time and size dependent induction of COX-2 and TNF-α expression was observed with both Ag and Al nanoparticles at mRNA and protein levels. While increase in the size of NPs showed slight decrease in the induction of COX-2 and TNF-α, the increase in exposure time showed gradual increase in COX-2 and TNF-α mRNA and protein induction up to 24 h and 48 h, respectively. Interestingly, when RAW 264.7 cells were exposed to Au NPs (20 nm and 40 nm) at concentration of 5 µg/ml for 6-48 h, there was no significant induction of COX-2 and TNF-α expression at both mRNA and protein levels. Macrophages secrete inflammatory mediators like

cytokines upon stimulation by various agents; one such cytokine IL-6 was measured in the medium when macrophages were exposed to various nanoparticles at 5 µg/ml concentration. The Ag NPs showed a significant release of IL-6 from RAW 264.7 macrophages after 48 h, followed by Al, CB and CAg NPs. Gold (20, 40 nm) NPs, however showed no appreciable release of IL-6 from RAW 264.7 cells. The results obtained are presented in the form of a schematic pathway in figure 6 below.

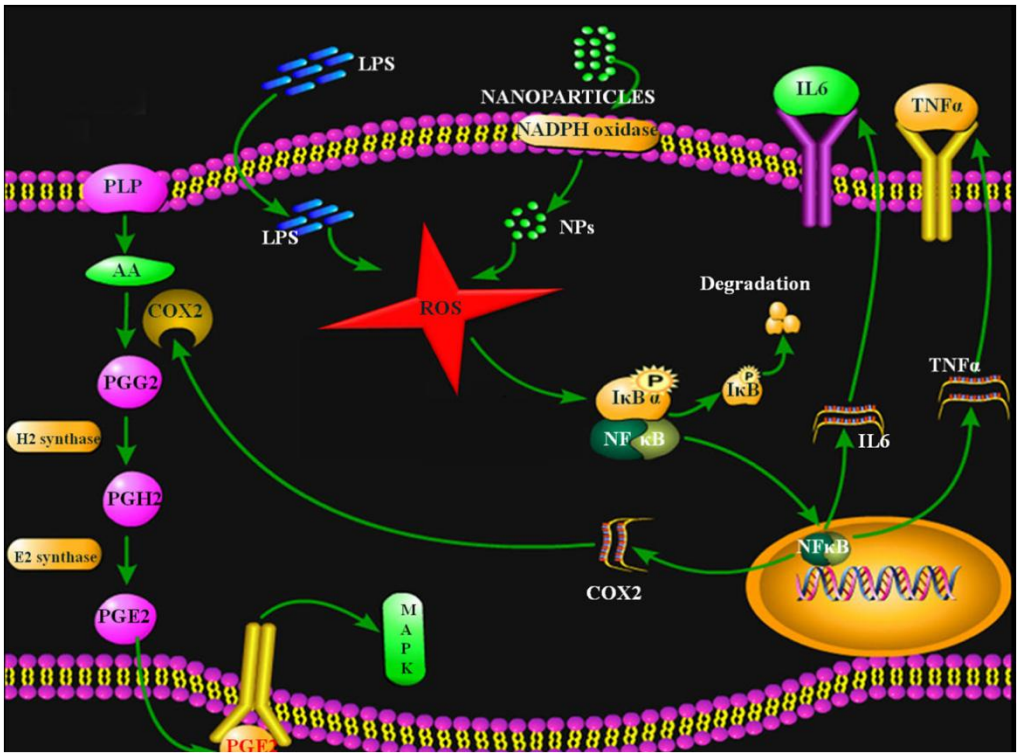

Figure 6. Schematic representation of the possible mode of nanoparticles induced inflammation

ii. Silver and Gold Nanoparticles Differentially Modulate the Proteome of Macrophages

A proteomics approach was employed to understand and identify the other key players involved in the effects of nanoparticles. Two dimensional electrophoresis (2DE) in combination with the MALDI-TOF-MS/MS is often used for such a purpose. The whole cell lysates were isoelectrofocused on the 4-7 pH strips and further resolved on 12% SDS gels to be analyzed by Image Master Platinum 6. The differentially expressed proteins were identified by MALDI-TOF-MS/MS followed by Mascot search.

A list of ten proteins were identified which were either up-regulated or down-regulated upon exposure to silver or gold nanoparticles. Among the ones identified Chloride intracellular ion channel (CLIC) and Cathepsin B were highly up-regulated. CLIC is a membrane associated protein that is most often associated with the autophagosomal lysosomes and is up-regulated in oxidative stress associated with the pathologies. Cathepsin B is a lysosomal protease that is involved in inflammaosome formation and trafficking TNF-α to the plasma membrane.

Enolase-1 was the other protein that was identified and this was down-regulated in the presence of gold nanoparticles. Enolase-1 a glycolytic enzyme when translocated to the plasma membrane, is detected as auto-antigen and

increase the inflammatory response in case of rheumatoid arthritis so this probably explains the role of gold nanoparticles in the Ayurvedic formulations that are used to treat the inflammatory conditions. These proteins could be good markers along with COX-2 and can be used for screening the nanoparticles.

iii. Silver and Gold Nanoparticles Affect the Stem Cell Proliferation and Differentiation

Stem cells are the undeveloped cells capable of self-renewal, proliferation and differentiation into any cell type in a multi-cellular organism. Recent studies make it more evident that every tissue in an organism has a repository of stem cells and there could be every possibility that the nanoparticles could interact with the stem cells. Therefore, the effects of nanoparticles were evaluated on human induced pluripotent stem cells.

The cell viability assay results obtained indicated that the silver nanoparticles were more toxic with an IC_{50} value of 4.6µg/ml as compared to gold nanoparticles that had an IC_{50} of 26.7µg/ml. According to the very preliminary setup to assess the effect on nanoparticles on random differentiation of nanoparticles it was observed that the formation of embryoid bodies was not largely affected in the presence of gold nanoparticles at 1µg as

well as 10µg concentrations. On the other hand, the EB formation was decreased in the presence of silver nanoparticles. There seems to be an increase in the debris as the days progressed indicating the increased cell death. There was also a dose dependent effect that was observed. These results were in correlation with the earlier results seen in case of macrophages.

iv. Effects of Silver and Gold Nanoparticles *In vivo*.

In vivo studies were carried out on the albino mice to evaluate the effects of the nanoparticles when the animals were exposed to them at sub-lethal doses. Effects of nanoparticles were evaluated in hepatic and pulmonary tissues. Hepatic tissue a major site of the xenobiotic metabolism was looked for ROS level change, antioxidant enzyme activities, and the inflammatory protein COX-2 expression.

Reactive oxygen species and nitrite levels showed an increase in the levels both in liver and lung tissues in mice treated. The antioxidant enzymes treated with Ag NPs however, were slightly reduced in both liver and lung tissues. These effects were observed to be dose dependent. The expression of COX-2 and Hsp70 was increased in dose dependent manner. Au NPs, on the other hand, had very limited changes in all the parameters studied in liver and lung tissues.

The histopathological observation of the liver tissue indicated that there was centrizonal necrosis with increased intercellular spaces. These effects were observed in silver nanoparticles treated animals. There was a size dependent effect of the nanoparticles where smaller size nanoparticles had more drastic effects compared to the bigger sizes. These effects were very mild in case of the gold nanoparticles treated animals. Similarly in case of lungs there was infiltration of inflammatory cells into the peribronchial regions especially in case of silver nanoparticles treated animals. This was also observed to be size dependent.

The transmission electron micrographs showed complete loss of the cellular morphology of the hepatocytes and the organelles within the cells were completely lost in case of silver nanoparticles treated nanoparticles. The damage observed was more drastic in case of silver smaller size treated animals as compared to bigger size treated animals. Also in case of pneumocytes there was severe damage observed in animals exposed to silver nanoparticles and this was dose and size dependent as well. These effects were not as prominent in case of gold nanoparticles treated animals. In conclusion the results observed *in vivo* upon treatment with nanoparticles showed correlation to the observations *in vitro*.

Overall the studies conducted *in vitro* and *in vivo* with selected nanoparticles indicate that the Ag NPs are pro-inflammatory and induce cytotoxic effects in somatic as well as stem cells. On the other hand, Au NPs which caused no such notable effects can be used for biomedical applications. Another important finding of the study in that COX-2 and macrophage based *in vitro* assay system could be employed to rapidly evaluate the biocompatibility of nanoparticles.

References

Aebersold R, Goodlett DR (2001) Mass spectrometry in proteomics. Chem Rev 101: 269-295.

Alshatwi AA, Subbarayan PV, Ramesh E, Al-Hazzani AA, Alsaif MA, et al. (2013) Aluminium oxide nanoparticles induce mitochondrial-mediated oxidative stress and alter the expression of antioxidant enzymes in human mesenchymal stem cells. Food Addit Contam Part A Chem Anal Control Expo Risk Assess 30: 1-10.

Alt V, Bechert T, Steinrucke P, Wagener M, Seidel P, et al. (2004) An in vitro assessment of the antibacterial properties and cytotoxicity of nanoparticulate silver bone cement. Biomaterials 25: 4383-4391.

An NT, Dong NT, Hanh PTB, Nhi TTY, Vu DA (2010) Silver-N-Carboxymethyl Chitosan Nanocomposites: Synthesis and its Antibacterial Activities. J Bioterr Biodef 1: 102.

Arora S, Jain J, Rajwade JM, Paknikar KM (2008) Cellular responses induced by silver nanoparticles: In vitro studies. Toxicol Lett 179: 93-100.

Asare N, Instanes C, Sandberg WJ, Refsnes M, Schwarze P, et al. (2012) Cytotoxic and genotoxic effects of silver nanoparticles in testicular cells. Toxicology 291: 65-72.

Asharani PV, Lian Wu Y, Gong Z, Valiyaveettil S (2008) Toxicity of silver nanoparticles in zebrafish models. Nanotechnology 19: 255102.

Averaimo S, Milton RH, Duchen MR, Mazzanti M (2010) Chloride intracellular channel 1 (CLIC1): Sensor and effector during oxidative stress. FEBS Lett 584: 2076-2084.

Bae S, Kim H, Lee N, Won C, Kim HR, et al. (2012) alpha-Enolase expressed on the surfaces of monocytes and macrophages induces robust synovial inflammation in rheumatoid arthritis. J Immunol 189: 365-372.

Baetz D, Shaw J, Kirshenbaum LA (2005) Nuclear factor-kappaB decoys suppress endotoxin-induced lung injury. Mol Pharmacol 67: 977-979.

Bankapur A, Krishnamurthy RS, Zachariah E, Santhosh C, Chougule B, et al. (2012) Micro-Raman spectroscopy of silver nanoparticle induced stress on optically-trapped stem cells. PLoS One 7: e35075.

Bantscheff M, Schirle M, Sweetman G, Rick J, Kuster B (2007) Quantitative mass spectrometry in proteomics: a critical review. Anal Bioanal Chem 389: 1017-1031.

Bosetti M, Masse A, Tobin E, Cannas M (2002) Silver coated materials for external fixation devices: in vitro biocompatibility and genotoxicity. Biomaterials 23: 887-892.

Bradford MM (1976) A rapid and sensitive method for the quantitation of microgram quantities of protein utilizing the principle of protein-dye binding. Anal Biochem 72: 248-254.

Braydich-Stolle L, Hussain S, Schlager JJ, Hofmann MC (2005) In vitro cytotoxicity of nanoparticles in mammalian germline stem cells. Toxicol Sci 88: 412-419.

Brown DM, Donaldson K, Borm PJ, Schins RP, Dehnhardt M, et al. (2004) Calcium and ROS-mediated activation of transcription factors and TNF-alpha cytokine gene expression in macrophages exposed to ultrafine particles. Am J Physiol Lung Cell Mol Physiol 286: L344-353.

Brown DM, Wilson MR, MacNee W, Stone V, Donaldson K (2001) Size-dependent proinflammatory effects of ultrafine polystyrene particles: a role for surface area and oxidative stress in the enhanced activity of ultrafines. Toxicol Appl Pharmacol 175: 191-199.

Brown SD, Nativo P, Smith JA, Stirling D, Edwards PR, et al. (2010) Gold nanoparticles for the improved anticancer drug delivery of the active component of oxaliplatin. J Am Chem Soc 132: 4678-4684.

Burklew CE, Ashlock J, Winfrey WB, Zhang B (2012) Effects of aluminum oxide nanoparticles on the growth, development, and microRNA expression of tobacco (Nicotiana tabacum). PLoS One 7: e34783.

Buzdugan E, Beckman EJ (2007) Propylene oxide copolymerization with carbon dioxide using sterically hindered aluminium catalysts. Materiale Plastice 44: 278-283.

Cai W, Gao T, Hong H, Sun J (2008) Applications of gold nanoparticles in cancer nanotechnology. Nanotech Sci App 1: 17–32.

Cao L, Wang X, Meziani MJ, Lu F, Wang H, et al. (2007) Carbon dots for multiphoton bioimaging. J Am Chem Soc 129: 11318-11319.

Carlson C, Hussain SM, Schrand AM, Braydich-Stolle LK, Hess KL, et al. (2008) Unique cellular interaction of silver nanoparticles: size-dependent generation of reactive oxygen species. J Phys Chem B 112: 13608-13619.

Castranova V (2004) Signaling pathways controlling the production of inflammatory mediators in response to crystalline silica exposure: role of reactive oxygen/nitrogen species. Free Radic Biol Med 37: 916-925.

Chae YJ, Pham CH, Lee J, Bae E, Yi J, et al. (2009) Evaluation of the toxic impact of silver nanoparticles on Japanese medaka (Oryzias latipes). Aquat Toxicol 94: 320-327.

Chandra S, Das P, Bag S, Laha D, Pramanik P (2011) Synthesis, functionalization and bioimaging applications of highly fluorescent carbon nanoparticles. Nanoscale 3: 1533-1540. 1.

Chen CD, Wang CS, Huang YH, Chien KY, Liang Y, et al. (2007) Overexpression of CLIC1 in human gastric carcinoma and its clinicopathological significance. Proteomics 7: 155-167.

Chen J, Wang D, Xi J, Au L, Siekkinen A, et al. (2007) Immuno gold nanocages with tailored optical properties for targeted photothermal destruction of cancer cells. Nano Lett 7: 1318-1322.

Chen L, Yokel RA, Hennig B, Toborek M (2008) Manufactured aluminum oxide nanoparticles decrease expression of tight junction proteins in brain vasculature. J Neuroimmune Pharmacol 3: 286-295.

Chen YH, Tsai CY, Huang PY, Chang MY, Cheng PC, et al. (2007) Methotrexate conjugated to gold nanoparticles inhibits tumor growth in a syngeneic lung tumor model. Mol Pharm 4: 713-722.

Cho WS, Cho M, Jeong J, Choi M, Cho HY, et al. (2009) Acute toxicity and pharmacokinetics of 13 nm-sized PEG-coated gold nanoparticles. Toxicol Appl Pharmacol 236: 16-24.

Cho WS, Cho M, Jeong J, Choi M, Han BS, et al. (2010) Size-dependent tissue kinetics of PEG-coated gold nanoparticles. Toxicol Appl Pharmacol 245: 116-123.

Claiborne A (1985) Catalase. In: Greenwald R, editor. Handbook of oxygen research radical research. New York: CRC Press 283–284.

de Hoog CL, Mann M (2004) Proteomics. Annu Rev Genomics Hum Genet 5: 267-293.

Diaz A, Chepenik KP, Korn JH, Reginato AM, Jimenez SA (1998) Differential regulation of cyclooxygenases 1 and 2 by interleukin-1 beta, tumor necrosis factor-alpha, and transforming growth factor-beta 1 in human lung fibroblasts. Exp Cell Res 241: 222-229.

Dunn MJ, Görg A (2001) Two-dimensional polyacrylamide gel electrophoresis for proteome analysis, in Proteomics, From Protein Sequence to function BIOS Scientific Publisher, Oxford 4: 43-63.

Dutta D, Sundaram SK, Teeguarden JG, Riley BJ, Fifield LS, et al. (2007) Adsorbed proteins influence the biological activity and molecular targeting of nanomaterials. Toxicol Sci 100: 303-315.

Fang CY, Vaijayanthimala V, Cheng CA, Yeh SH, Chang CF, et al. (2011) The Exocytosis of Fluorescent Nanodiamond and Its Use as a Long-Term Cell Tracker. Small 7: 3363-3370.

Ferreira L, Karp JM, Nobre L, Langer R (2008) New opportunities: The use of Nanotechnologies to manipulate and track stem cells. Cell Stem Cell 3: 136-146.

Floyd RA, West M, Hensley K (2001) Oxidative biochemical markers; clues to understanding aging in long-lived species. Exp Gerontol 36: 619-640.

Fontes A, Macarthur CC, Lieu PT, Vemuri MC (2013) Generation of human-induced pluripotent stem cells (hiPSCs) using episomal vectors on defined Essential 8™ Medium conditions. Methods Mol Biol 997: 57-72.

Fuchs E, Segre JA (2000) Stem cells: a new lease on life. Cell 100: 143-155.

Garcia-Contreras R, Argueta-Figueroa L, Mejia-Rubalcava C, Jimenez-Martinez R, Cuevas-Guajardo S, et al. (2011) Perspectives for the use

of silver nanoparticles in dental practice. International Dental Journal 61: 297-301.

Gediminas C, Tao R, Peter RK (2002) Vascular dysfunction and Free radicals. Free Rad biol Med 33: 433-440.

Greenacre SA, Rocha FA, Rawlingson A, Meinerikandathevan S, Poston RN, et al. (2002) Protein nitration in cutaneous inflammation in the rat: essential role of inducible nitric oxide synthase and polymorphonuclear leukocytes. Br J Pharmacol 136: 985-994.

Grodzik M, Sawosz E, Zielinska M, Chwalibog A (2009) Influence of silver nanoparticles on hsp70 expression in bursa of fabricius and serum immunoglobulin levels in chicken embryos. The International Nanotechnology Conference.

Ha SD, Martins A, Khazaie K, Han JH, Chan BMC, et al. (2008) Cathepsin B is involved in the trafficking of TNF-alpha-containing vesicles to the plasma membrane in macrophages. Journal of Immunology 181: 690-697.

Hackenberg S, Scherzed A, Kessler M, Hummel S, Technau A, et al. (2011) Silver nanoparticles: Evaluation of DNA damage, toxicity and functional impairment in human mesenchymal stem cells. Toxicology Letters 201: 27-33.

Harris RE (2009) Cyclooxygenase-2 (cox-2) blockade in the chemoprevention of cancers of the colon, breast, prostate, and lung. Inflammopharmacology 17: 55-67.

Hashimoto M, Toshima H, Yonezawa T, Kawai K, Narushima T, Kaga M, Endo K (2013) Responses of RAW264.7 macrophages to water-dispersible gold and silver nanoparticles stabilized by metal-carbon σ-bonds. J Biomed Mater Res A. 2013

Haworth O, Levy BD (2007) Endogenous lipid mediators in the resolution of airway inflammation. Eur Respir J 30: 980-992.

HEI Review Panel on Ultrafine Particles. (2013) Understanding the Health Effects of Ambient Ultrafine Particles. HEI Perspectives 3. Health Effects Institute, Boston, MA.

Hendel J, Nielsen OH (1997) Expression of cyclooxygenase-2 mRNA in active inflammatory bowel disease. Am J Gastroenterol 92: 1170-1173.

Hirsch LR, Stafford RJ, Bankson JA, Sershen SR, Rivera B, et al. (2003) Nanoshell-mediated near-infrared thermal therapy of tumors under magnetic resonance guidance. Proc Natl Acad Sci U S A 100: 13549-13554.

Hiura TS, Kaszubowski MP, Li N, Nel AE (1999) Chemicals in diesel exhaust particles generate reactive oxygen radicals and induce apoptosis in macrophages. J Immunol 163: 5582-5591.

Hornung V, Bauernfeind F, Halle A, Samstad EO, Kono H, et al. (2008) Silica crystals and aluminum salts activate the NALP3 inflammasome through phagosomal destabilization. Nature Immunology 9: 847-856.

Hsin YH, Chena CF, Huang S, Shih TS, Lai PS, et al. (2008) The apoptotic effect of nanosilver is mediated by a ROS- and JNK-dependent mechanism involving the mitochondrial pathway in NIH3T3 cells. Toxicology Letters 179: 130-139.

Hussain SM, Frazier JM (2002) Cellular toxicity of hydrazine in primary rat hepatocytes. Toxicological Sciences 69: 424-432.

Hussain SM, Hess KL, Gearhart JM, Geiss KT, Schlager JJ (2005) In vitro toxicity of nanoparticles in BRL 3A rat liver cells. Toxicology in Vitro 19: 975-983.

Hyun JS, Lee BS, Ryu HY, Sung JH, Chung KH, et al. (2008) Effects of repeated silver nanoparticles exposure on the histological structure and mucins of nasal respiratory mucosa in rats. Toxicology Letters 182: 24-28.

Ilic V, Saponjic Z, Vodnik V, Mihailovic D, Jovancic P, et al. (2009) The study of coloration and antibacterial efficiency of corona activated dyed polyamide and polyester fabrics loaded with Ag nanoparticles. Fibers and Polymers 10: 650-656.

Jain P, Pradeep T (2005) Potential of silver nanoparticle-coated polyurethane foam as an antibacterial water filter. Biotechnology and Bioengineering 90: 59-63.

Jani P, Halbert GW, Langridge J, Florence AT (1990) Nanoparticle uptake by the rat gastrointestinal mucosa: quantitation and particle size dependency. J Pharm Pharmacol 42: 821-826.

Janssen YM, Barchowsky A, Treadwell M, Driscoll KE, Mossman BT (1995) Asbestos induces nuclear factor kappa B (NF-kappa B) DNA-binding activity and NF-kappa B-dependent gene expression in tracheal epithelial cells. Proc Natl Acad Sci U S A 92: 8458-8462.

Jiang LL, Salao K, Li H, Rybicka JM, Yates RM, et al. (2012) Intracellular chloride channel protein CLIC1 regulates macrophage function through modulation of phagosomal acidification. Journal of Cell Science 125: 5479-5488.

Kaewamatawong T, Shimada A, Okajima M, Inoue H, Morita T, et al. (2006) Acute and subacute pulmonary toxicity of low dose of ultrafine colloidal silica particles in mice after intratracheal instillation. Toxicologic Pathology 34: 958-965.

Keren S, Zavaleta C, Cheng Z, de la Zerda A, Gheysens O, et al. (2008) Noninvasive molecular imaging of small living subjects using Raman spectroscopy. Proceedings of the National Academy of Sciences of the United States of America 105: 5844-5849.

Kim JH, Kim JH, Kim KW, Kim MH, Yu YS (2009) Intravenously administered gold nanoparticles pass through the blood-retinal barrier depending on the particle size, and induce no retinal toxicity. Nanotechnology 20(50): 505101.

Kim TW, Chung PW, Slowing II, Tsunoda M, Yeung ES, et al. (2008) Structurally Ordered Mesoporous Carbon Nanoparticles as Transmembrane Delivery Vehicle in Human Cancer Cells. Nano Letters 8: 3724-3727.

Kim Y, Suh HS, Cha HJ, Kim SH, Jeong KS, et al. (2009) A Case of Generalized Argyria After Ingestion of Colloidal Silver Solution. American Journal of Industrial Medicine 52: 246-250.

Kim YS, Kim JS, Cho HS, Rha DS, Kim JM, et al. (2008) Twenty-eight-day oral toxicity, genotoxicity, and gender-related tissue distribution of silver nanoparticles in Sprague-Dawley rats. Inhalation Toxicology 20: 575-583.

Klose J (1975) Protein mapping by combined isoelectric focusing and electrophoresis of mouse tissues. A novel approach to testing for induced point mutations in mammals. Humangenetik 26: 231-243.

Kohler JM, Abahmane L, Wagner J, Albert J, Mayer G (2008) Preparation of metal nanoparticles with varied composition for catalytical applications in microreactors. Chemical Engineering Science 63: 5048-5055.

Koike E, Kobayashi T (2006) Chemical and biological oxidative effects of carbon black nanoparticles. Chemosphere 65: 946-951.

Lee HJ, Yeo SY, Jeong SH (2003) Antibacterial effect of nanosized silver colloidal solution on textile fabrics. Journal of Materials Science 38: 2199-2204.

Lim DH, Jang J, Kim S, Kang T, Lee K, Choi IH (2012) The effects of sub-lethal concentrations of silver nanoparticles on inflammatory and stress genes in human macrophages using cDNA microarray analysis. Biomaterials 18: 4690-4699.

Littler DR, Harrop SJ, Goodchild SC, Phang JM, Mynott AV, et al. (2010) The enigma of the CLIC proteins: Ion channels, redox proteins, enzymes, scaffolding proteins? Febs Letters 584: 2093-2101.

Liu P, Zhao MF (2009) Silver nanoparticle supported on halloysite nanotubes catalyzed reduction of 4-nitrophenol (4-NP). Applied Surface Science 255: 3989-3993.

Liu Z, Chen K, Davis C, Sherlock S, Cao QZ, et al. (2008) Drug delivery with carbon nanotubes for in vivo cancer treatment. Cancer Research 68: 6652-6660.

Lu YB, Wahl LM (2005) Oxidative stress augments the production of matrix metalloproteinase-1, cyclooxygenase-2, and prostaglandin E2 through enhancement of NF-kappa B activity in lipopolysaccharide-activated human primary monocytes. Journal of Immunology 175: 5423-5429.

Lukin ES, Tarasova SV, Korolev AV (2001) Application of ceramics based on aluminum oxide in medicine (a review). Glass and Ceramics 58: 105-107.

Ma LL, Feldman MD, Tam JM, Paranjape AS, Cheruku KK, et al. (2009) Small Multifunctional Nanoclusters (Nanoroses) for Targeted Cellular Imaging and Therapy. Acs Nano 3: 2686-2696.

Magrez A, Kasas S, Salicio V, Pasquier N, Seo JW, et al. (2006) Cellular toxicity of carbon-based nanomaterials. Nano Letters 6: 1121-1125.

Manno D, Filippo E, Di Giulio M, Serra A (2008) Synthesis and characterization of starch-stabilized Ag nanostructures for sensors applications. Journal of Non-Crystalline Solids 354: 5515-5520.

Masaki M, Ikeda A, Shiraki E, Oka S, Kawasaki T (2003) Mixed lineage kinase LZK and antioxidant protein-1 activate NF-kappaB synergistically. Eur J Biochem 270: 76-83.

McGrath ME (1999) The lysosomal cysteine proteases. Annu Rev Biophys Biomol Struct 28: 181-204.

Medina C, Santos-Martinez MJ, Radomski A, Corrigan OI, Radomski MW (2007) Nanoparticles: pharmacological and toxicological significance. Br J Pharmacol 150: 552-558.

Miziolek A (2002) Nanoenergetics: An emerging technology area of national importance. AMPTIACQ 6 (1): 43-48.

Mroz RM, Schins RP, Li H, Drost EM, Macnee W, Donaldson K (2007) Nanoparticle Carbon Black Driven DNA Damage Induces Growth Arrest and AP-1 and NFkappa B DNA Binding in Lung Epithelial A549 Cell Line. J Physiol Pharmacol 58: 461-470.

Nagesha D, Laevsky GS, Lampton P, Banyal R, Warner C, et al. (2007) In vitro imaging of embryonic stem cells using multiphoton luminescence of gold nanoparticles. International Journal of Nanomedicine 2: 813-819

Nakao S, Ogtata Y, Shimizu E, Yamazaki M, Furuyama S, Sugiya H (2002) Tumor Necrosis Factor Alpha (TNF-α)-Induced Prostaglandin E2 Release is Mediated by the Activation of Cyclooxygenase-2 (Cox-2) Transcription Via NFκB in Human Gingival Fibroblasts. Mol Cell Biochem 238: 11–18.

Nam JM, Thaxton CS, Mirkin CA (2003) Nanoparticle-based bio-bar codes for the ultrasensitive detection of proteins. Science 301: 1884-1886.

Nel A, Xia T, Madler L, Li N (2006) Toxic potential of materials at the nanolevel. Science 311: 622-627.

Niemeyer CM (2001) Nanoparticles, proteins, and nucleic acids: Biotechnology meets materials science. Angewandte Chemie-International Edition 40: 4128-4158.

Nishanth RP, Jyotsna RG, Schlager JJ, Hussain SM, Reddanna P (2011) Inflammatory responses of RAW 264.7 macrophages upon exposure to nanoparticles: role of ROS-NFκB signaling pathway. Nanotoxicology 4: 502-516.

Niwa Y, Hiura Y, Sawamura H, Iwai N (2008) Inhalation exposure to carbon black induces inflammatory response in rats. Circulation Journal 72: 144-149.

Novarino G, Fabrizi C, Tonini R, Denti MA, Malchiodi-Albedi F, et al. (2004) Involvement of the intracellular ion channel CLIC1 in microglia-mediated beta-amyloid-induced neurotoxicity. Journal of Neuroscience 24: 5322-5330.

Nowack B, Bucheli TD (2007) Occurrence, behavior and effects of nanoparticles in the environment. Environmental Pollution 150: 5-22.

Oberdorster G, Finkelstein JN, Johnston C, Gelein R, Cox C, et al. (2000) Acute pulmonary effects of ultrafine particles in rats and mice. Res Rep Health Eff Inst: 5-74; disc 75-86.

Oberdorster G, Oberdorster E, Oberdorster J (2005) Nanotoxicology: an emerging discipline evolving from studies of ultrafine particles. Environ Health Perspect 113: 823-839.

Oberdorster G (2001) Pulmonary effects of inhaled ultrafine particles. Int Arch Occup Environ Health 74: 1-8.

O'Farrell PH (1975) High resolution two-dimensional electrophoresis of proteins. J Biol Chem 250: 4007-4021.

Olofsson L, Rindzevicius T, Pfeiffer I, Kall M, Hook F (2003) Surface-based gold-nanoparticle sensor for specific and quantitative DNA hybridization detection. Langmuir 19: 10414-10419.

Pakrashi S, Dalai S, Prathna TC, Trivedi S, Myneni R, et al. (2013) Cytotoxicity of aluminium oxide nanoparticles towards fresh water algal isolate at low exposure concentrations. Aquatic Toxicology 132: 34-45.

Panyam J, Labhasetwar V (2003) Biodegradable nanoparticles for drug and gene delivery to cells and tissue. Advanced Drug Delivery Reviews 55: 329-347.

Park EJ, Park K (2009) Oxidative stress and pro-inflammatory responses induced by silica nanoparticles in vivo and in vitro. Toxicology Letters 184: 18-25.

Park MVDZ, Neigh AM, Vermeulen JP, de la Fonteyne LJJ, Verharen HW, et al. (2011) The effect of particle size on the cytotoxicity, inflammation, developmental toxicity and genotoxicity of silver nanoparticles. Biomaterials 32: 9810-9817.

Patra HK, Banerjee S, Chaudhuri U, Lahiri P, Dasgupta AK (2007) Cell selective response to gold nanoparticles. Nanomedicine-Nanotechnology Biology and Medicine 3: 111-119.

Pinkus R, Weiner LM, Daniel V (1996) Role of Oxidants and Antioxidants in the Induction of AP-1, NF-Kappa B, and Glutathione S-Transferase Gene Expression. J Biol Chem 271: 13422–13429.

Pitsillides CM, Joe EK, Wei X, Anderson RR, Lin CP (2003) Selective cell targeting with light-absorbing microparticles and nanoparticles. Biophys J 84: 4023-4032.

Platonov OI, Tsernekhman LS, Kalinkin PN, Kovalenko ON (2007) Analysis of the activity of an aluminum oxide claus catalyst in commercial operation. Russian Journal of Applied Chemistry 80: 2031-2035.

Quercia L, Loffredo F, Alfano B, La Ferrara V, Di Francia G (2004) Fabrication and characterization of carbon nanoparticles for polymer based vapor sensors. Sensors and Actuators B-Chemical 100: 22-28.

Rabinovich GA, Sotomayor CE, Riera CM, Bianco I, Correa SG (2000) Evidence of a role for galectin-1 in acute inflammation. European Journal of Immunology 30: 1331-1339.

Reddy MC, Subliashini J, Mahipal SVK, Bhat VB, Reddy PS, et al. (2003) C-Phycocyanin, a selective cyclooxygenase-2 inhibitor, induces apoptosis in lipopolysaccharide-stimulated RAW 264.7 macrophages. Biochemical and Biophysical Research Communications 304: 385-392.

Roit IM (1997) Roitt's Essential Immunolgy Oxford: Blackwell Science Ltd.

Rojanasakul Y, Ye JP, Chen F, Wang LY, Cheng NL, et al. (1999) Dependence of NF-kappa B activation and free radical generation on silica-induced TNF-alpha production in macrophages. Molecular and Cellular Biochemistry 200: 119-125.

Ruan SY, Schuh CA (2012) Towards electroformed nanostructured aluminum alloys with high strength and ductility. Journal of Materials Research 27: 1638-1651.

Rubakhin SS, Jurchen JC, Monroe EB, Sweedler JV (2005) Imaging mass spectrometry: fundamentals and applications to drug discovery. Drug Discovery Today 10: 823-837.

Salata O (2004) Applications of nanoparticles in biology and medicine. J Nanobiotechnology 2: 3.

Sanford JC, Smith FD, Russell JA (1993) Optimizing the biolistic process for different biological applications. Methods Enzymol 217: 483-509.

Scott WA, Zrike JM, Hamill AL, Kempe J, Cohn ZA (1980) Regulation of arachidonic acid metabolites in macrophages. J Exp Med 152: 324-335.

Scown TM, Santos EM, Johnston BD, Gaiser B, Baalousha M, et al. (2010) Effects of aqueous exposure to silver nanoparticles of different sizes in rainbow trout. Toxicol Sci 115: 521-534.

Sell S (2005) Adult stem cell plasticity: introduction to the first issue of stem cell reviews. Stem Cell Rev 1: 1-7.

Shukla R, Bansal V, Chaudhary M, Basu A, Bhonde RR, et al. (2005) Biocompatibility of gold nanoparticles and their endocytotic fate inside the cellular compartment: A microscopic overview. Langmuir 21: 10644-10654.

Smithies O, Poulik MD (1956) Two-dimentional electrophoresis for serum proteins. Nature 177 (4518): 1033.

Steen H, Mann M (2004) The ABC's (and XYZ's) of peptide sequencing. Nat Rev Mol Cell Biol 5: 699-711.

Stone V, Shaw J, Brown DM, Macnee W, Faux SP, et al. (1998) The role of oxidative stress in the prolonged inhibitory effect of ultrafine carbon black on epithelial cell function. Toxicology in Vitro 12: 649-659.

Stone V, Tuinman M, Vamvakopoulos JE, Shaw J, Brown D, et al. (2000) Increased calcium influx in a monocytic cell line on exposure to ultrafine carbon black. Eur Respir J 15: 297-303.

Sung JH, Ji JH, Park JD, Yoon JU, Kim DS, et al. (2009) Subchronic inhalation toxicity of silver nanoparticles. Toxicol Sci 108: 452-461.

Suresh AK, Pelletier DA, Wang W, Morrell-Falvey JL, Gu BH, et al. (2012) Cytotoxicity Induced by Engineered Silver Nanocrystallites Is Dependent on Surface Coatings and Cell Types. Langmuir 28: 2727-2735.

Sutherland WS, Winefordner JD (1992) Colloid Filtration a Novel Substrate Preparation Method for Surface-Enhanced Raman-Spectroscopy. J Colloid Interface Sci 48:129–141.

Takenaka S, Karg E, Roth C, Schulz H, Ziesenis A, et al. (2001) Pulmonary and systemic distribution of inhaled ultrafine silver particles in rats. Environ Health Perspect 109 Suppl 4: 547-551.

Thannickal VJ, Fanburg BL (2000) Reactive oxygen species in cell signaling. American Journal of Physiology-Lung Cellular and Molecular Physiology 279: L1005-L1028.

Theng BKG, Yuan GD (2008) Nanoparticles in the Soil Environment. Elements 4: 395-399.

Tian F, Cui D, Schwarz H, Estrada GG, Kobayashi H (2006) Cytotoxicity of single-wall carbon nanotubes on human fibroblasts. Toxicology in Vitro 20: 1202-1212.

Tkachenko AG, Xie H, Coleman D, Glomm W, Ryan J, et al. (2003) Multifunctional gold nanoparticle-peptide complexes for nuclear targeting. J Am Chem Soc 125: 4700-4701.

Trop M, Novak M, Rodl S, Hellbom B, Kroell W, et al. (2006) Silver-coated dressing acticoat caused raised liver enzymes and argyria-like symptoms in burn patient. J Trauma 60: 648-652.

Tuch BE (2006) Stem cells--a clinical update. Aust Fam Physician 35: 719-721.

Tzeng HP, Yang RS, Ueng TH, Liu SH (2007) Upregulation of cyclooxygenase-2 by motorcycle exhaust particulate-induced reactive oxygen species enhances rat vascular smooth muscle cell proliferation. Chem Res Toxicol 20: 1170-1176.

Van Bramer SE (1998) An Introduction to Mass Spectrometry.

Wagner AJ, Bleckmann CA, Murdock RC, Schrand AM, Schlager JJ, et al. (2007) Cellular interaction of different forms of aluminum nanoparticles in rat alveolar macrophages. J Phys Chem B 111: 7353-7359.

Walter JL, Maire EP, Theo PK (2005) Nanomolar aluminum induces pro-inflammatory and pro-apoptotic gene expression in human brain cells in primary culture. J Inorg Biochem 99: 1895-1898.

Wang H, Joseph JA (1999) Quantifying cellular oxidative stress by dichlorofluorescein assay using microplate reader. Free Radical Biology and Medicine 27: 612-616.

Westermeier R (2005) Electrophoresis in practice: A guide to methods and applications of DNA and protein separations. (fourth edition). Wiley VCH.

Whiteman M, Hong HS, Jenner A, Halliwell B (2002) Loss of oxidized and chlorinated bases in DNA treated with reactive oxygen species: implications for assessment of oxidative damage in vivo. Biochemical and Biophysical Research Communications 296: 883-889.

Wu W, Li RT, Bian XC, Zhu ZS, Ding D, et al. (2009) Covalently Combining Carbon Nanotubes with Anticancer Agent: Preparation and Antitumor Activity. Acs Nano 3: 2740-2750.

Xia L, Lenaghan SC, Zhang M, Zhang Z, Li Q (2010) Naturally occurring nanoparticles from English ivy: an alternative to metal-based nanoparticles for UV protection. J Nanobiotechnology 8: 12.

Xu A, Chai Y, Nohmi T, Hei TK (2009) Genotoxic responses to titanium dioxide nanoparticles and fullerene in gpt delta transgenic MEF cells. Part Fibre Toxicol 6: 3.

Yan S, Sloane BF (2003) Molecular regulation of human cathepsin B: implication in pathologies. Biol Chem 384: 845-854.

Yarmush ML, Jayaraman A (2002) Advances in proteomic technologies. Annu Rev Biomed Eng 4: 349-373.

Yu J, Hu K, Smuga-Otto K, Tian S, Stewart R, et al. (2009) Human induced pluripotent stem cells free of vector and transgene sequences. Science 324: 797-801.

Yu J, Vodyanik MA, Smuga-Otto K, Antosiewicz-Bourget J, Frane JL, et al. (2007) Induced pluripotent stem cell lines derived from human somatic cells. Science 318: 1917-1920.